ERDC/CHL TR-00-23

US Army Corps
of Engineers®
Engineer Research and
Development Center

Design of Sediment Trap at Rollover Pass, Texas

Trimbak M. Parchure, Ben Brown,
and Robert T. McAdory

September 2000

Coastal and Hydraulics Laboratory

The contents of this report are not to be used for advertising, publication, or promotional purposes. Citation of trade names does not constitute an official endorsement or approval of the use of such commercial products.

The findings of this report are not to be construed as an official Department of the Army position, unless so designated by other authorized documents.

PRINTED ON RECYCLED PAPER

ERDC/CHL TR-00-23
September 2000

Design of Sediment Trap at Rollover Pass, Texas

by Trimbak M. Parchure, Ben Brown, Robert T. McAdory

Coastal and Hydraulics Laboratory
U.S. Army Engineer Research and Development Center
3909 Halls Ferry Road
Vicksburg, MS 39180-6199

Final report

Prepared for U.S. Army Corps of Engineers
Washington, DC 20314-1000

Engineer Research and Development Center Cataloging-In-Publication Data

Parchure, T. M. (Trimbak Mukund), 1943-
Design of sediment trap at Rollover Pass, Texas / by Trimbak M. Parchure, Ben Brown, Robert T. McAdory ; prepared for U.S. Army Corps of Engineers.
113 p. : ill. ; 28 cm. -- (ERDC/CHL ; TR-00-23)
Includes bibliographic references.
1.Sediment control -- Texas -- Rollover Pass. 2. Sedimentation and deposition -- Texas -- Rollover Pass. 3. Rollover Pass (Tex.) I. Brown, Ben. II. McAdory, Robert T. III. United States. Army. Corps of Engineers. IV. Engineer Research and Development Center (U.S.) V. Coastal and Hydraulics Laboratory (U.S.) VI. Series: ERDC/CHL TR ; 00-23.
TA7 E8 no.ERDC/CHL TR-00-23

Contents

List of Figures

List of Tables

Preface

A numerical model study for design of a sediment trap at Rollover Pass, TX, was conducted at the Coastal and Hydraulics Laboratory of the U.S. Army Engineer Research and Development Center (ERDC), Vicksburg, MS, during 1999. The U.S. Army Engineer District, Galveston, provided funding for this study. Dr. Trimbak M. Parchure, Research Hydraulic Engineer, was the Principal Investigator for the project. Dr. Parchure prepared this report jointly with Mr. Ben Brown. Dr. Parchure and Mr. Ben Brown conducted the work under general supervision of Messers Allen M. Teeter, Leader, Sedimentation Engineering and Dredging Group, Dr. Robert T. McAdory, Chief, Tidal Hydraulics Branch, Dr. William H. McAnally, Chief, Estuaries and Hydrosciences Division, and Dr. James R. Houston, former Director, Coastal and Hydraulics Laboratory.

The ERDC Coastal and Hydraulics Laboratory (CHL) published this report. CHL was formed in October 1996 with the merger of the Waterways Experiment Station Coastal Engineering Research Center and the Hydraulics Laboratory. WES has now become part of ERDC.

During the preparation and publication of this report, Dr. James R. Houston was Director of ERDC, and COL James S. Weller, EN, was Commander.

1 Introduction

Background

Rollover Pass, TX, is located in the Gulf of Mexico about 29 km (18 miles) northeast of the Galveston Bay entrance (Figure 1). Rollover Bay is a small semicircular bay in the southeastern part of East Bay, which forms a part of Galveston Bay. Rollover Pass is a narrow manmade channel which connects the Gulf of Mexico and Rollover Bay (Figure 2). Most of Rollover Bay consists of shallow depths of about 0.3 to 0.9 m (1 to 3 ft) with extensive areas covered by marshland. The Gulf Intracoastal Waterway (GIWW) separates Rollover Bay and East Bay. Rollover Pass provides tidal connection between the sea and Rollover Bay. The U.S. Army Engineer District, Galveston, (SWG) maintains a navigation channel within the GIWW for commercial barge traffic. The GIWW has a bottom width of 38 m (125 ft). An authorized depth of 3.6 m (12 ft) [plus 0.61 m (2 ft) advance maintenance] is maintained for the existing dredge channel. The dredged material is deposited along the beach on the west side of the pass. Rollover Pass does not permit navigation of any vessels from the ocean to Rollover Bay because of two limitations. The first is a weir constructed in the channel to restrict tidal velocities. The crest of the weir is about 1.5 m (5 ft) below mean sea level (msl). The second limitation is imposed by the low elevation of a bridge on Highway 87 that crosses Rollover Pass.

The Problem

Over the past several years considerable siltation has occurred inside the GIWW and the Rollover Bay area, which has required periodic dredging for maintaining navigable depths. Although no direct field measurements were available, it was believed that substantial sediment might be entering Rollover Bay from the sea as well as from the land areas adjacent to the bay. It was presumed that sediment from the sea enters the bay under the action of flood tidal currents.

The Galveston District is considering the possibility of providing a sediment trap near the GIWW and wanted to know whether such a trap would be feasible and effective in reducing the frequency of dredging in GIWW. The District requested the U.S. Army Engineer Research and Development Center (ERDC), Coastal and Hydraulics Laboratory (CHL), Vicksburg, to examine the problem and suggest necessary measures.

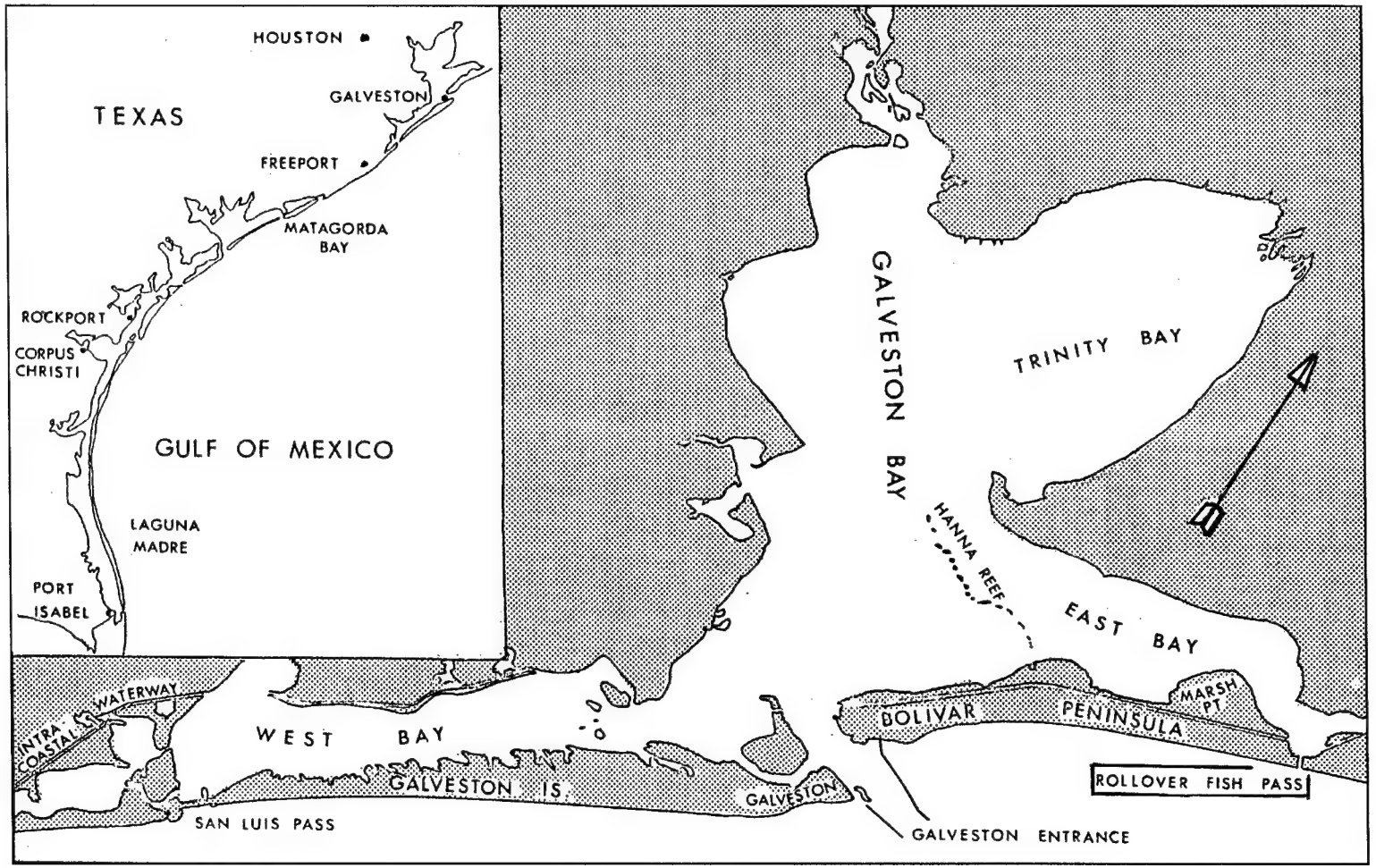

Figure 1. Location map of Rollover Pass

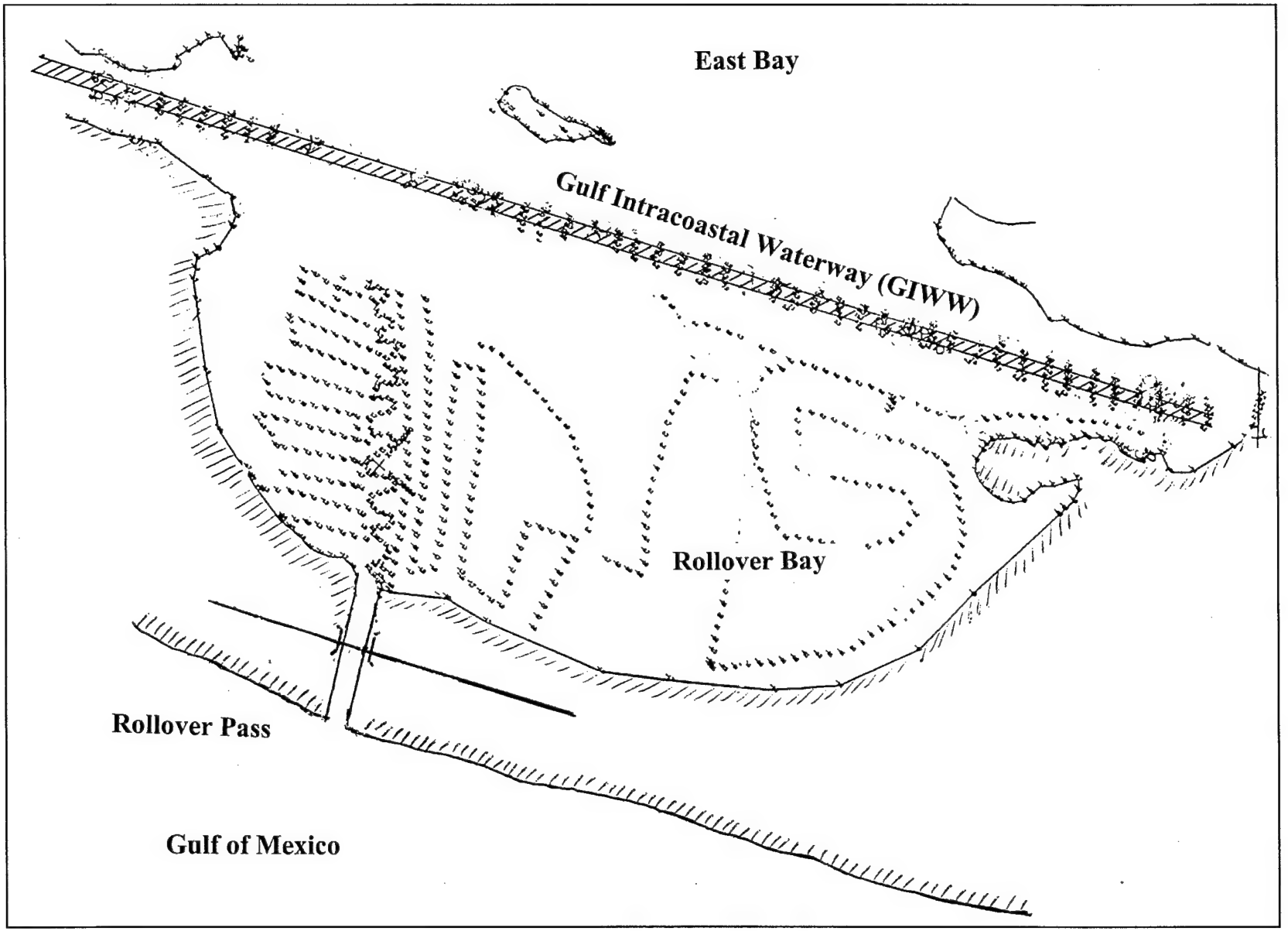

Figure 2. Map of Rollover Bay, Rollover Pass, and East Bay

Objective

The objective of the proposed study was to construct a working numerical model of the Rollover Pass area and to use the model for addressing problems related to the siltation and maintenance of the present navigation channel including the design of a sediment trap.

Scope of Study

A two-dimensional hydraulic numerical model study was considered to be appropriate and adequate for the study. Furthermore, it was presumed on the basis of anecdotal evidence that the sediment predominantly consisted of sand and therefore salinity was not expected to have a significant influence in the sediment transport dynamics in the area. The assumption on the type of sediment was subsequently proved to be correct based on the results of analysis of bed samples collected at site. Salinity was not reproduced in the model because it does not influence dynamics of noncohesive sediments.

A numerical model study of the Galveston Bay area was done at ERDC, CHL a few years ago (Lin 1992). The model was retrieved and the model grid was modified to provide improved resolution and updated bathymetry by incorporating results of the latest hydrographic survey of the area of interest. The model was then run for the revised tidal conditions and appropriate boundary conditions.

Velocity patterns under selected tidal conditions were generated and results were stored for necessary use. Computation and analysis of bed shear stress patterns were used with the velocities to estimate where and by how much sediment deposition was expected to occur. The sediment depositing in the channel was presumed to be noncohesive sediment. Hence, only this type of sediment was taken into account for the study.

Three alternatives of sediment trap configuration were examined with the model:

a. A sand trap proposed by the Galveston District was studied first.

b. The location, shape, size, and depth of a sand trap based on intuition and experience were tested as the second alternative.

c. Based on the results of the first layout, configuration of final layout was evolved for recommendation.

Approach

The hydrodynamic model code RMA2 (see Appendix A), available at ERDC, CHL was used to calculate the hydrodynamics of the system. The area

included in the model was decided in consultation with the Galveston District. Grid generation for the selected area (Figure 3) (SMS 1995) was prepared by using the Surface Water Modeling System (Brigham Young University 1995). Bathymetry of the entire area is shown in Figure 4. Bathymetry of the Rollover Bay area is shown in Figure 30. The model generated flow patterns under the same tidal conditions for which field data were collected. Verification of the model was based on the available field data for tides and current velocities. Results of the hydrodynamic model were used to analytically estimate the effect of currents on sediment transport.

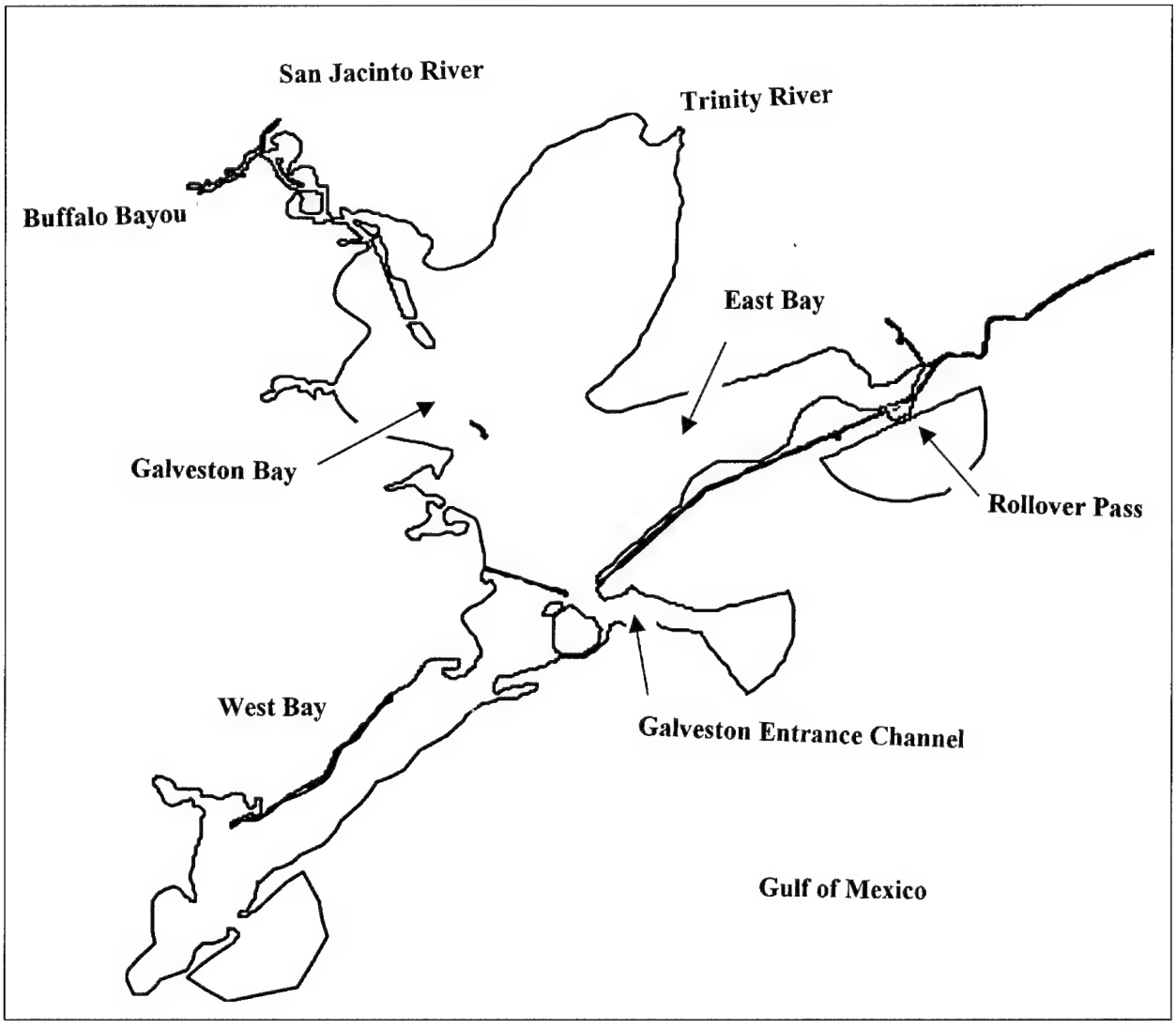

Figure 3. Grid used for hydrodynamic numerical model of Rollover Pass

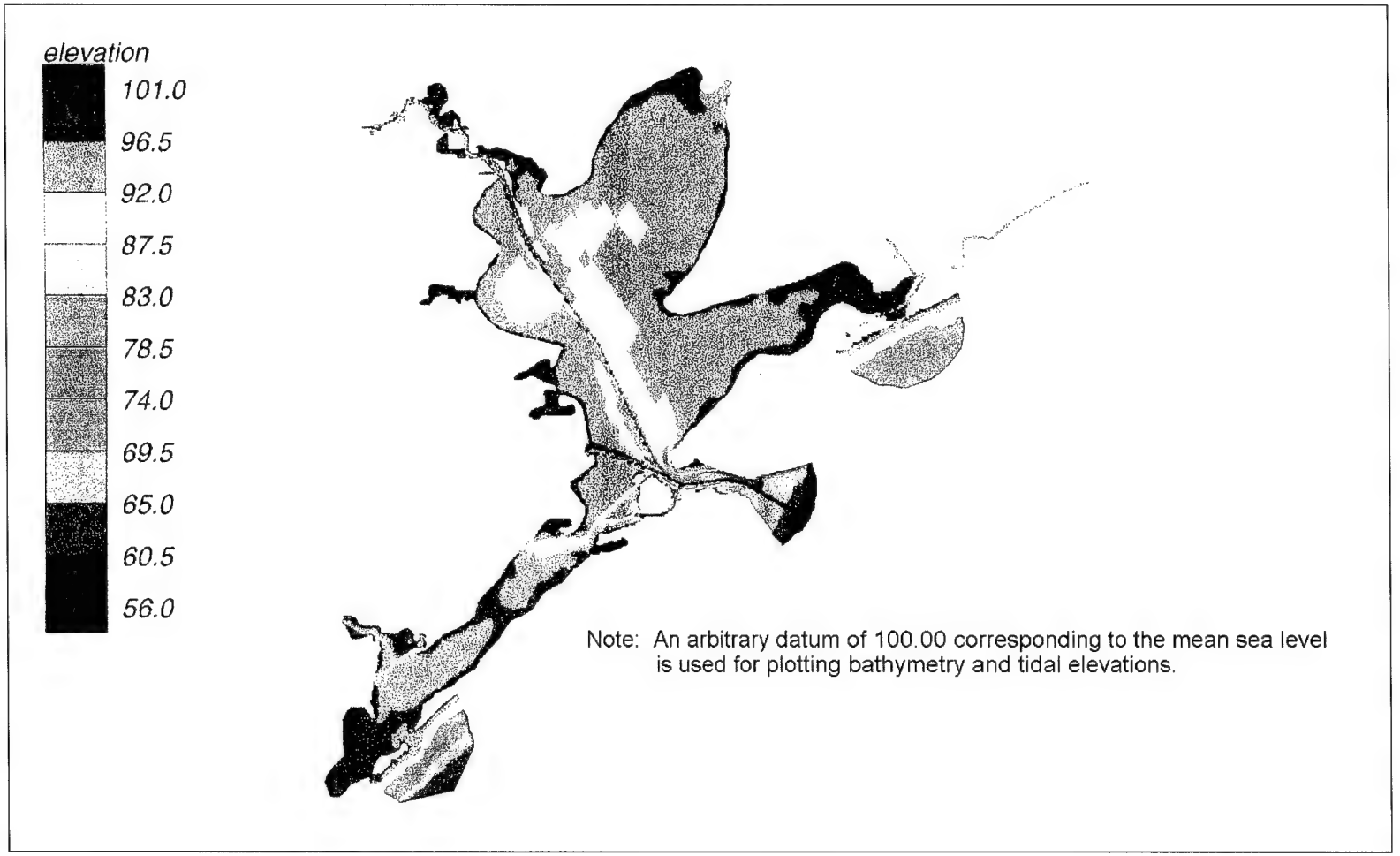

Figure 4. Bathymetry of the numerical model area (Elevation is in feet. To convert feet to meters, multiply by 0.3048)

2 Field Data Analysis

Introduction

ERDC, CHL conducted field investigations in the area in 1994 in the context of numerical model investigations related to Houston-Galveston navigation channels. These data were collected only for the Galveston Bay area and did not extend to the East Bay area, which is the area of interest for the present study. Hence ERDC, CHL collected additional field data in 1999. The data included a hydrographic survey of East Bay and Rollover Bay, tide and velocity data, and water and sediment samples. Field data available from the SWG consisted of cross sections of GIWW measured before dredging and after dredging during the years 1995, 1997, and 1999. The cross sections were taken at every 61-m-(200-ft-) interval. The District also supplied data on the locations of sections, quantities of dredging, and frequency of dredging. All these data were analyzed and results have been used in this report.

Tides

ERDC, CHL made tidal measurements at the Rollover Bay and Rollover Pass area during March 1999. The results are contained in a ERDC, CHL Memorandum for Record (MFR). [1]

Four locations were established in the study area for obtaining water level changes during the data collection period. Three locations (TG1, TG2, and TG3) are shown in Figure 5. The fourth gauge (TG4) was located in the western part of East Bay. No data were obtained at location TG1 because of the loss of the water level recorder. This recorder was positioned on a temporary platform placed near the shoreline along the GIWW. The platform and recorder were lost after apparently being hit by a passing towboat. Also, the water level recorder at location TG2 in the GIWW developed internal recording problems and data recording failed without warning immediately after deployment. Two water level recorders (A and B) were installed at location TG3 to ensure data recovery

[1] Fagerburg, T. L. (1999). Memorandum for Record. "Field data collection at Rollover Bay and Gulf Intracoastal Waterway, Galveston, TX," CEERD-HE-TH, Research Hydraulics Engineer, Hydraulic Analysis Group, Tidal Hydraulics Branch, Coastal and Hydraulics Laboratory.

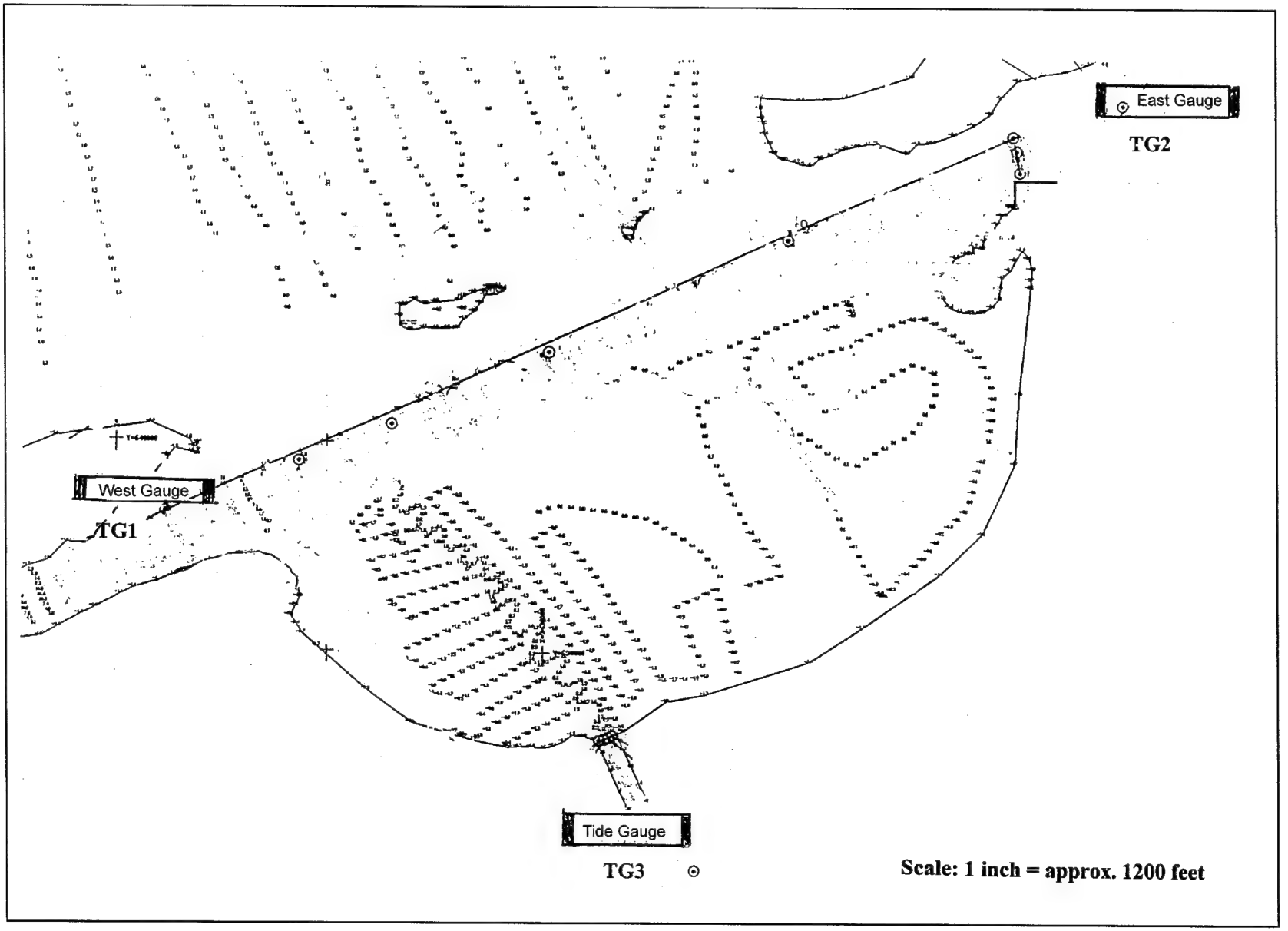

Figure 5. Locations of tide gauges installed in field (To convert feet to meters, multiply by 0.3048)

in the event one of the recorders failed. During the data collection period, the first recorder (TG3A) at location TG3 provided a full deployment record of the data shown in Figure 6. The second recorder (TG3B) at this location malfunctioned and stopped recording data within two days after installation (Figure 7). Tidal data collected at location TG4 are shown in Figure 8. Observed tides at TG3 and TG4 over the period 16-17 March 1999 are shown in Figures 9 and 10, respectively. The water level elevations have been corrected to the mean low tide (mlt) for Galveston Bay.

Fischer (1972) mentioned that strong northerly (coming from the north) or offshore winds tend to push water out of the bays and marshes around Rollover Pass. Because of this effect, ebb tides and flows through Rollover Pass are amplified and flood tides and flows are reduced during northerly winds. Prior to the data collection effort, an extended period of wind coming from the north produced low tide conditions in the bay area which simultaneously resulted in shallow water conditions in East Bay. These shallow depth conditions prevented deployment of the water level recorder at location 4 until the water levels returned to normal. The original plans were to have all the water level recorders installed 15 to 30 days prior to the start of the data collection effort.

Ocean tides in the study area are predominantly diurnal with a relatively small drop in water level near high-water stage, giving two high-water values. The diurnal tidal range is small, varying from 0.46 to 0.67 m (1.5 to 2.2 ft). Local wind is known to have a substantial effect on the water levels in the Rollover Bay area. When strong wind blows towards the north, sea water piles up in the Rollover Bay, whereas when the wind blows towards the south, the bay gets partially emptied and shallow areas are exposed above water level.

Currents

ERDC made velocity measurements at the Rollover Bay and Rollover Pass areas during March 1999. The results are contained in an ERDC, CHL MFR.[1]

The measurements were made at six ranges labeled 1, 2, 3, 4, 5, and 40 (Figure 11). Current data were obtained by using Acoustic Doppler Current Profiler (ADCP) equipment. The measurements showed that the maximum velocity magnitude at Range 1 in Rollover Pass (see Figure 11 for location) was 0.79 m/s (2.6 ft/s). Location of corresponding node in the numerical hydrodynamic model is shown in Figure 12, and the current velocity obtained at the location is shown in Figure 13. It is seen from this figure that the maximum velocity in the numerical model was also on the same order of magnitude (2.6 to 2.8 ft/s) with the exception of one peak, which had a magnitude of 3.1 ft/s. The maximum velocity at Range 5 near the entrance to the East Bay was 2.5 ft/s. The maximum velocity in GIWW was 4 ft/s.

The ADCP field measurements were also used for plotting velocity contours as illustrated in Figure 14. Since the numerical hydrodynamic model was a

[1] Fagerburg (1999), op cit.

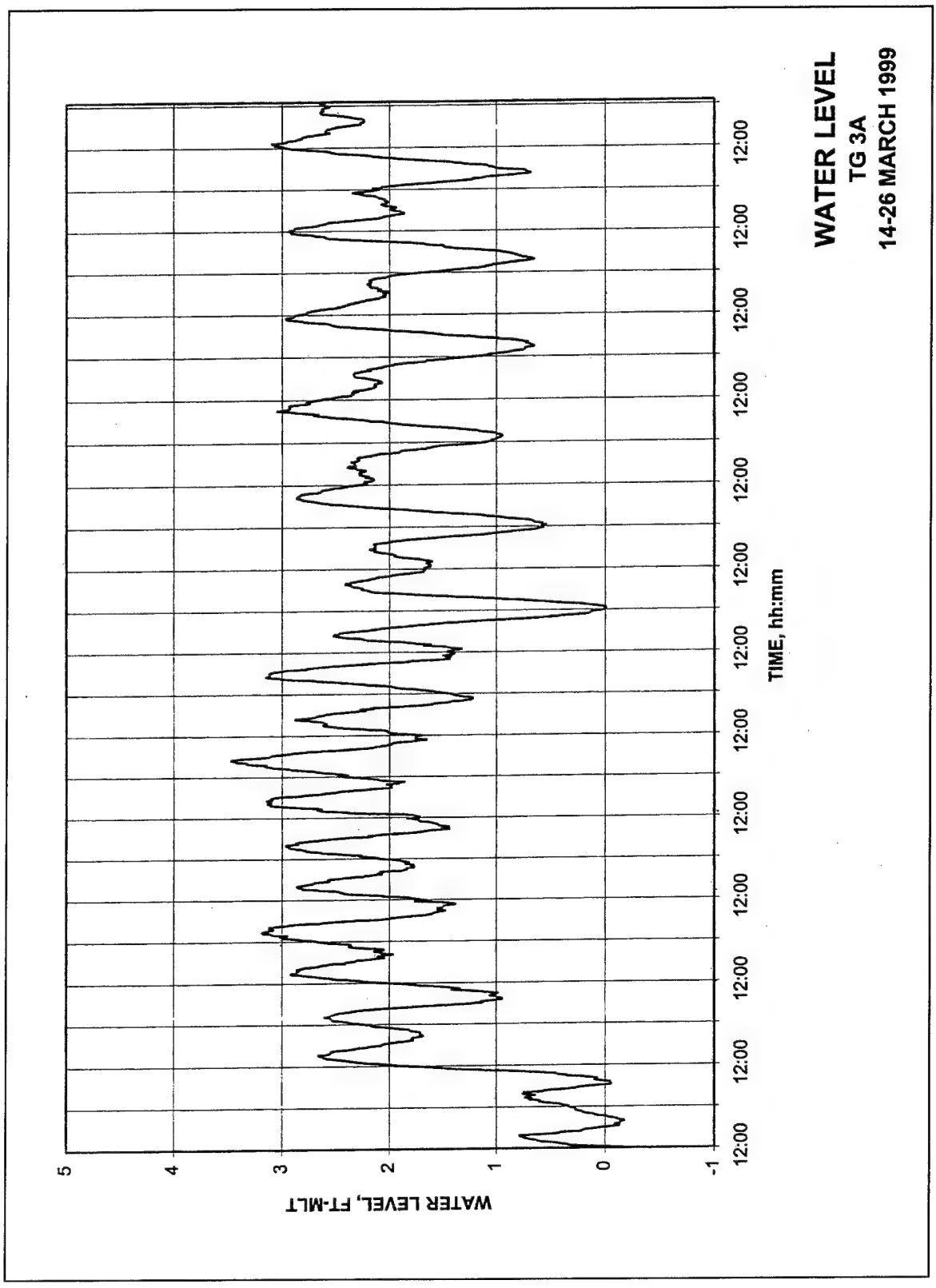

Figure 6. Observed tides at TG3A (14-26 March 1999) (Water level is in feet. To convert feet to meters, multiply by 0.3048)

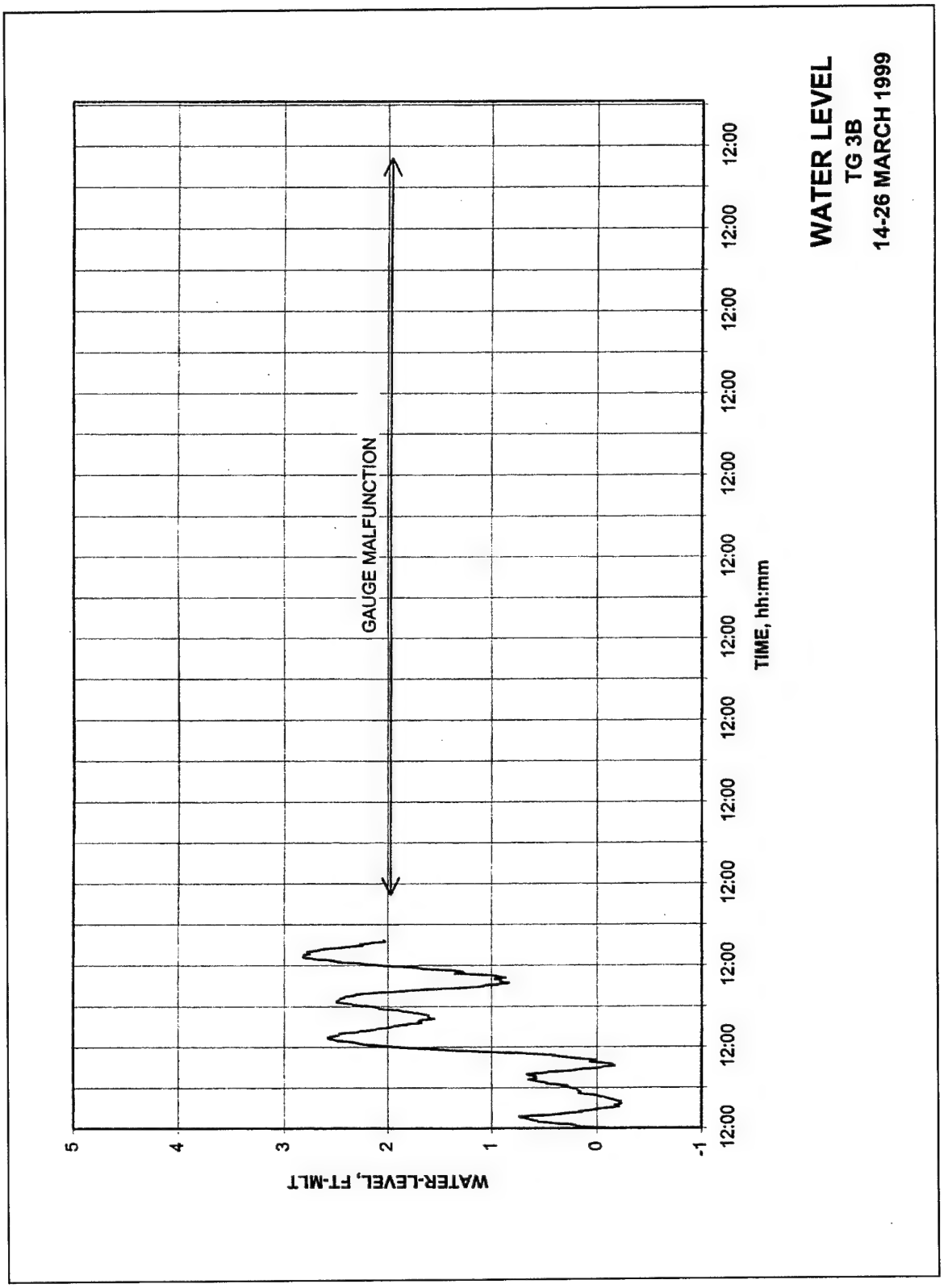

Figure 7. Observed tides at TG3B (14-26 March 1999) (Water level is in feet. To convert feet to meters, multiply by 0.3048)

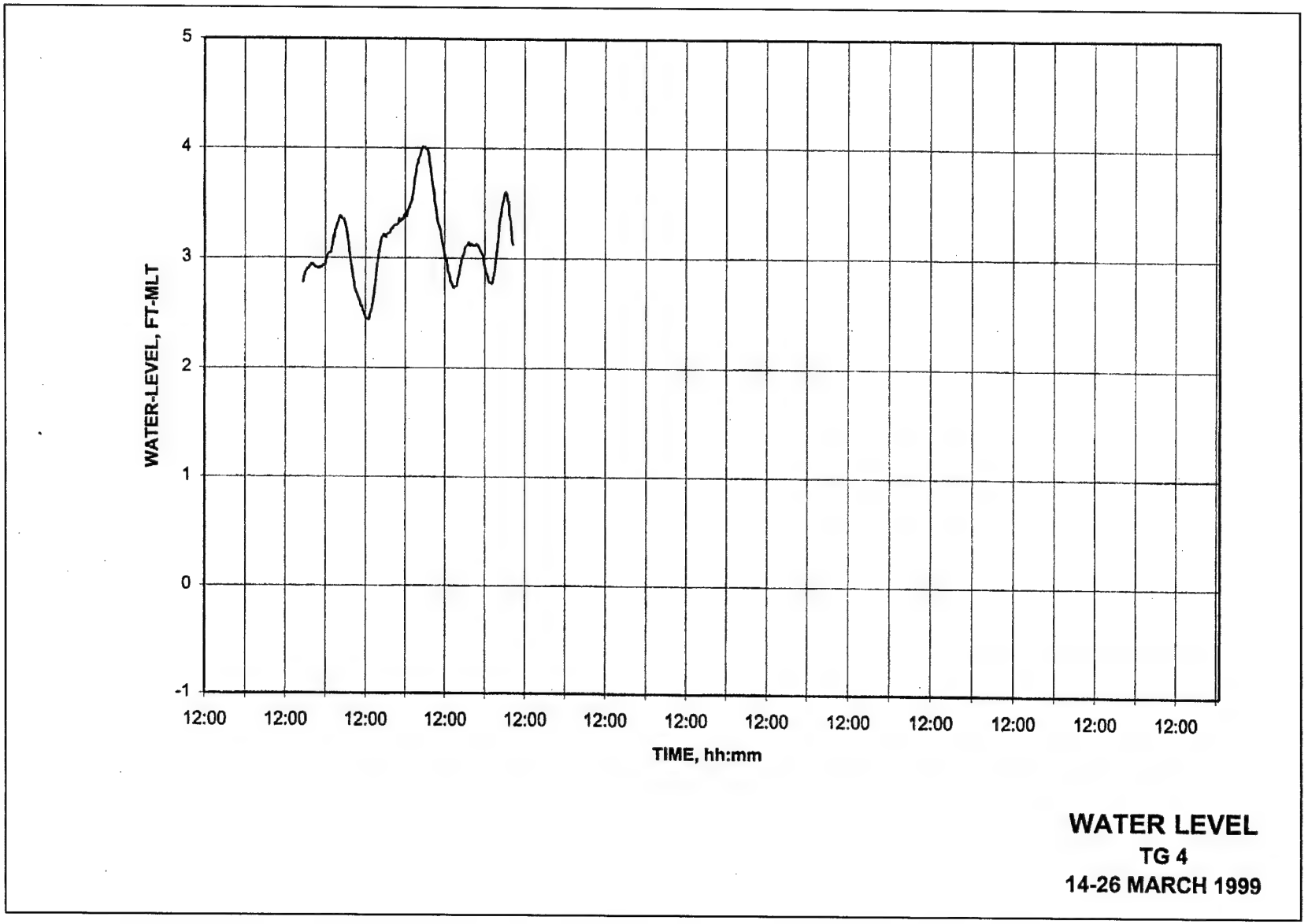

Figure 8. Observed tides at TG4 (14-26 March 1999) (Water level is in feet. To convert feet to meters, multiply by 0.3048)

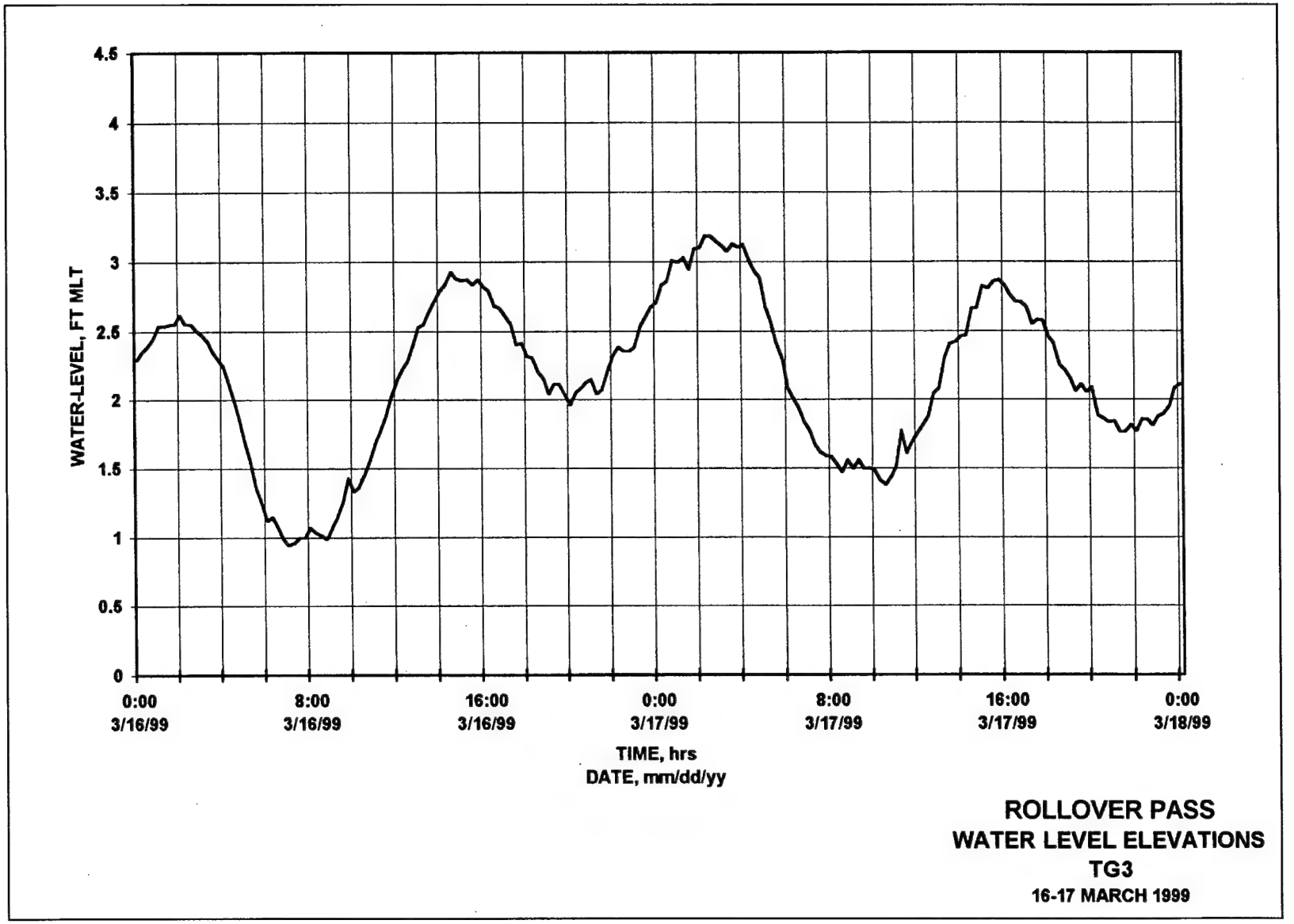

Figure 9. Observed tides at TG3 (16-17 March 1999) (Water level is in feet. To convert feet to meters, multiply by 0.3048)

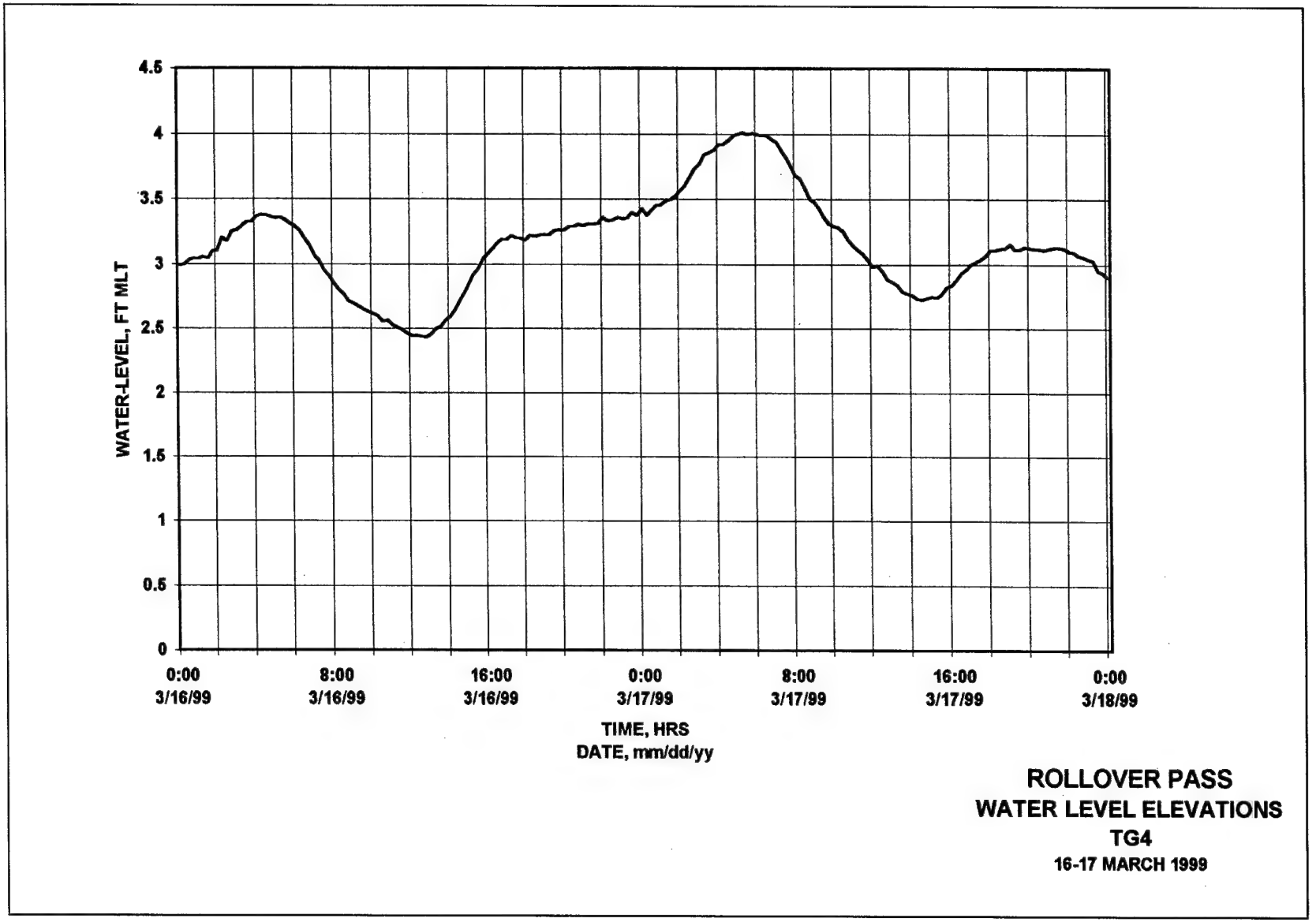

Figure 10. Observed tides at TG4 (16-17 March 1999) (Water level is in feet. To convert feet to meters, multiply by 0.3048)

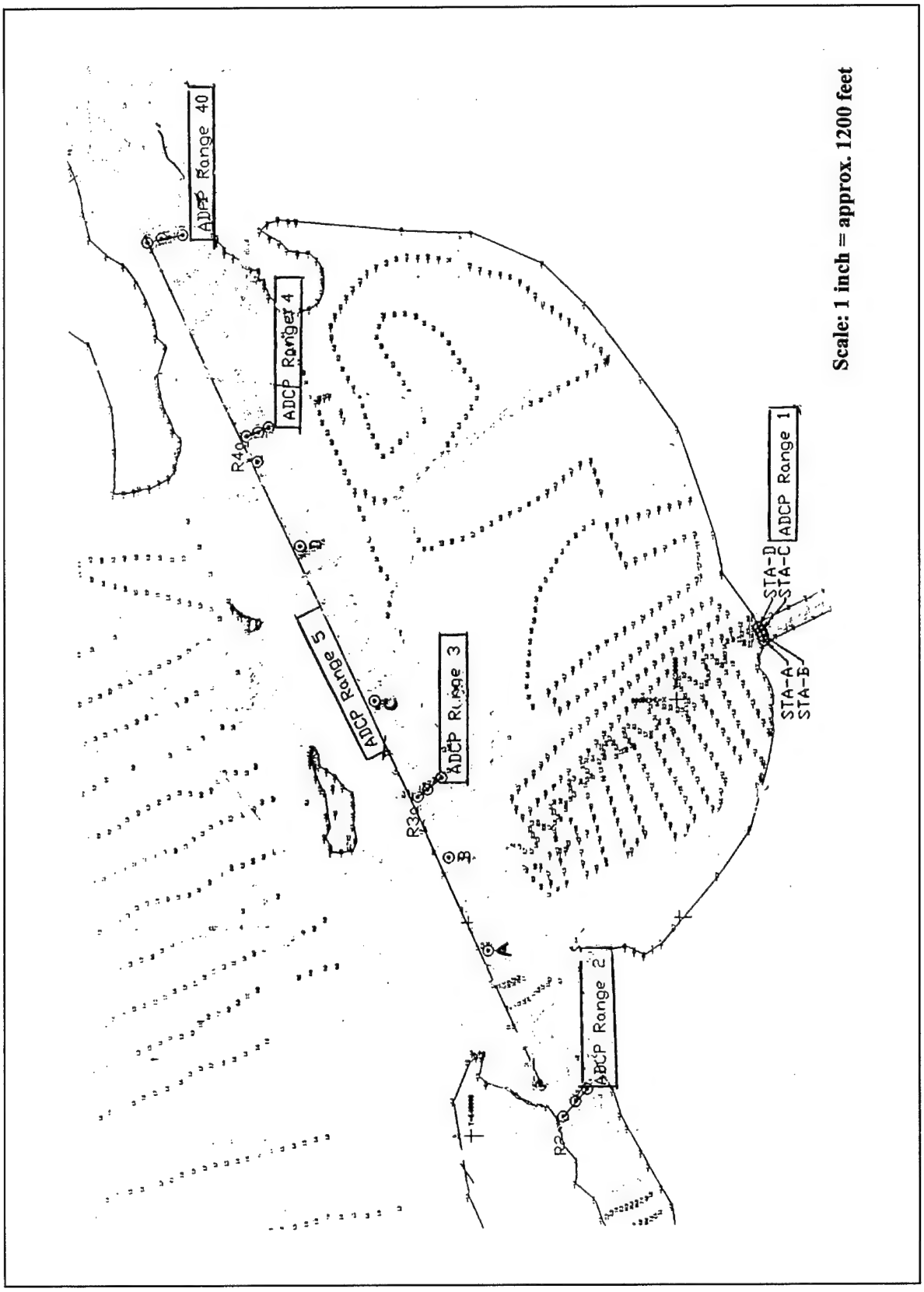

Figure 11. Locations of ADCP data collection transects (To convert feet to meters, multiply by 0.3048)

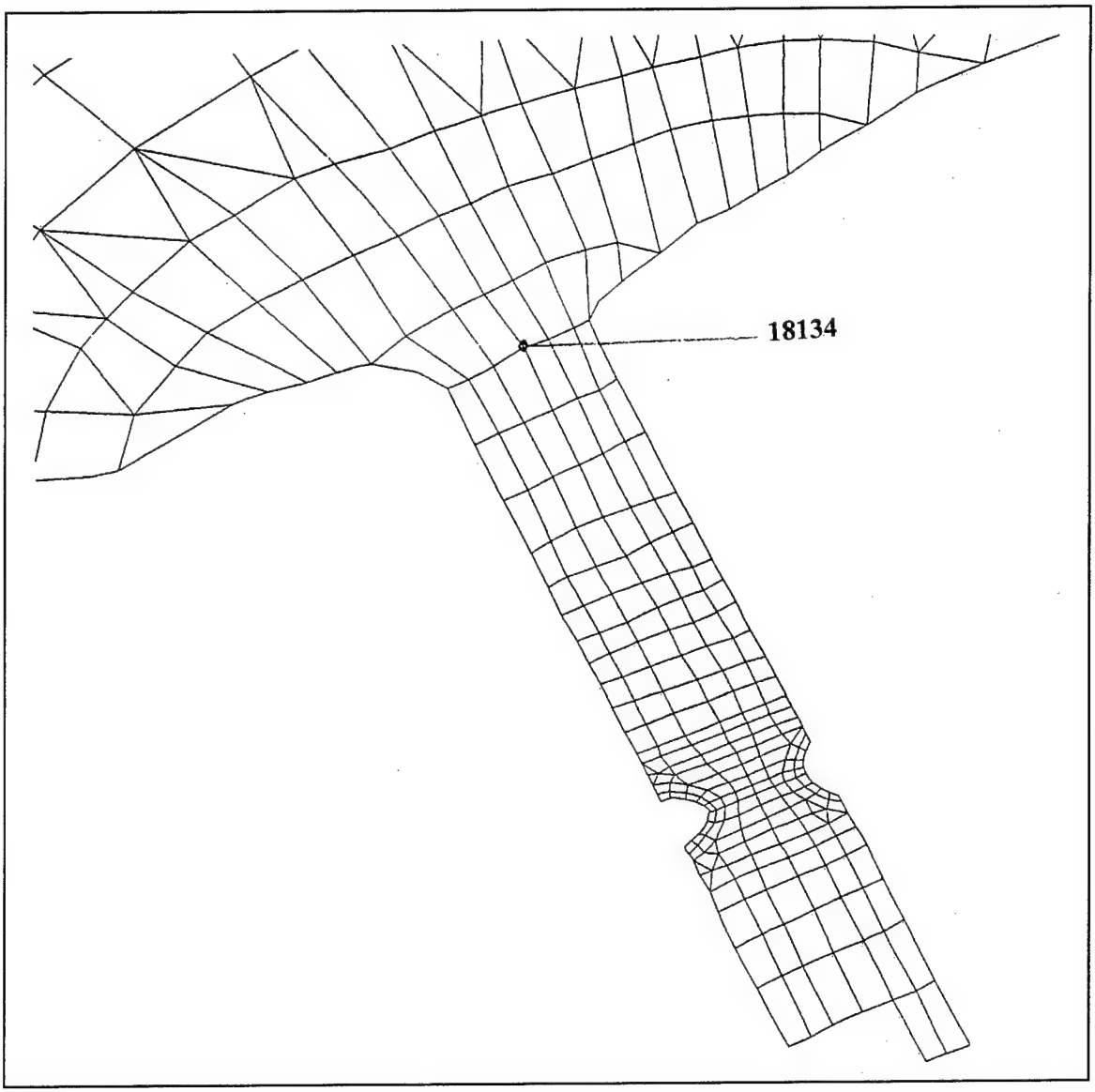

Figure 12. Location of model node 18134

vertically averaged two-dimensional model, such data could not be obtained on the model.

Dredging

Dredging data available from the Galveston District for the GIWW area were supplied to ERDC for the years 1997 and 1999. The data were supplied in the form of cross sections of the navigation channel maintained by the District within the GIWW. Illustrations of cross sections for 1997 and 1999 are shown in Figures 15 and 16, respectively. The locations of cross sections are shown in Figure 17. The sections, which are 61 m (200 ft) apart from each other, were supplied for the "before-dredging" status measured May 29, 1997, and again on

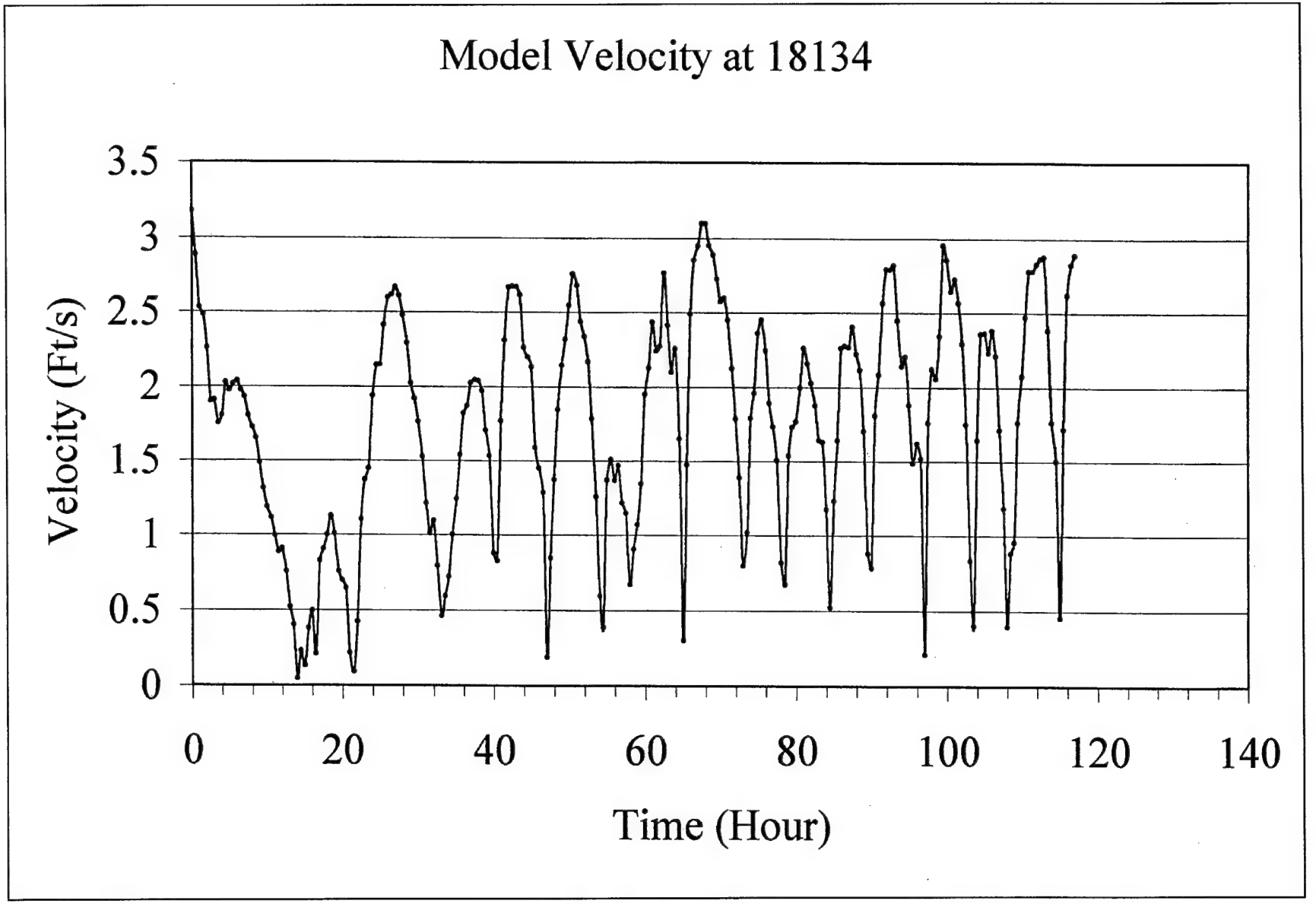

Figure 13. Model velocity at node 18134 (Velocity is in feet per second. To convert feet to meters per second, multiply by 0.3048)

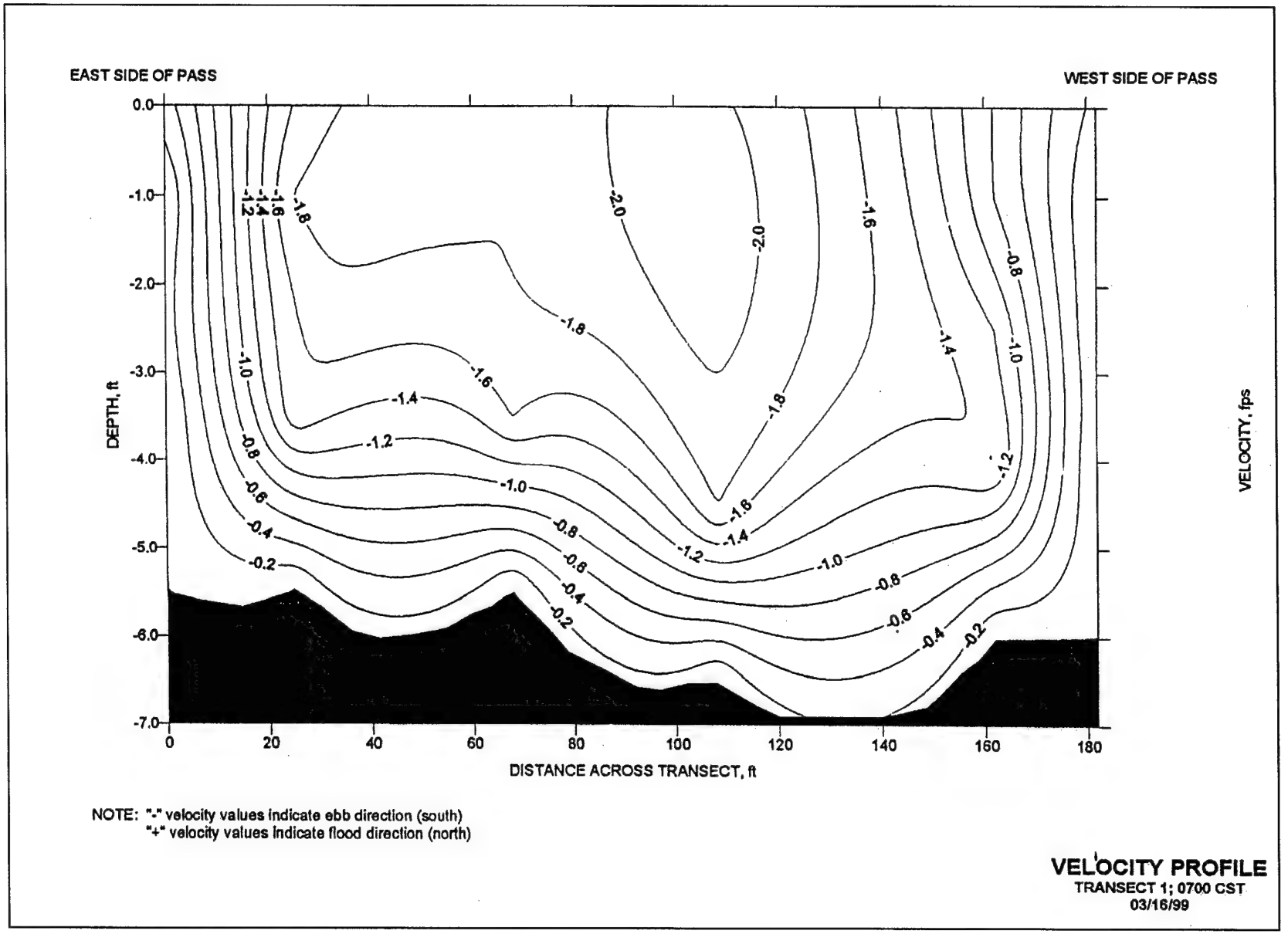

Figure 14. Illustration of velocity profile measured in field at Transect 1 (Velocity is in feet per second. To convert feet to meters, multiply by 0.3048)

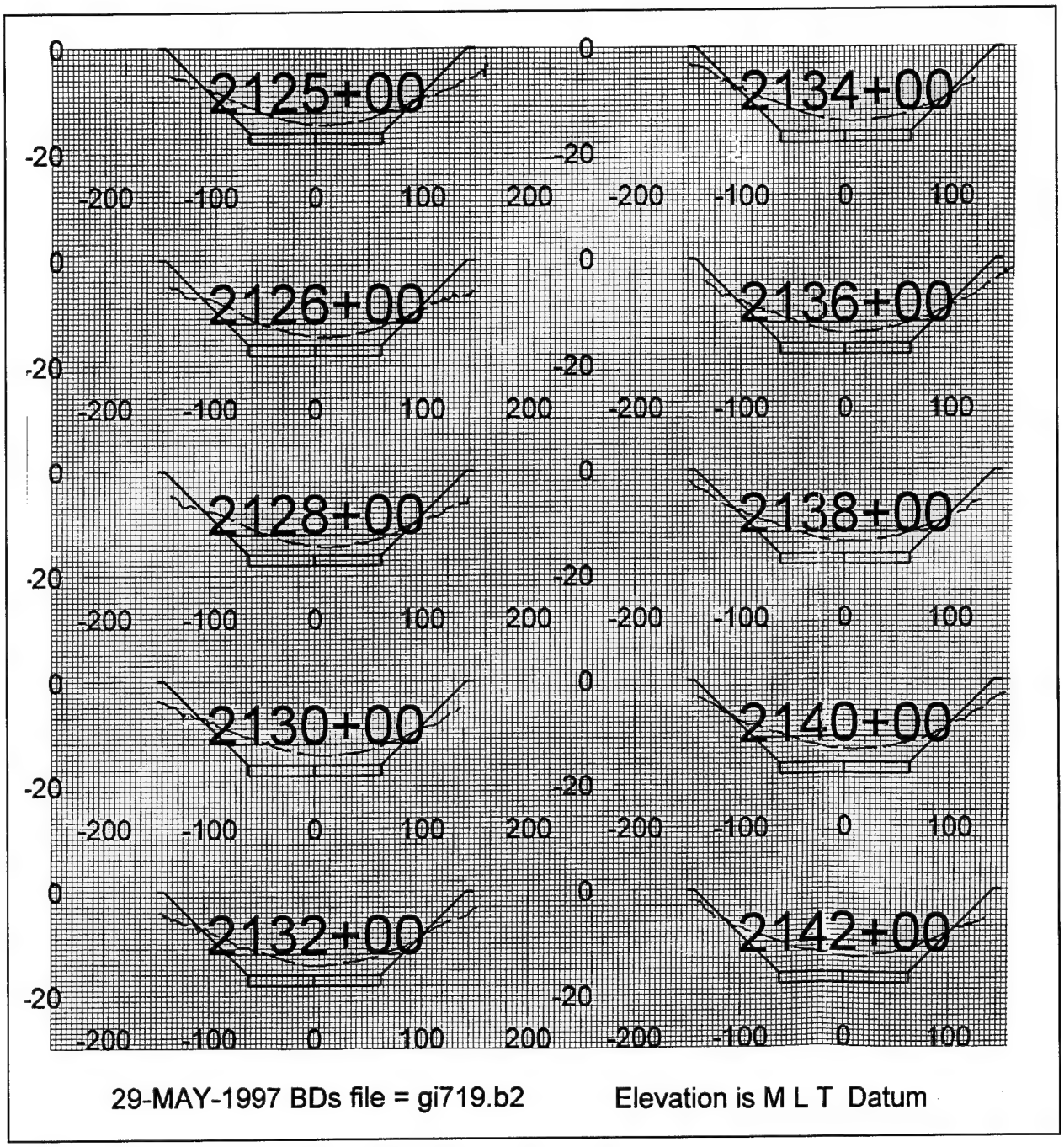

Figure 15. Illustration of bed profile measurements in GIWW (29 May 1997) (All dimensions are in feet. To convert feet to meters, multiply by 0.3048)

January 9, 1999. The cross sections supplied for the "after-dredging" conditions were measured June 18, 1997, and February 24, 1999. Both the "after-dredging" sections show that dredging restored the entire trapezoidal "template" cross sections and in addition, excess dredging was done across the bottom width to a bed level of 5.48 m (-18 ft). These trapezoidal sections get partially filled as a result of siltation. The quantity of sediment accumulated within the trapezoidal sections was computed using the cross sections for the "after-dredging" status.

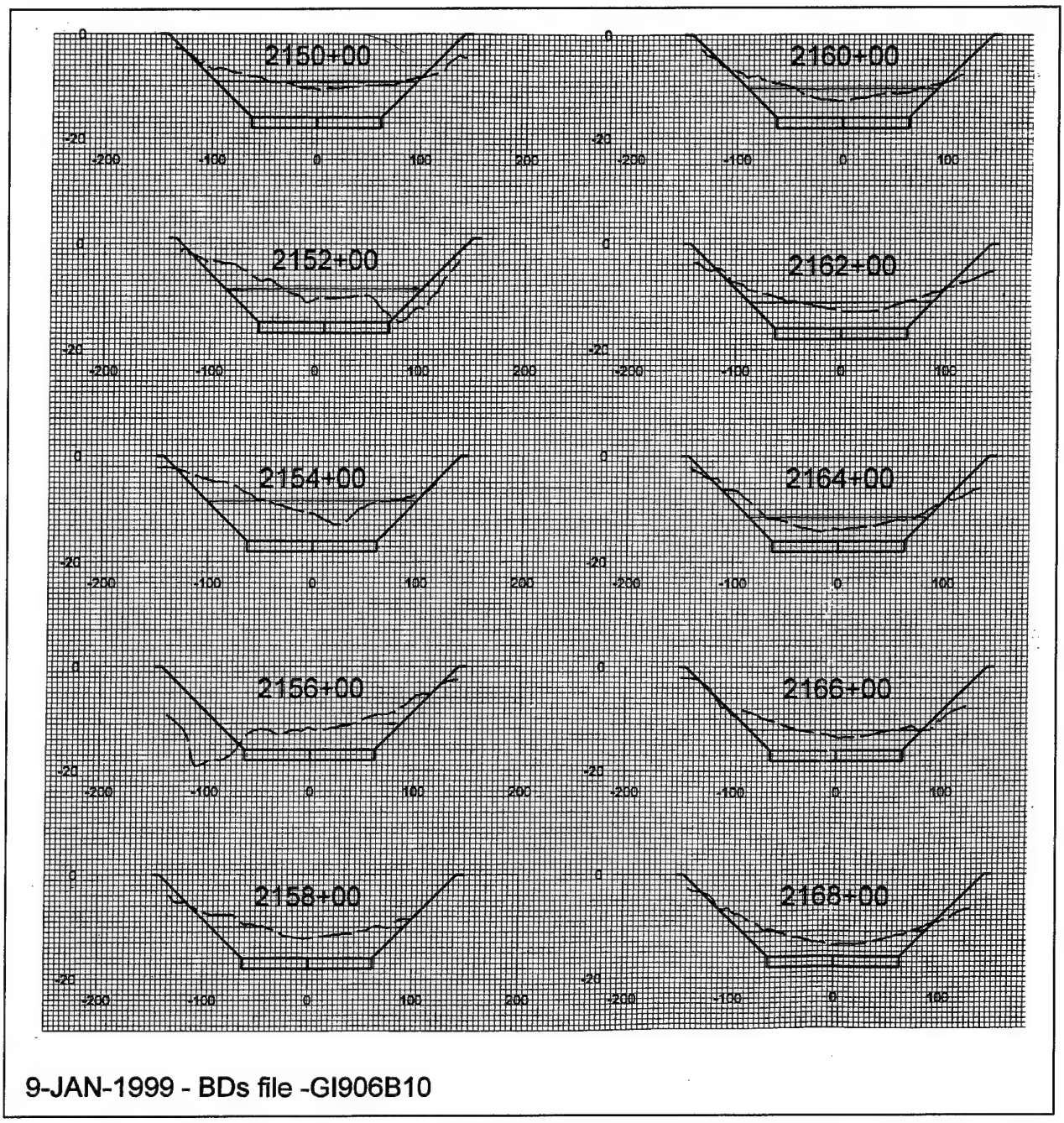

Figure 16. Illustration of bed profile measurements in GIWW (9 January 1999) (All dimensions are in feet. To convert feet to meters, multiply by 0.3048)

Since the sections were 61 m (200 ft) apart, volume of sediment deposited within each 61-m- (200-ft-) long-reach of the GIWW could be computed. Before June 1997, dredging was done in May 1995. Hence, computations give volume of sediment accumulated during a two-year period from May 1995 to May 1997. Dredging data also provided information that no dredging was done between May 1997 and February 1999. Hence, computations give sediment accumulated from May 1997 until January 1999.

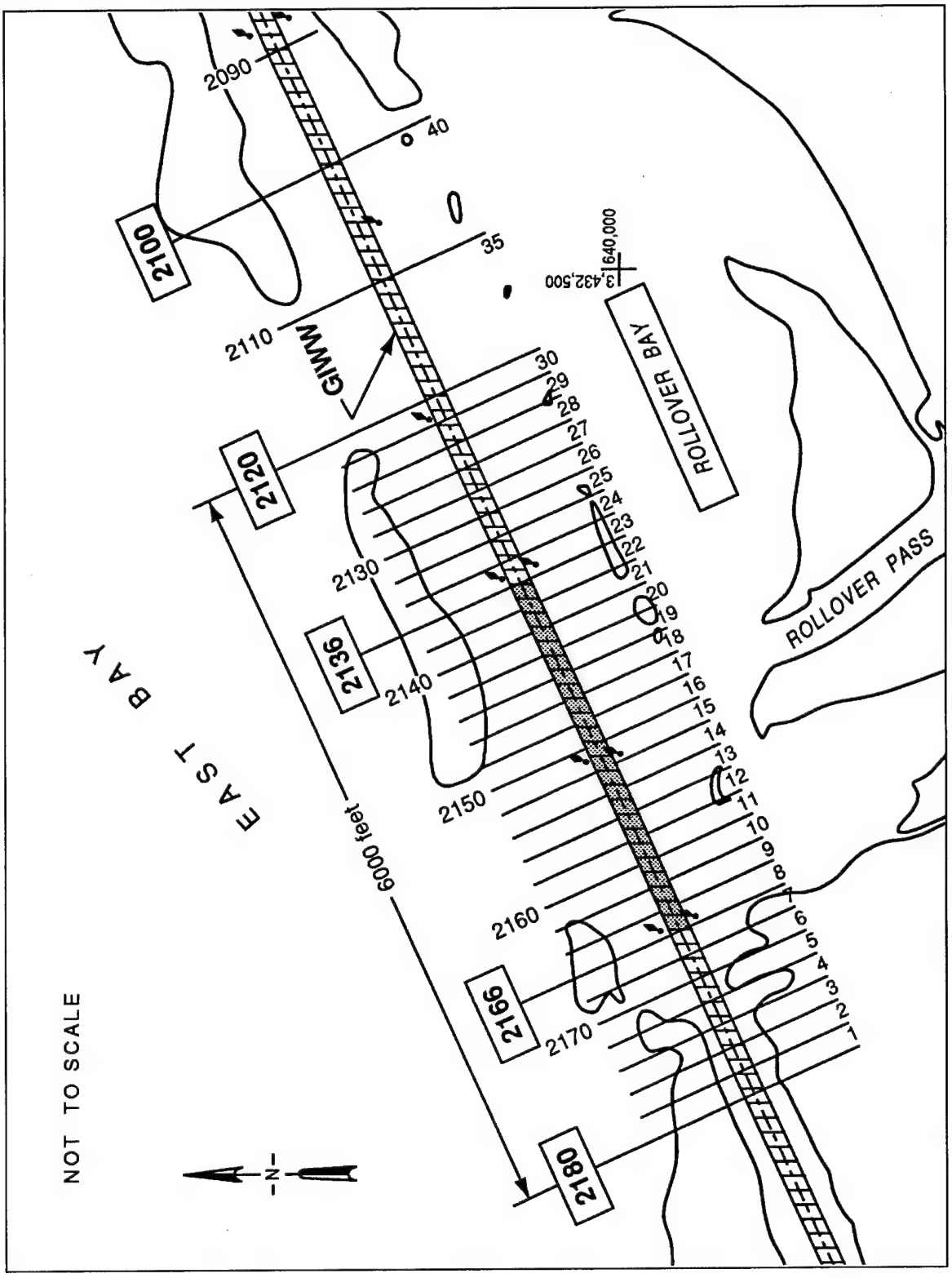

Figure 17. Location of transects for bed profile measurements (To convert feet to meters, multiply by 0.3048)

All the cross sections are plotted "looking west." Hence, the left side bank on the map of cross sections represents the slope on the entrance side of GIWW whereas the right side of cross sections represents slope on the East Bay side. An examination of the sections shows that the sediment-water interface within the navigation channel is curved like the shape of a bowl for most of the sections. This may be an indication that the sections are filled from both sides and sediment appears to have entered the navigation channel by sliding over the slopes predominantly as bed load. However, it is also possible that the shape of bed profile has evolved from the combined action of longitudinal tidal currents within GIWW and the action of propellers of vessels navigating in GIWW.

Table 1 shows the volume of sediment deposited between each two adjacent cross sections for the years 1995 to 1997 and for 1997 to 1999. The values are given for the reach of GIWW that lies within Rollover Bay, namely section 2100 to section 2180 (see Figure 17 for locations). This zone is denoted as A-A in Table 1. The computed volumes are plotted in Figure 18. It is seen that Zone A-A has a base accumulation on the order of 4,302 cu m (152,000 cu ft) between each two consecutive sections 61 m (200 ft) apart.

For convenience of reference, different reaches of the GIWW are denoted under the following four zones: A-A: Sections 2180 to 2100; B-B: Sections 2166 to 2100; C-C: Sections 2180 to 2120; D-D: Sections 2166 to 2136 (Figure 17).

It is noted from Table 1 that the measured dredging data are not fully available for both periods over the entire reach between Sections 2100 and 2180. Hence, the missing data were filled by picking up values from the column where data are available. Table 2 gives "estimated" quantities of sediment accumulation in Zone D-D. Table 3 gives measured sediment accumulation in Zone D-D, the reach of GIWW between Sections 2136 (serial number 22) and 2166 (serial number 8). Table 4 gives percentage of sediment accumulation in Zone D-D with respect to siltation in Zone A-A. It is noted that Zone D-D of the GIWW catches about 45 percent of sediment depositing in Zone A-A from Section 2100 to 2180. Table 5 gives excess siltation in Zone D-D relative to the siltation in other reaches of the GIWW. The quantity is on the order of 22,640 cu m (800,000 cu ft). If a sand trap could collect at least this volume before it reaches the GIWW, then excessive local shoaling in Zone D-D can be reduced, which will result in reduced frequency of dredging and hence, a reduced maintenance cost. Zone D-D between Sections 2136 and 2166 is therefore selected for locating the sediment trap.

Bed Sediment

Bottom sediment samples were collected at each ADCP transect using a clamshell bottom sediment sampler. The locations of transects are shown in Figure 19. The bed samples were brought to ERDC for determining grain size distribution. The results are given in ERDC, CHL MFR.[1]

[1] Fagerburg (1999), op cit.

Table1
Measured Siltation in Zone A-A of GIWW (1995-1997) and (1997-1999)

Zone	Sections	Element #	Zone	1995 - 1997	Zone	1997 - 1999
A-A	2178-80	1			C-C	141,000
	2176-78	2				141,874
2180	2174-76	3			2180	141,874
To 2100	2172-74	4			To	141,000
	2170-72	5			2120	169,250
	2168-70	6				197,500
	2166-68	7				180,750
	2164-66	8	B-B	165,000		165,000
	2162-64	9	2166	184,250		181,750
	2160-62	10	To	217,750		207,500
	2158-60	11	2100	216,500		225,250
	2156-58	12		183,000		215,250
	2154-56	13		181,750		243,750
	2152-54	14		235,750		270,750
	2150-52	15		253,500		261,000
	2148-50	16		217,750		253,250
	2146-48	17		217,750		236,000
	2144-46	18		233,000		226,750
	2142-44	19		233,000		207,500
	2140-42	20		215,250		181,750
	2138-40	21		180,750		166,000
	2136-38	22		165,000		166,000
	2134-36	23		166,000		166,000
	2132-34	24		166,000		165,000
	2130-32	25		166,000		164,000
	2128-30	26		166,000		164,000
	2126-28	27		166,000		164,000
	2124-26	28		166,000		164,000
	2122-24	29		165,000		164,000
	2120-22	30		165,000		164,000
	2118-20	31		165,000		
	2116-18	32		164,000		
	2114-16	33		164,000		
	2112-14	34		165,000		
	2110-12	35		166,000		
	2108-10	36		165,000		
	2106-08	37		129,000		
	2104-06	38		134,000		
	2102-04	39		134,000		
	2100-02	40		134,000		
		Total (cu ft)		5,946,000 cu ft		5,635,748 cu ft

Note: All siltation quantities are in cubic feet. To convert feet to meters, multiply by 0.3048.

Sediments from Transects R2 and R3 (see Figure 19 for locations) can be classified as medium to fine sand with minor fractions of clays. Sediments from Transect R4 were found to have significantly higher silt contents. Transect R5 was taken parallel to the GIWW and was located just north of GIWW. Sediments along Transect R5 were varied. Sediments in one segment of this transect were mostly medium to fine sands as found at Transects R2 and R3, while in another section of the transect significantly higher silt contents were found. Other bottom samples were obtained during the bathymetric survey of the eastern portion of East Bay. Locations of these samples are shown in Figure 20. The sediments from the East Bay area are generally uniform in composition and classified as fine sands with considerable silt content.

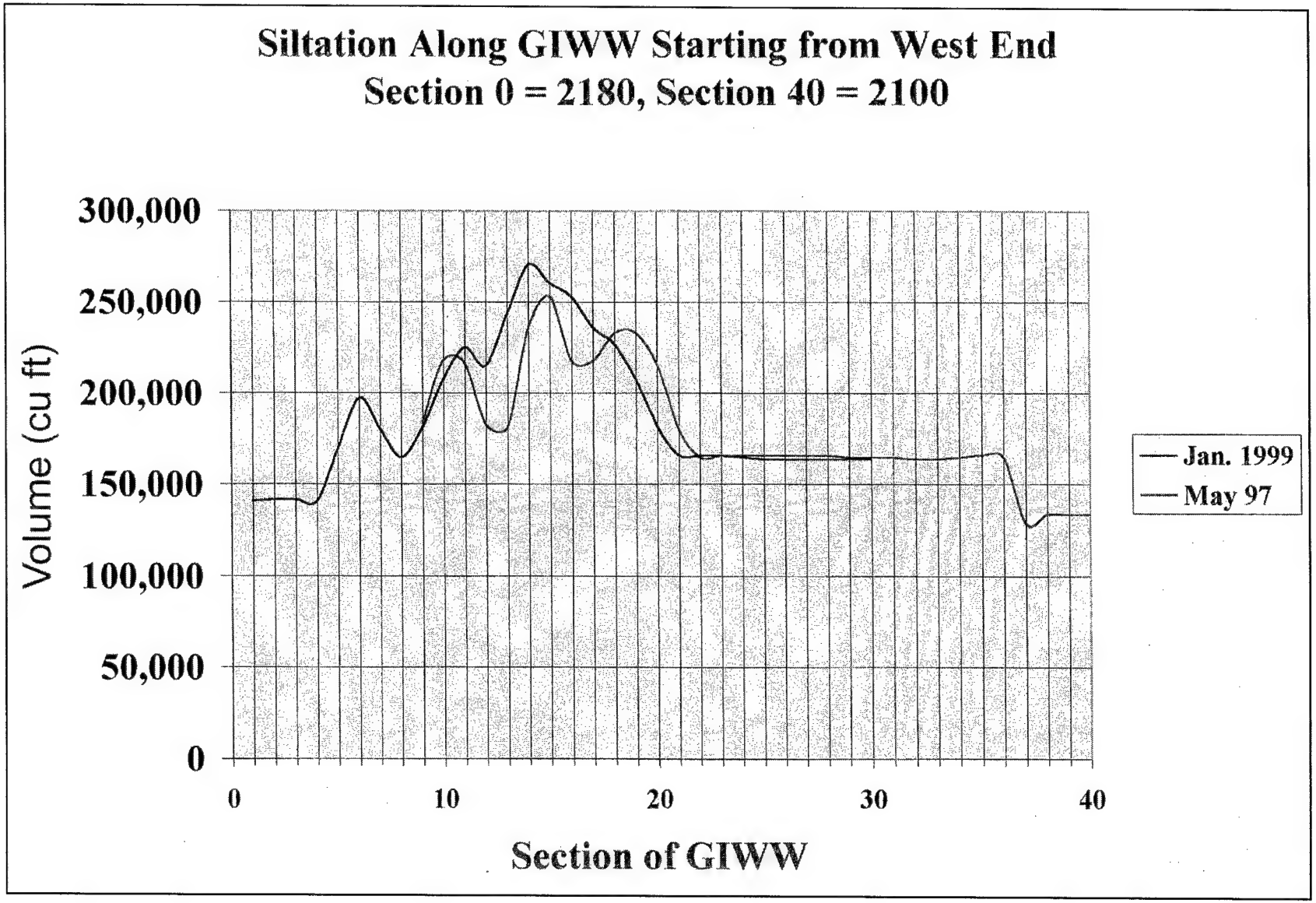

Figure 18. Computed volumes of sediment accumulation in GIWW (Volume is in cubic feet. To convert to cubic meters, multiply cubic feet by 0.3048)

Table 2
Estimated Siltation in GIWW (1995-1997) and (1997-1999)

Zone	Sections	Element #	1995 - 1997	1997 - 1999
A-A	2178-80	1	141,000	141,000
	2176-78	2	141,874	141,874
2180	2174-76	3	141,874	141,874
To	2172-74	4	141,000	141,000
2100	2170-72	5	169,250	169,250
	2168-70	6	197,500	197,500
	2166-68	7	180,750	180,750
	2164-66	8	165,000	165,000
	2162-64	9	184,250	181,750
	2160-62	10	217,750	207,500
	2158-60	11	216,500	225,250
	2156-58	12	183,000	215,250
	2154-56	13	181,750	243,750
	2152-54	14	235,750	270,750
	2150-52	15	253,500	261,000
	2148-50	16	217,750	253,250
	2146-48	17	217,750	236,000
	2144-46	18	233,000	226,750
	2142-44	19	233,000	207,500
	2140-42	20	215,250	181,750
	2138-40	21	180,750	166,000
	2136-38	22	165,000	166,000
	2134-36	23	166,000	166,000
	2132-34	24	166,000	165,000
	2130-32	25	166,000	164,000
	2128-30	26	166,000	164,000
	2126-28	27	166,000	164,000
	2124-26	28	166,000	164,000
	2122-24	29	165,000	164,000
	2120-22	30	165,000	164,000
	2118-20	31	165,000	165,000
	2116-18	32	164,000	164,000
	2114-16	33	164,000	164,000
	2112-14	34	165,000	165,000
	2110-12	35	166,000	166,000
	2108-10	36	165,000	165,000
	2106-08	37	129,000	129,000
	2104-06	38	134,000	134,000
	2102-04	39	134,000	134,000
	2100-02	40	134,000	134,000
		Total (cu ft)	7,059,248	7,155,748

Note: All siltation quantities are in cubic feet. To convert feet to meters, multiply by 0.3048.

An average median diameter size of surface sediment samples is shown in Figure 19. It is seen from this figure that the sediment within Sections 2136 and 2166 is much coarser than the sediment outside this reach. This is an indication that this reach catches more of the sand and silt, presumably transported from the sea. These data again confirm that the site for locating the sediment trap should be between Sections 2136 and 2166.

Table 3
Measured Sediment Accumulation in Zone D-D of GIWW Between Sections 2136 and 2166

Zone	Section	Element #	1995 - 1997	1997 - 1999
D-D			Volume (cu ft)	Volume (cu ft)
2166 To 2136	2164-66	8	165,000	165,000
	2162-64	9	184,250	181,750
	2160-62	10	217,750	207,500
	2158-60	11	216,500	225,250
	2156-58	12	183,000	215,250
	2154-56	13	181,750	243,750
	2152-54	14	235,750	270,750
	2150-52	15	253,500	261,000
	2148-50	16	217,750	253,250
	2146-48	17	217,750	236,000
	2144-46	18	233,000	226,750
	2142-44	19	233,000	207,500
	2140-42	20	215,250	181,750
	2138-40	21	180,750	166,000
	2136-38	22	165,000	166,000
		Total (cu ft)	3,100,000	3,207,500

Note: All siltation quantities are in cubic feet. To convert feet to meters, multiply by 0.3048.

Table 4
Percentage of Sediment Accumulation in "High Siltation Zone" Relative to Total Siltation in Rollover Pass Reach of GIWW

Zone	Section # From - To	1995 - 1997	1997 - 1999
		Estimated Cumulative Volume (cu ft)	Estimated Cumulative Volume (cu ft)
A-A	2180 to 2100	7,059,248	7,155,748
D-D	2166 to 2136	3,100,000	3,207,500
	Percentage of Siltation in Zone D-D to Zone A-A	43.91 %	44.82 %

Note: All siltation quantities are in cubic feet. To convert feet to meters, multiply by 0.3048.

Table 5
Excess Siltation in "High Siltation Zone" D-D Relative to Siltation in Other Reach of GIWW

Zone D-D From 2166 To 2136	1995 - 1997	1997 - 1999
	Estimated Cumulative Volume (cu ft)	Estimated Cumulative Volume (cu ft)
Actual siltation	3,100,000	3,207,500
Based on average siltation	2,375,550	2,368.950
Excess siltation	724,450	838,550

Note: All siltation quantities are in cubic feet. To convert feet to meters, multiply by 0.3048.

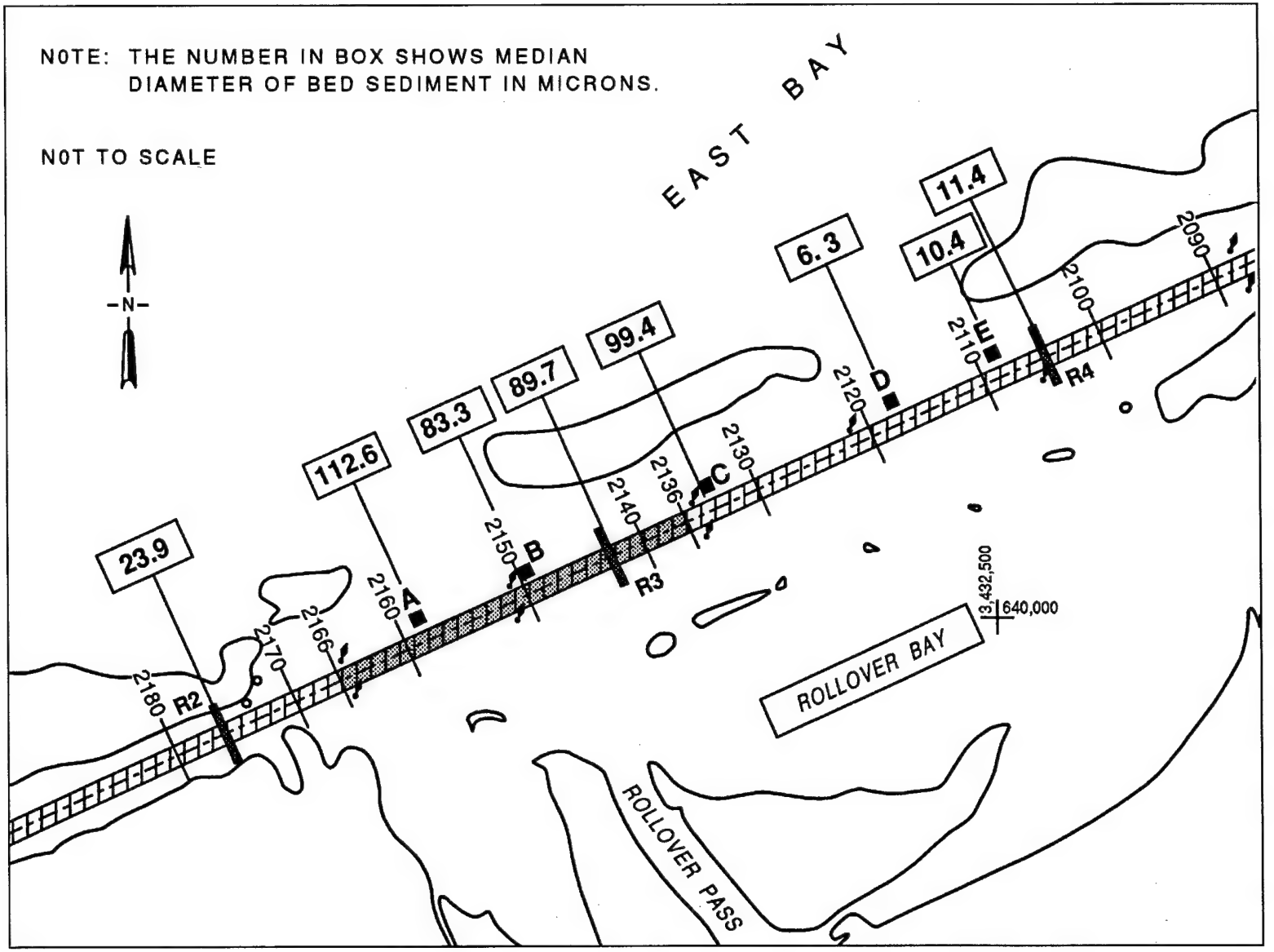

Figure 19. Median size of bed sediment along GIWW

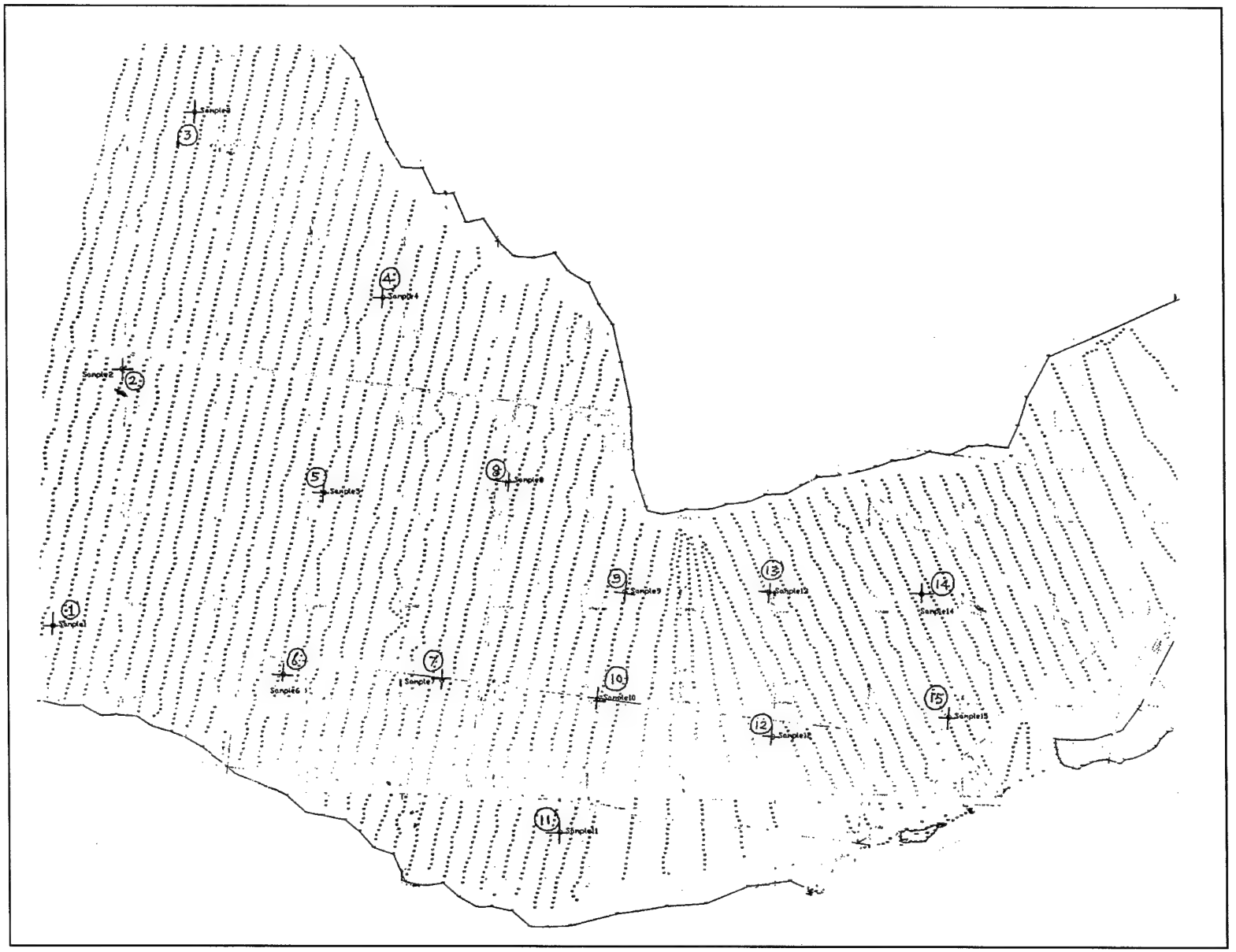

Figure 20. Locations of bed sediment samples collected in East Bay

Suspended Sediment

Water samples were collected by ERDC, CHL at a minimum of three depths at each ADCP transect. Samples were pumped from a predetermined depth into 100-ml plastic bottles for storage and transport. These samples were analyzed in the CHL laboratory for determining salinity and suspended sediment concentrations. The results are given in WES MFR "Field data collection at Rollover Bay and Gulf Intracoastal waterway, Galveston, TX," dated September 1999.[1]

The salinity within the study area indicated very small differences over the two days of data collection. The values ranged from 12 ppt to 23 ppt. The most significant salinity changes occurred at Range 1.

Water samples analyzed for Total Suspended Material (TSM) concentrations are given in Figures 21 through 22. It was noted that the total suspended material concentrations were generally higher on the ebb cycle than on the flood. Maximum TSM concentrations ranged from 50 - 325 mg/L in Rollover Pass, from 25 - 525 mg/L in the GIWW and from 20 - 375 mg/L at the entrances into East Bay. The concentrations are reasonable and appear to be in order for the prevailing conditions at the site.

Wind

It has been reported that wind has a significant influence on the hydrodynamics of Rollover Bay because the water depth in the bay varies from about 0.3 to 0.9 m (1 to 3 ft) over most of its area. A wind to the north brings sea water inside the bay resulting in water piling to abnormally high levels. On the other hand, wind blowing southward empties the bay and exposes shallow areas above water level. Wind data at the site of Rollover Pass are not available. Hence, wind data were obtained from NOAA Internet site for the Galveston Pleasure Pier (Figure 24) for the month of March 1999 during which ERDC, CHL collected field data. The wind speed and wind direction for March 1999 are shown in Figures 25 and 26, respectively. Ignoring fluctuations in the data, the maximum wind speed was about 11 m/s and predominant wind directions were 105 and 360 deg.

[1] Fagerburg (1999), op cit.

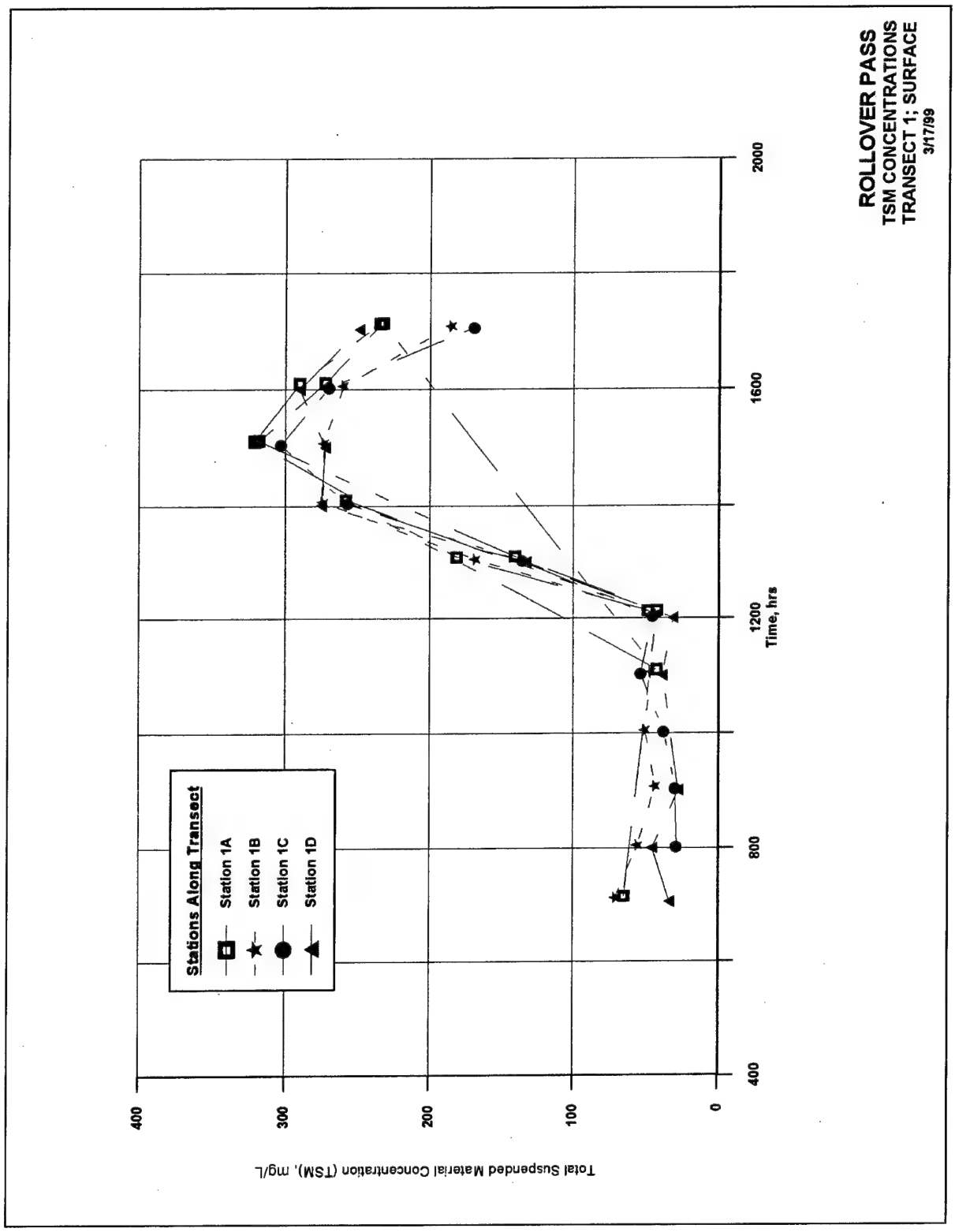

Figure 21. Total suspended matter concentration at Transect 1 near surface

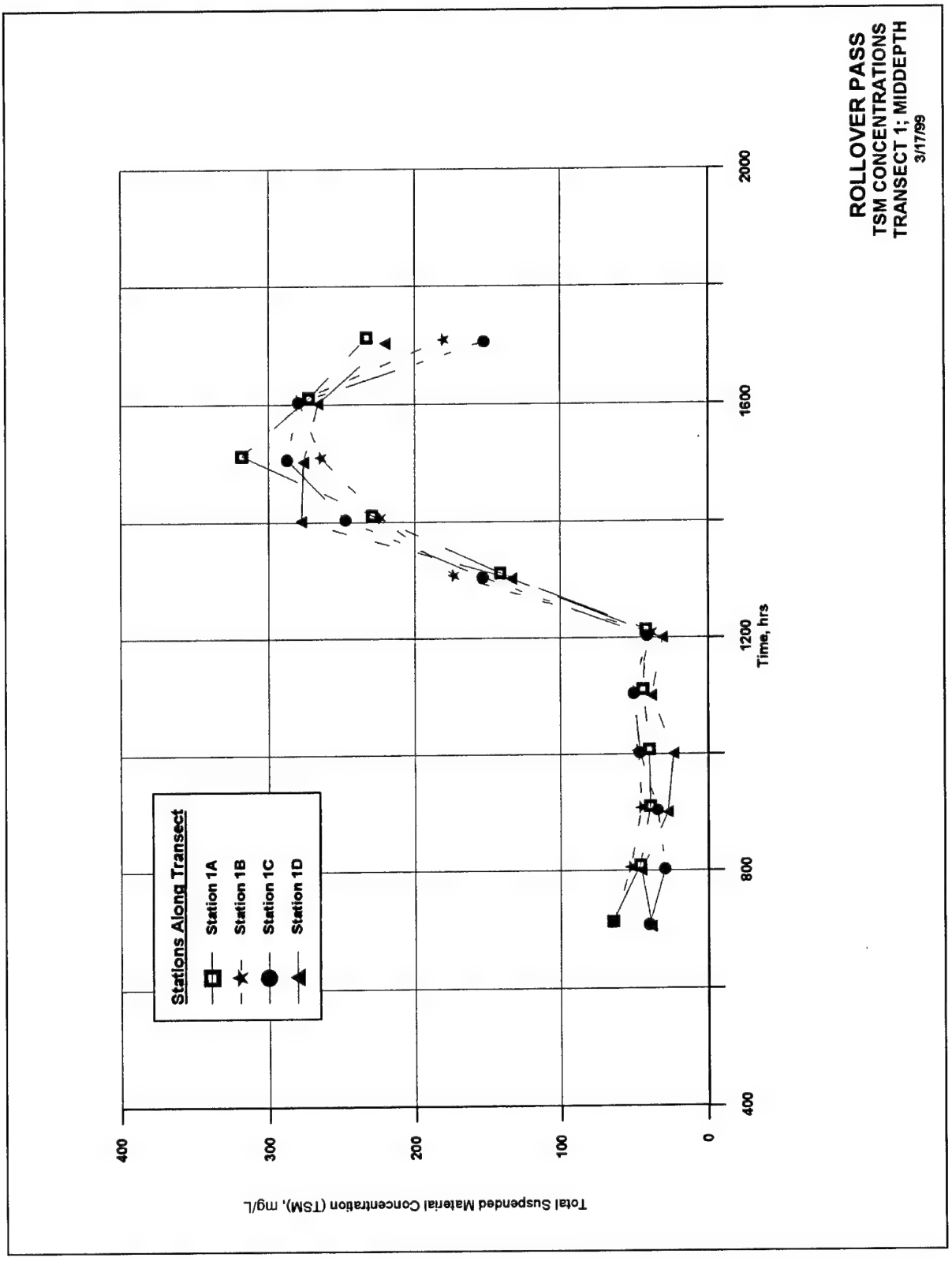

Figure 22. Total suspended matter concentration at Transect 1 at middepth

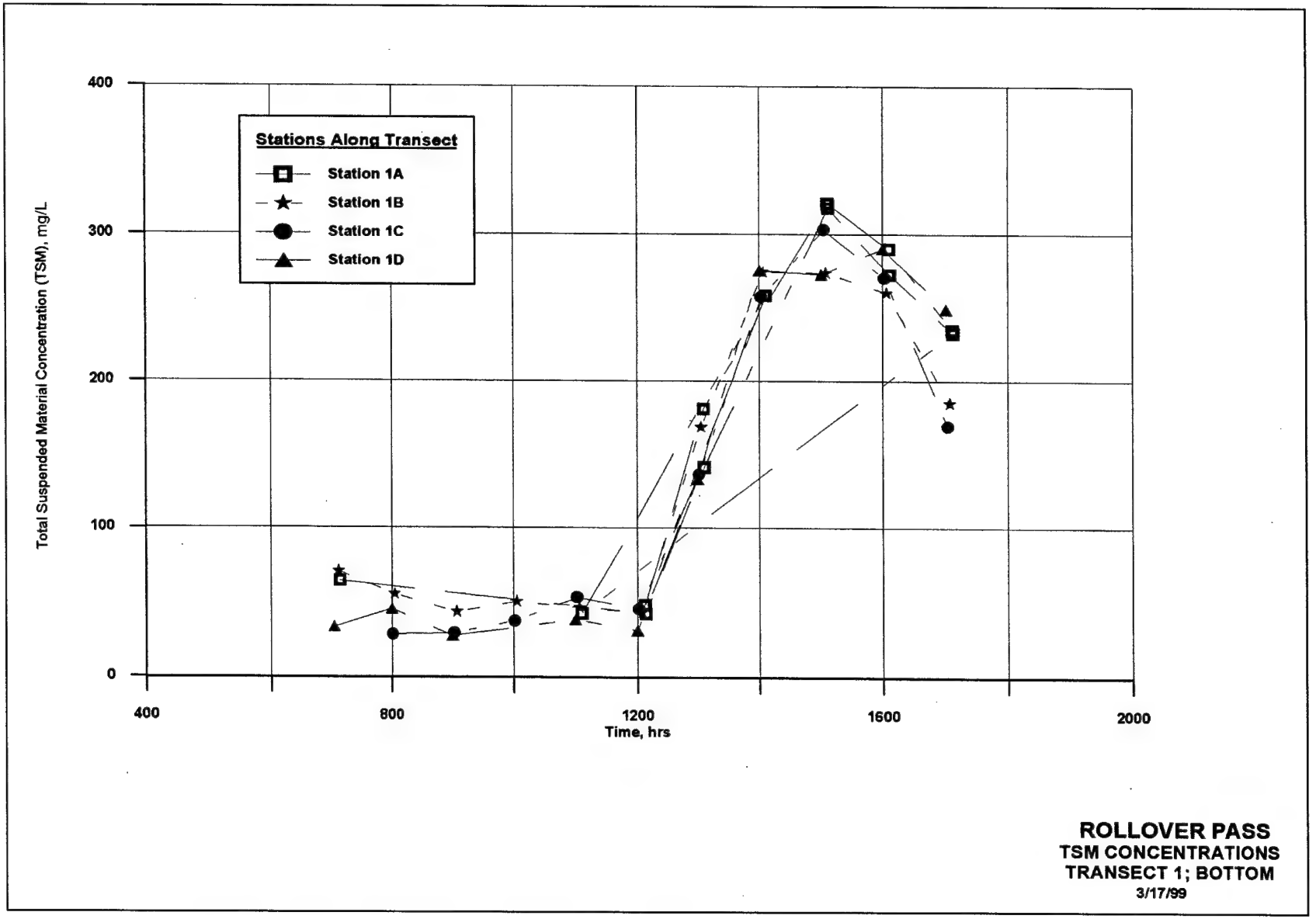

Figure 23. Total suspended matter concentration at Transect 1 near bottom

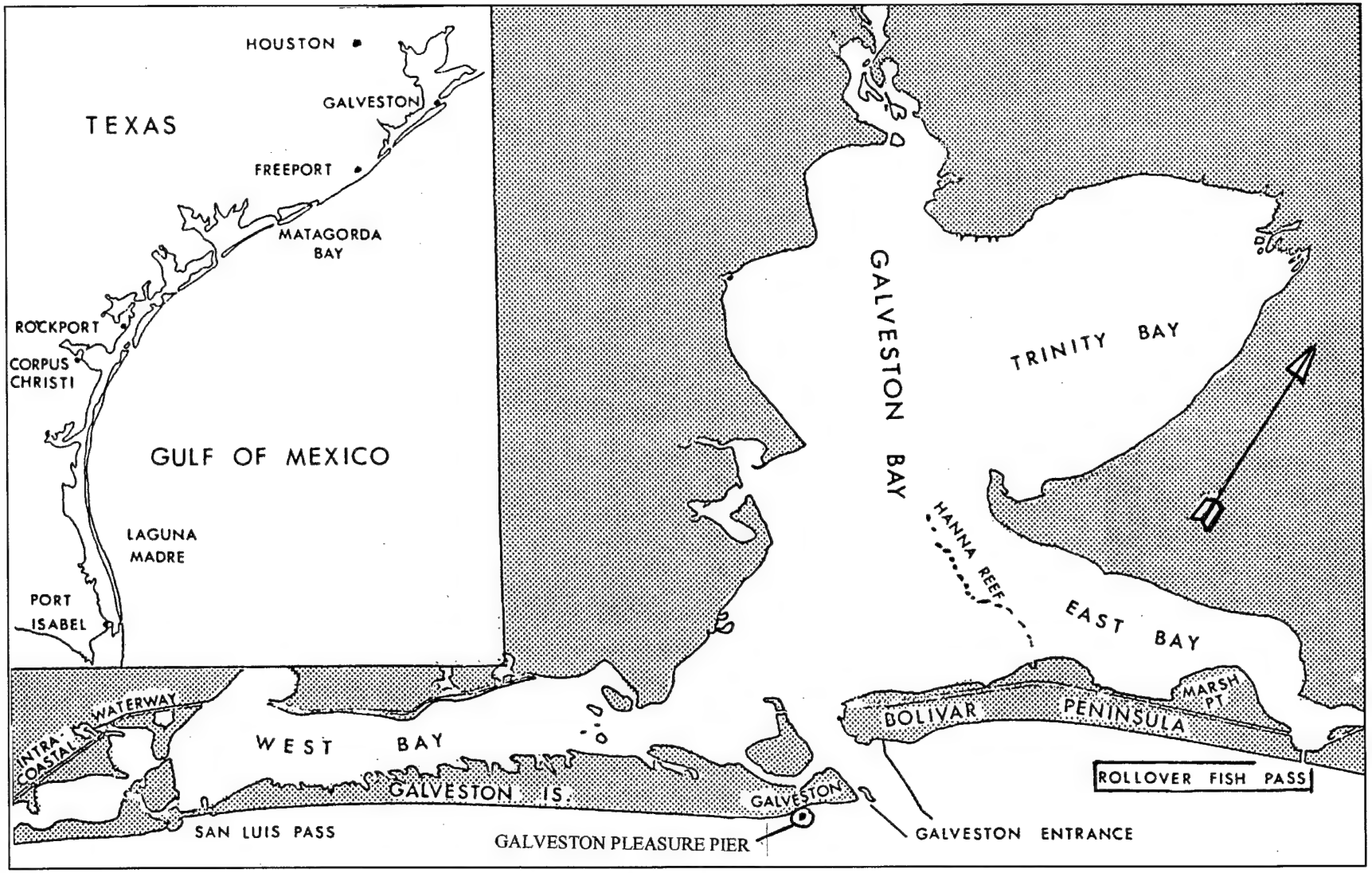

Figure 24. Map showing location of Galveston Pleasure Pier

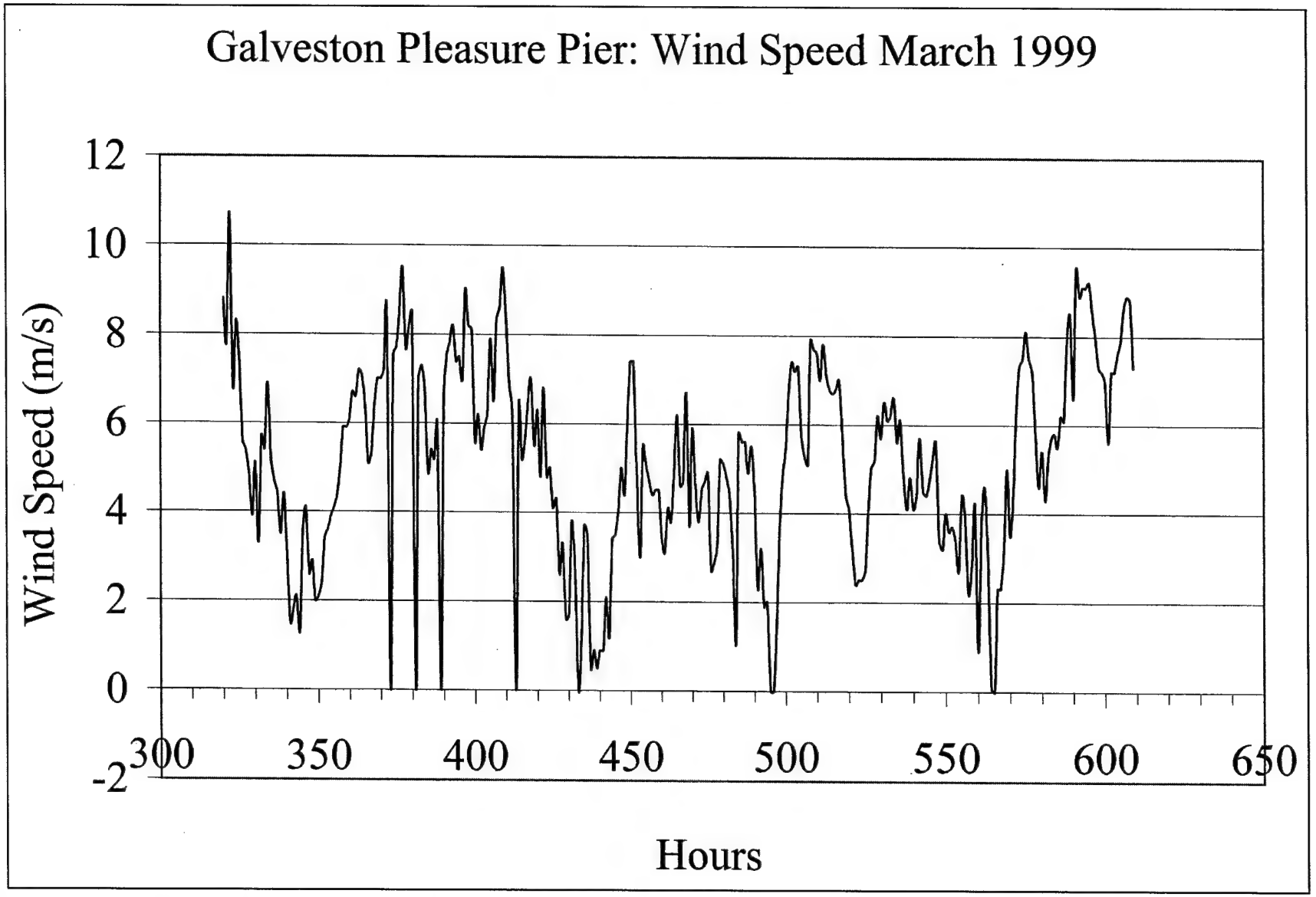

Figure 25. Wind speed at Galveston Pleasure Pier, March 1999

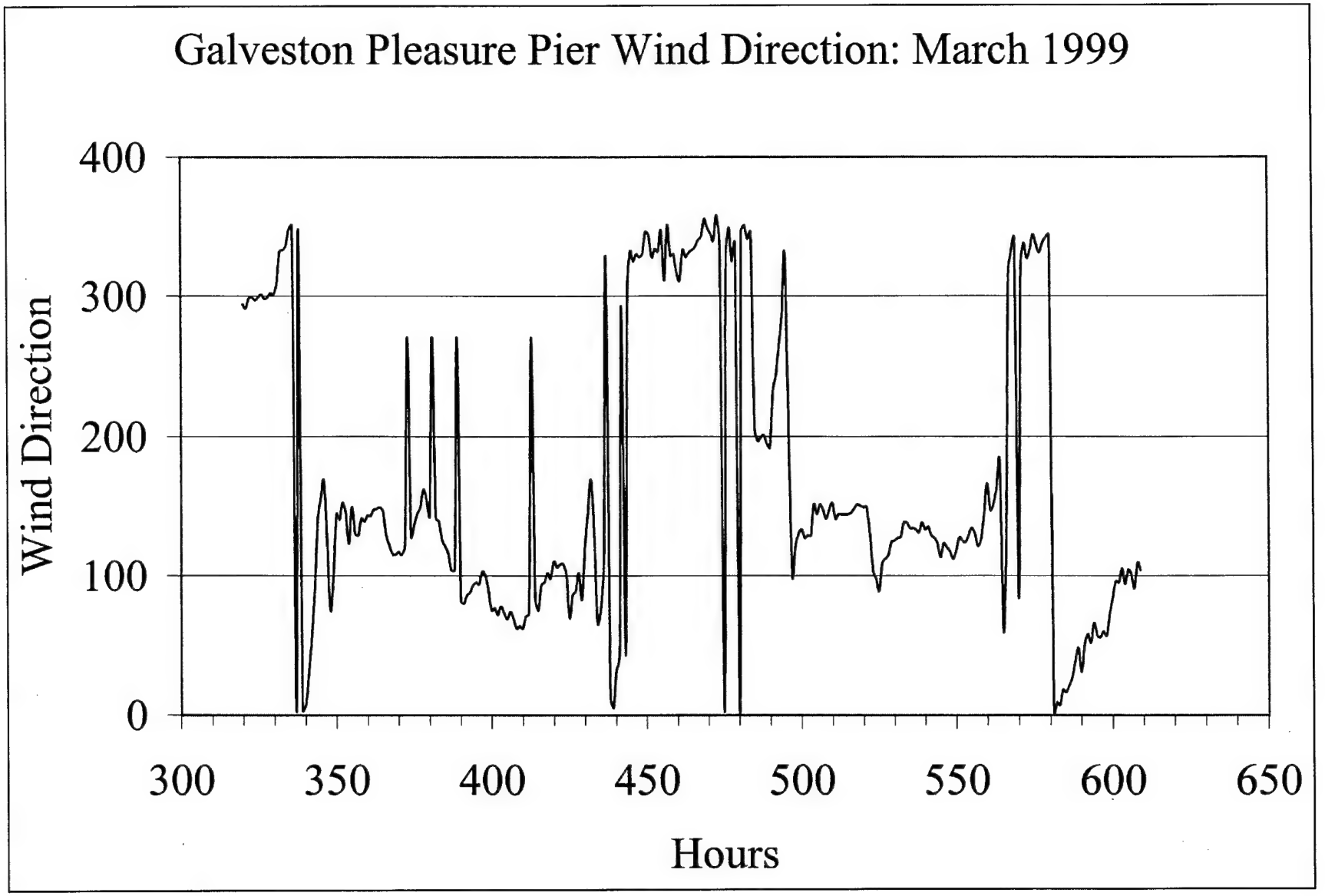

Figure 26. Wind direction at Galveston Pleasure Pier, March 1999

3 Numerical Hydrodynamic Model

Description

The numerical model used for the present study, RMA-2, is a part of the TABS-MD modeling system developed by the Coastal and Hydraulics Laboratory, ERDC for two-dimensional hydrodynamic modeling of open channel flow, transport processes and sediment problems in rivers, reservoirs, bays, and estuaries. Computational methods such as iteration and approximation are used to solve mathematical expressions that describe physical phenomena. This modeling system has been successfully used in the past at ERDC, CHL and elsewhere for solving hydraulic problems.

Mesh

A numerical mesh of nodes and elements was constructed for the entire area selected for the model (Figure 27). The mesh was developed primarily to study the Rollover Pass area; however, it also includes other adjacent areas such as the East Bay, Galveston Bay, a part of the Gulf of Mexico, and rivers and streams joining the water body. Large elements were used in the ocean and bays. Smaller elements providing higher resolution were used in the entrance channel, GIWW, and the Rollover Bay area (Figures 28 and 29). Higher resolution enabled accurate calculation of the velocity field in sufficient detail in the area of interest. A large geographical area was incorporated in the mesh to locate model boundaries sufficiently away from the area of investigation and thus reduce the influence of boundaries on the velocity field and tidal propagation. The mesh shown in Figure 27 represents existing conditions, which contain 7,380 elements and 20,700 nodes.

Bathymetry

Horizontal plane representation of the system and bed elevations were essential to describe the system. Bathymetry and geometry information for the system was obtained from the National Ocean Service / National Oceanic and Atmospheric Administration (NOAA) nautical charts shown in Table 6. These

Figure 27. Grid used for numerical model study

charts were also used to determine the location (x and y coordinate) of each corner node of each element.

In addition to the bathymetric data obtained from the preceding charts, results of hydrographic survey of Rollover Bay and vicinity conducted by ERDC, CHL in 1999 were incorporated in the numerical model. Also, details of the small islands and shoals, weir in the entrance channel, the GIWW and navigation channel within GIWW were incorporated. Figure 30 shows the bathymetry incorporated into the model.

Boundary Conditions

Tidal boundaries were provided at the entrance to West Bay, Galveston Bay, and Rollover Bay. The tide used as input at the model tidal boundaries was that taken at TG3 and is shown in Figure 31. Discharge inflows were specified at three locations, namely Buffalo Bayou, San Jacinto River, and the Trinity River. Figure 32 shows locations of all the tidal and river discharge boundaries.

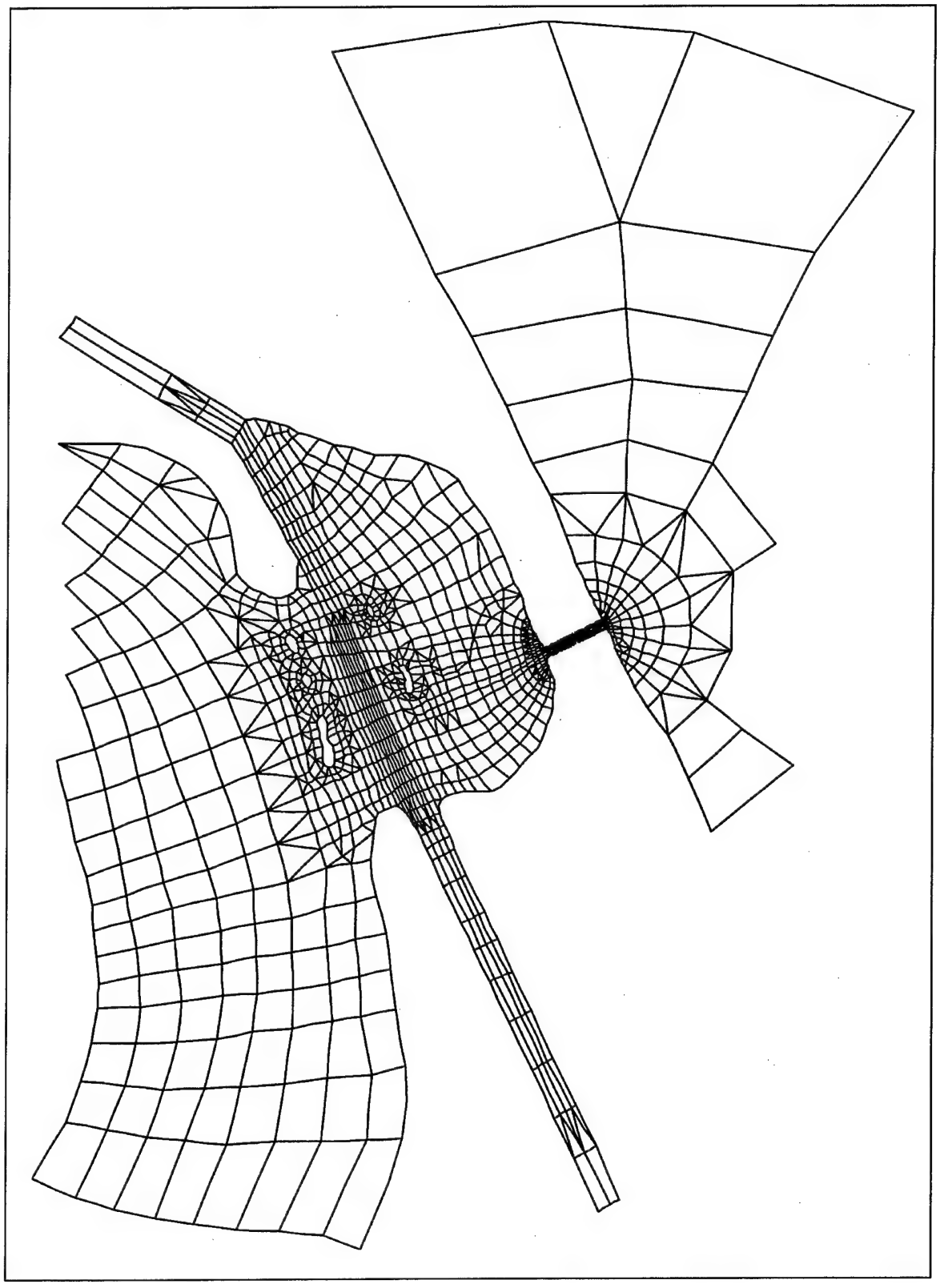

Figure 28. Details of grid in the study area

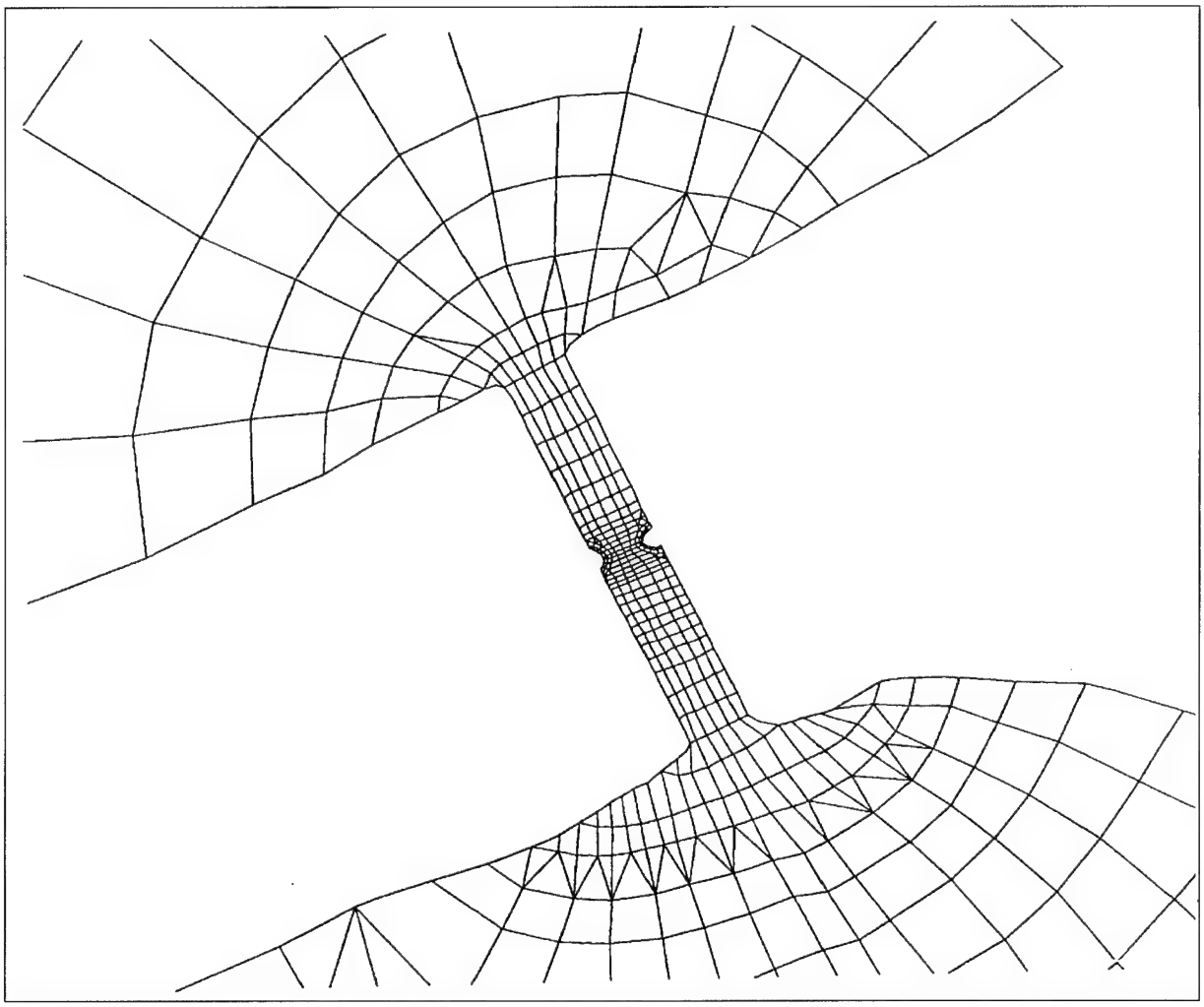

Figure 29. Details of grid in the channel connecting Rollover Bay to ocean

Table 6
NOAA Charts Used for Constructing Geometry and Bathymetry for Numerical Model

Chart No	Location	Year
11323	Approach to Galveston Bay	1986
11326	Galveston	1985
11327	Upper Galveston Bay	1984
11328	Houston Ship Channel, Atkins Island to Alexander Island	1983
11329	Houston Ship Channel, Carpenter Bayou to Houston	1987

Verification for Tide

Verification of the hydrodynamic model consisted of conducting several test runs to adjust boundary conditions, model mesh, and internal coefficients so the numerical model would reproduce current velocities and water surface elevations comparable to those measured during field data collection.

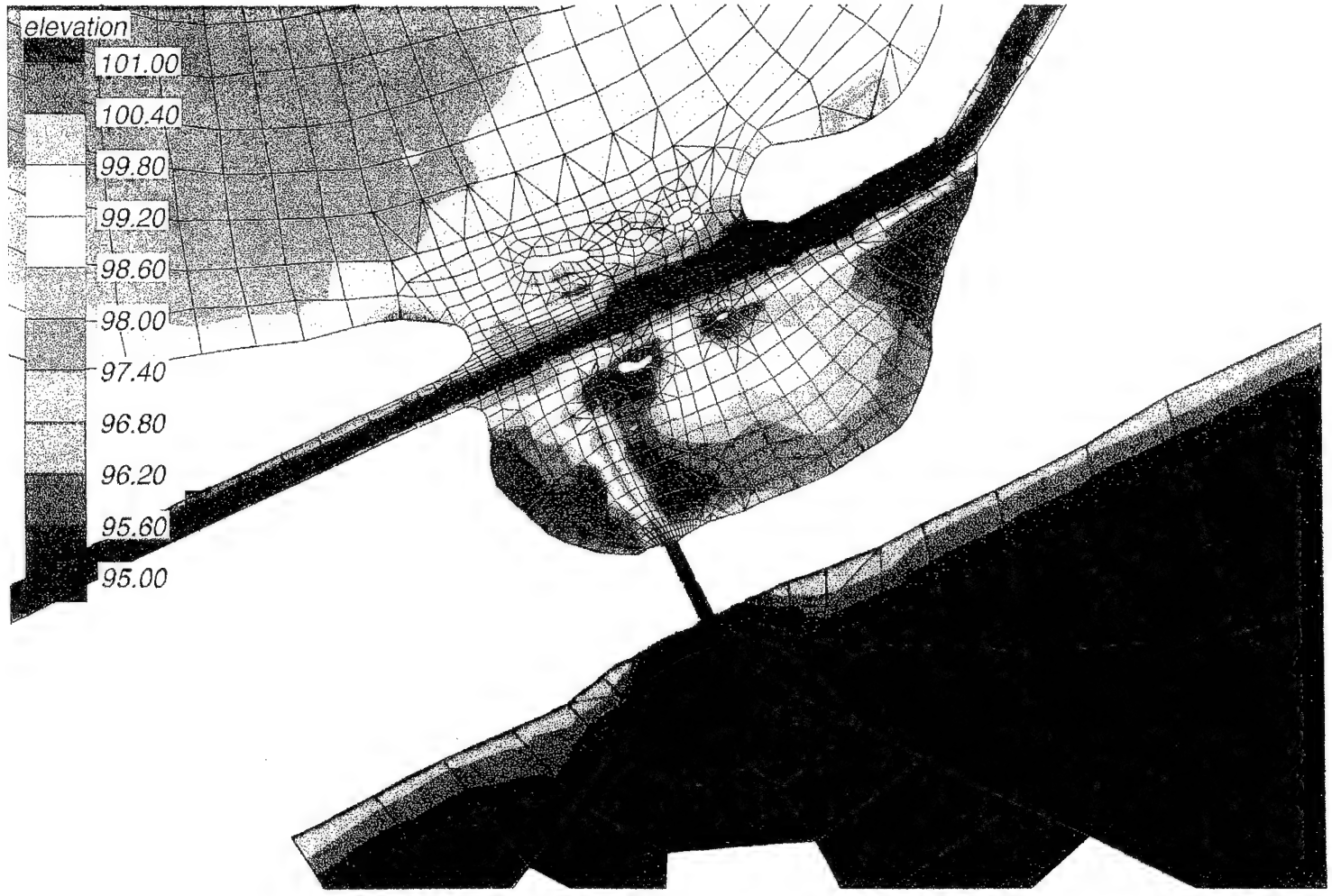

Note: An arbitrary datum of 100.00 corresponding to the mean sea level is used for plotting bathymetry and tidal elevations.

Figure 30. Bathymetry of study area [(All elevations (el) are in feet referenced to the National Geodetic Vertical Datum (NGVD)] (To convert feet to meters, multiply feet by .03048)

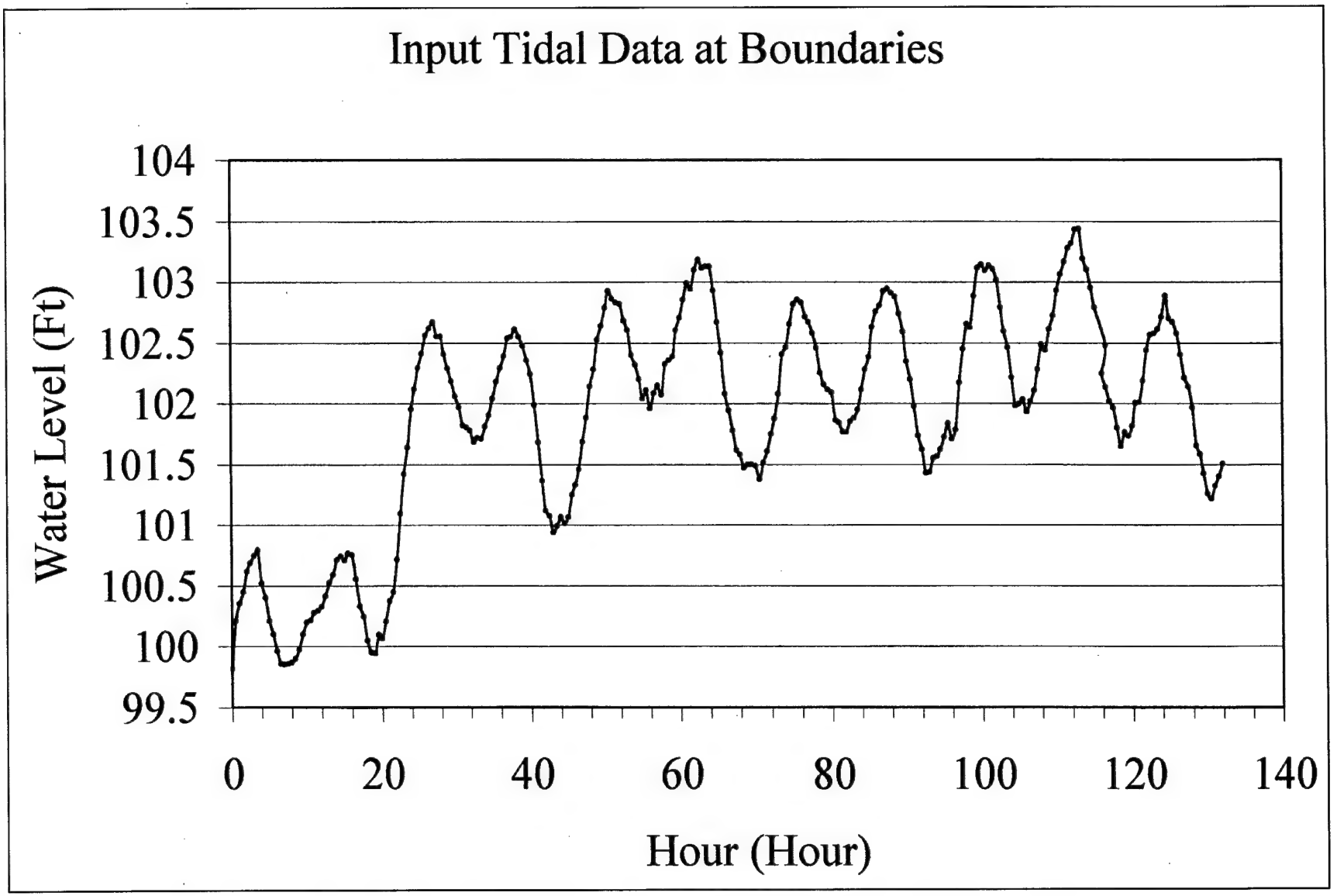

Figure 31. Input tidal data at model boundaries (Water level is in feet. To convert feet to meters, multiply by 0.3048)

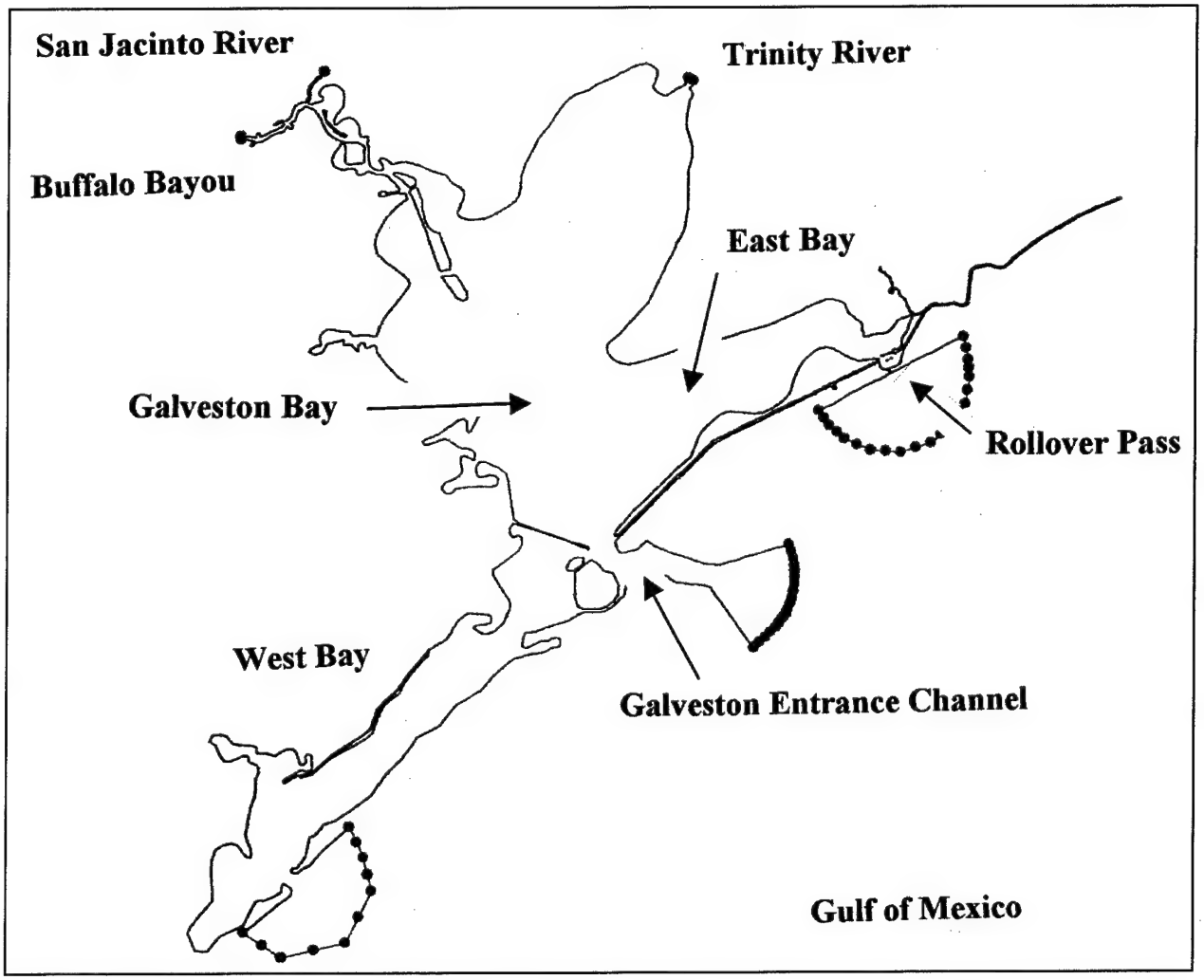

Figure 32. Locations of boundary nodes in numerical model

Tide gauges were installed at four locations during field data collection in March 1999. Out of these four gauges, data at two locations were lost; leaving two locations, namely Rollover Bay entrance and East Bay.

Figure 33 shows locations of three nodes where tidal data were obtained from the numerical model. All the three nodes are located near the entrance of the Rollover Pass. Tides obtained from the model at these nodes are compared in Figure 34 with the field tide at the entrance, which shows good agreement between model and field tides at the entrance. The three model tidal curves are not seen separately because they are identical and appear as one superposed curve.

In the East Bay area, tidal data were obtained from the numerical model at three nodes shown in Figure 35. Superposed tides obtained in the model at these nodes are compared with field tide at the entrance in Figure 36. This figure shows a blue line, which indicates tidal data collected in the field at a location in the East Bay. The model tides at three nodes (20116, 20118, and 20124) are

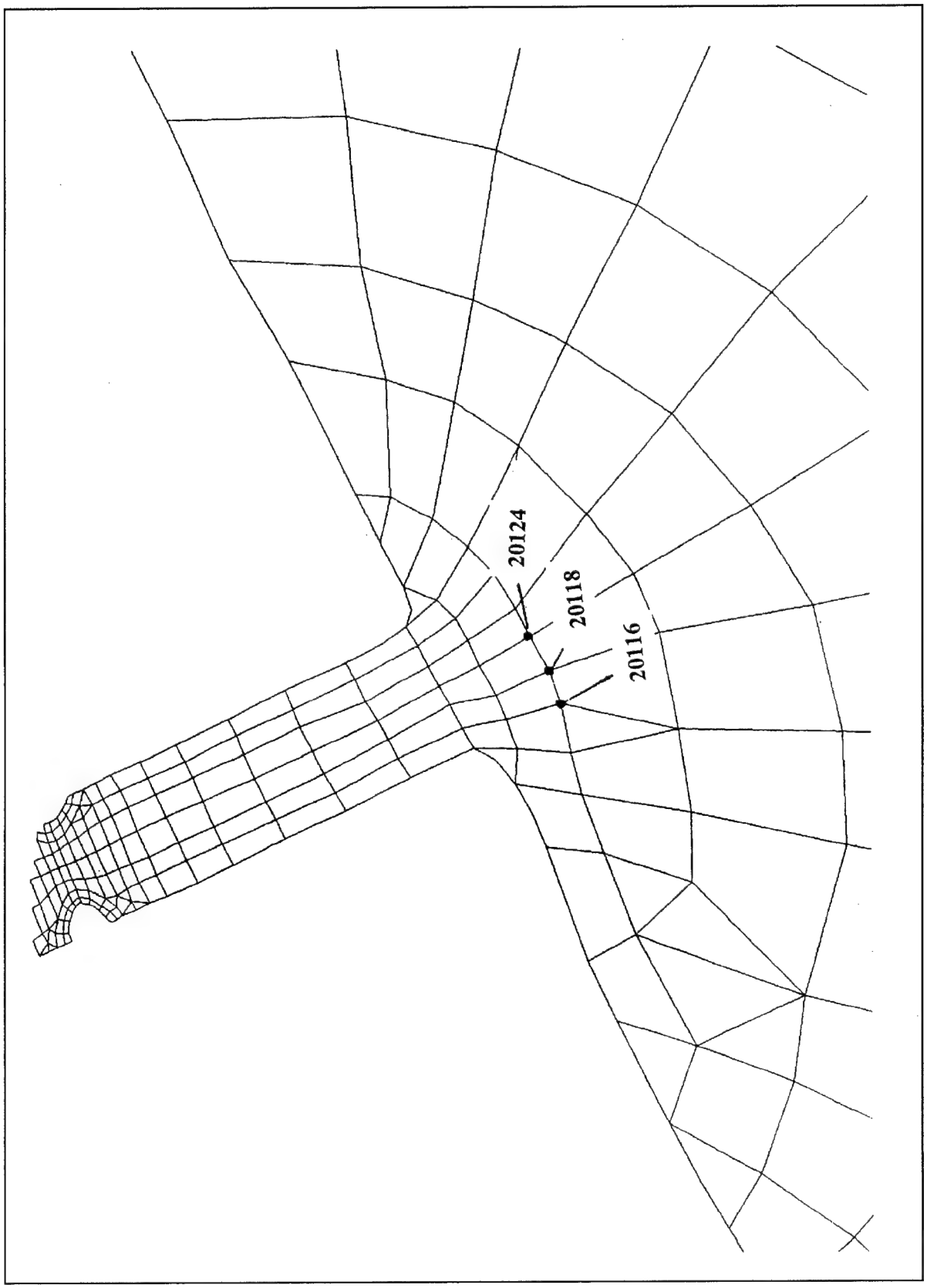

Figure 33. Locations of nodes where model tides were obtained for comparison

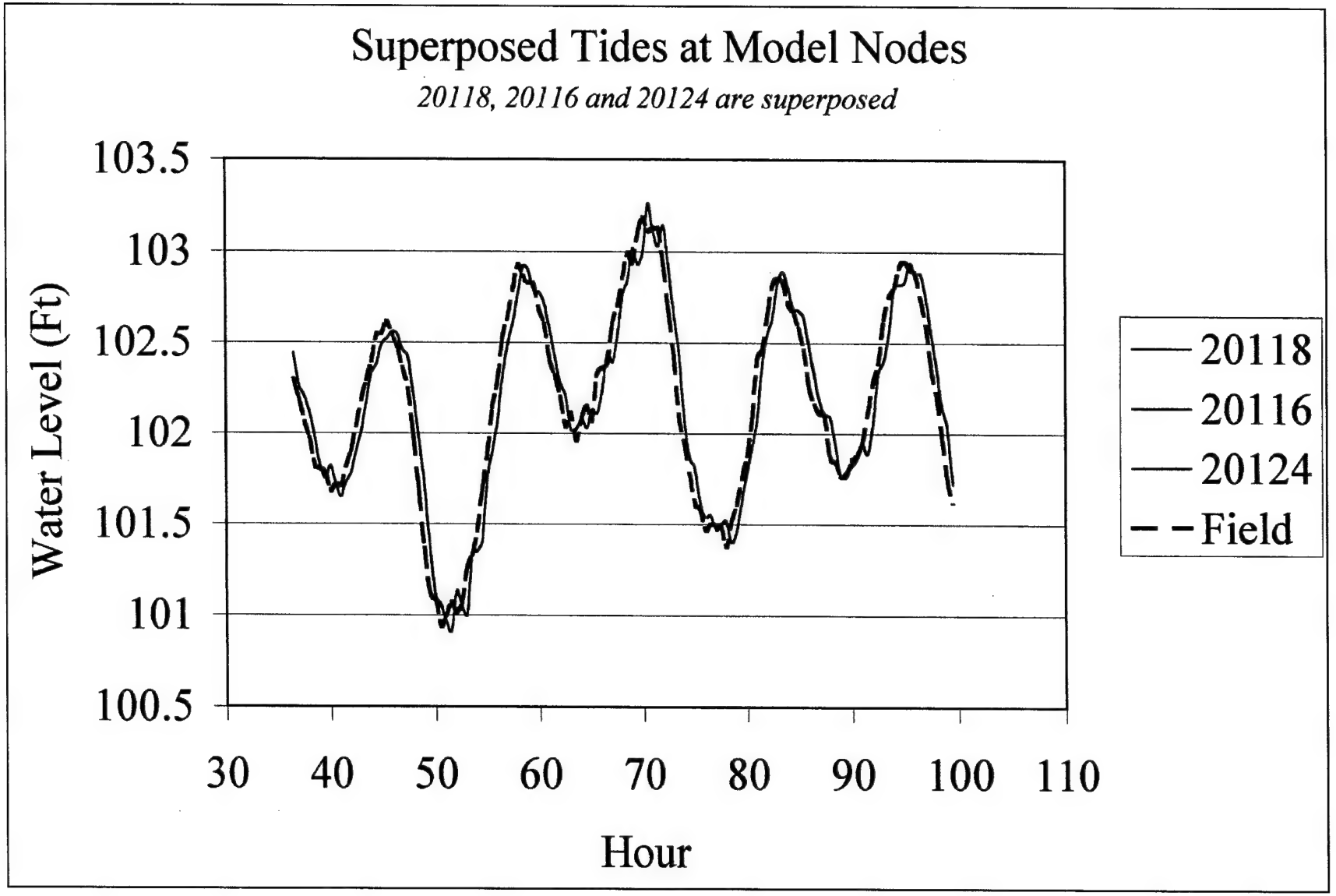

Figure 34. Superposed tides at field and three model nodes (Water level is in feet. To convert feet to meters, multiply by 0.3048)

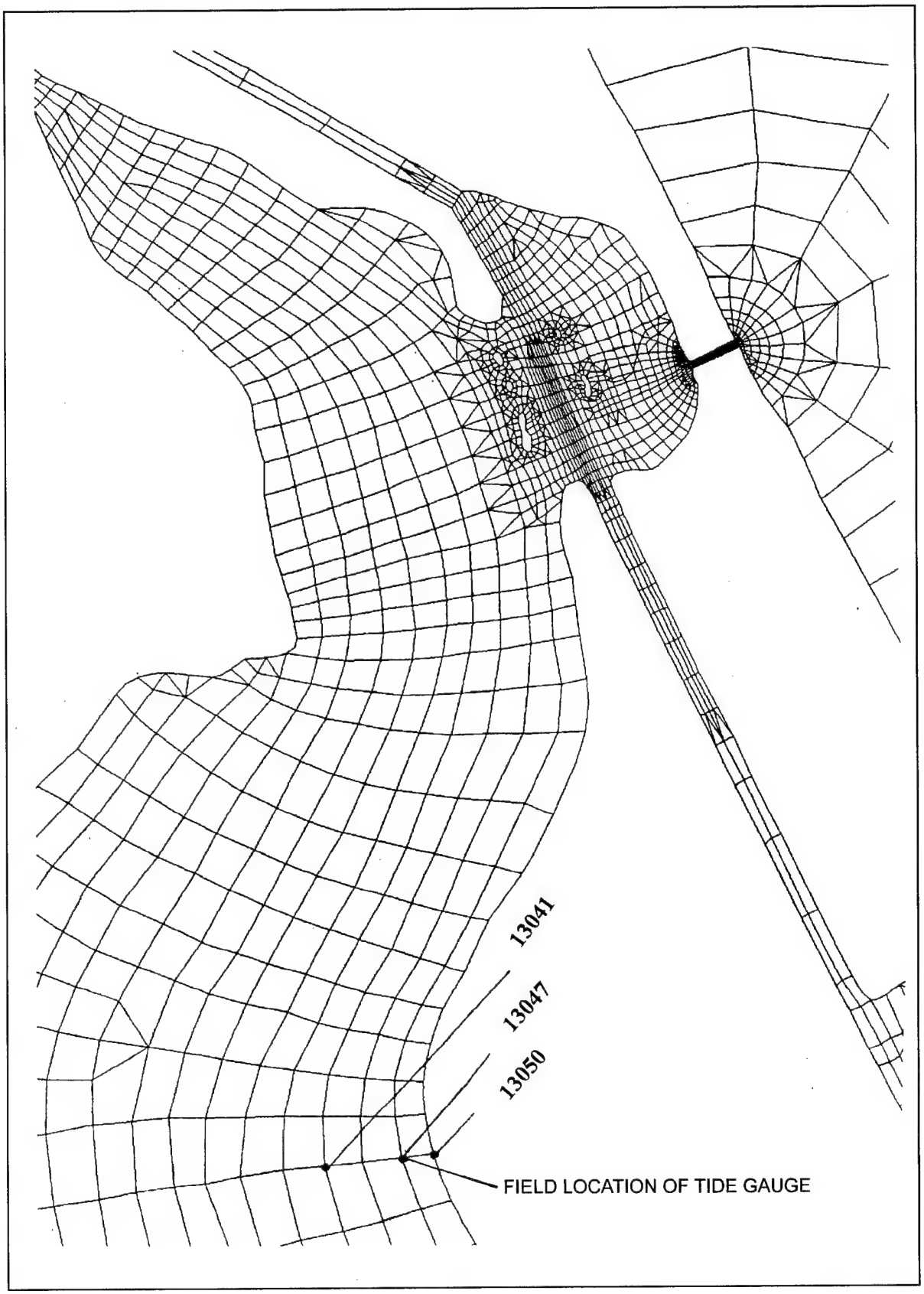

Figure 35. Locations of field tide gauge and model nodes 13041, 13047, and 13050

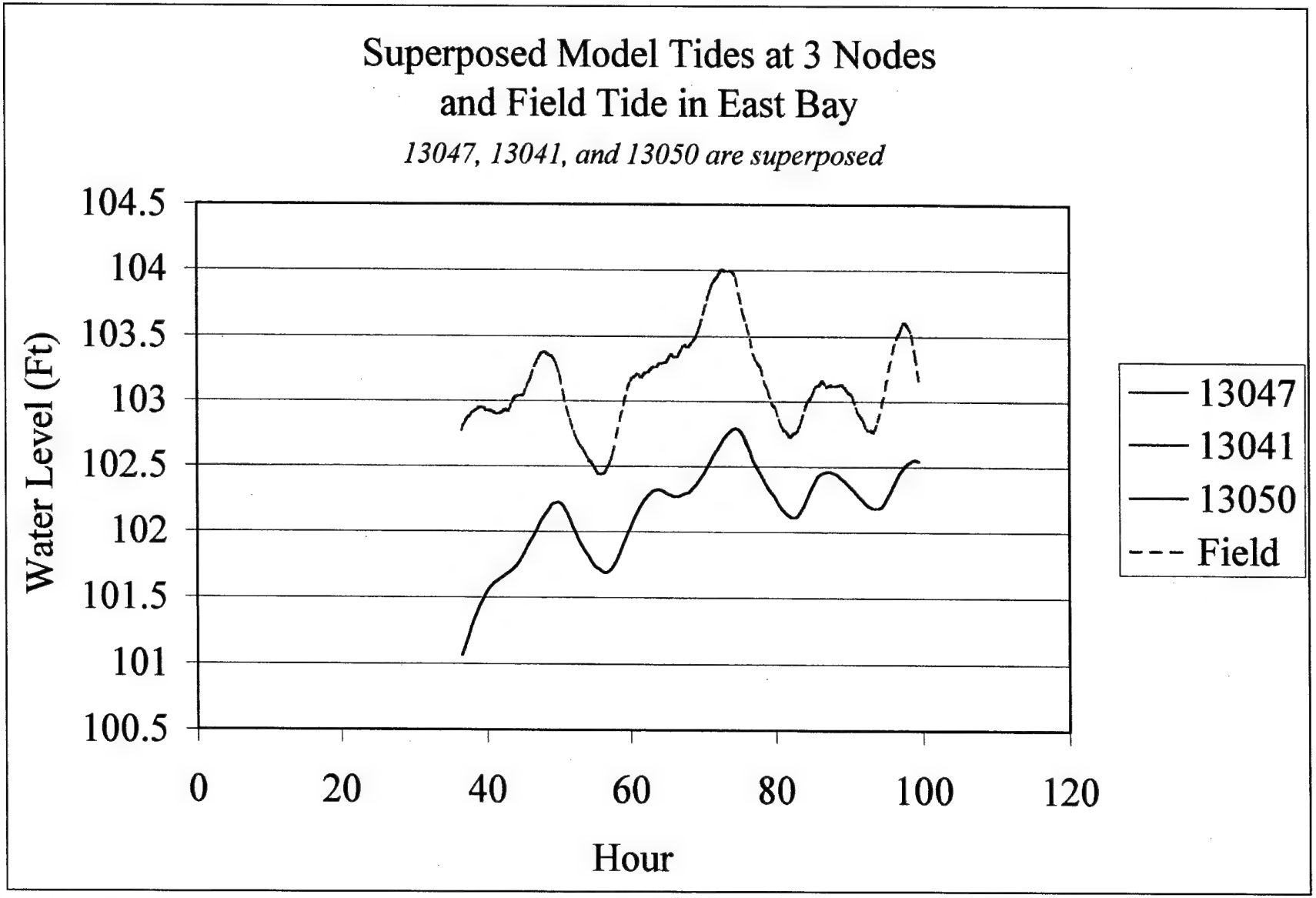

Figure 36. Superposed field tide and model tides at three nodes in East Bay (Water level is in feet. To convert feet to meters, multiply by 0.3048)

identical because the nodes are located close to each other. Hence, all three lines appear as a single red line in Figure 36. The model tide was lower than the recorded field tide, but the profile shape had a very good agreement. Model tides at nearby locations were not different from each other. This may suggest a datum shift between the two field locations, namely the Rollover Bay entrance and the East Bay tide gauge location. Since the tide at the entrance compared well in the model and field, the numerical model was considered verified for tides.

Verification for Velocity

Velocity measurements in the field have been described in the "Currents" section of this report. These measurements were taken at six transects, denoted as ADCP Range 1, 2, 3, 4, 5, and 40. Locations of these transects are shown in Figure 11. Time-history plots of velocity magnitudes in the numerical model were obtained at six nodes. Locations of these are shown in Figure 37. Comparison of model and field velocity plots at these six nodes is shown in Figures 38 through 43 corresponding to the field data collection at ranges 1, 2, 3, 4, 5, and 40, respectively.

The field measurements showed that the maximum velocity magnitude at Range 1 in Rollover Pass (see Figure 11 for location) was 0.79 m/s (2.6 ft/s). It is seen from Figure 13 that the maximum velocity in the numerical model was also on the same order of magnitude 0.79 to 0.85 m/s (2.6 to 2.8 ft/s) with the exception of one peak, which had a magnitude of 0.94 m/s (3.1 ft/s). The maximum velocity at range 5 near the entrance to the East Bay was 0.76 m/s (2.5 ft/s). The maximum velocity in GIWW was 0.76 m/s (4 ft/s). The numerical model velocities were comparable to these values.

Reasonably close agreement between model and field velocities was obtained. Hence, it was concluded that simulation of tides and velocities in the numerical model under the existing conditions was acceptable for purposes of the present study.

Flow Patterns

One of the advantages of a numerical hydrodynamic model is that flow patterns over different reaches of the area under investigation can be easily obtained for examination. Examples of flow patterns obtained from the numerical model are given in Figures 44 and 45 for the flood and ebb conditions respectively. Velocity vectors showing the flow pattern near the weir in the entrance channel of the Rollover Bay are shown in Figure 46. The flow pattern in the model appears to be consistent and in order.

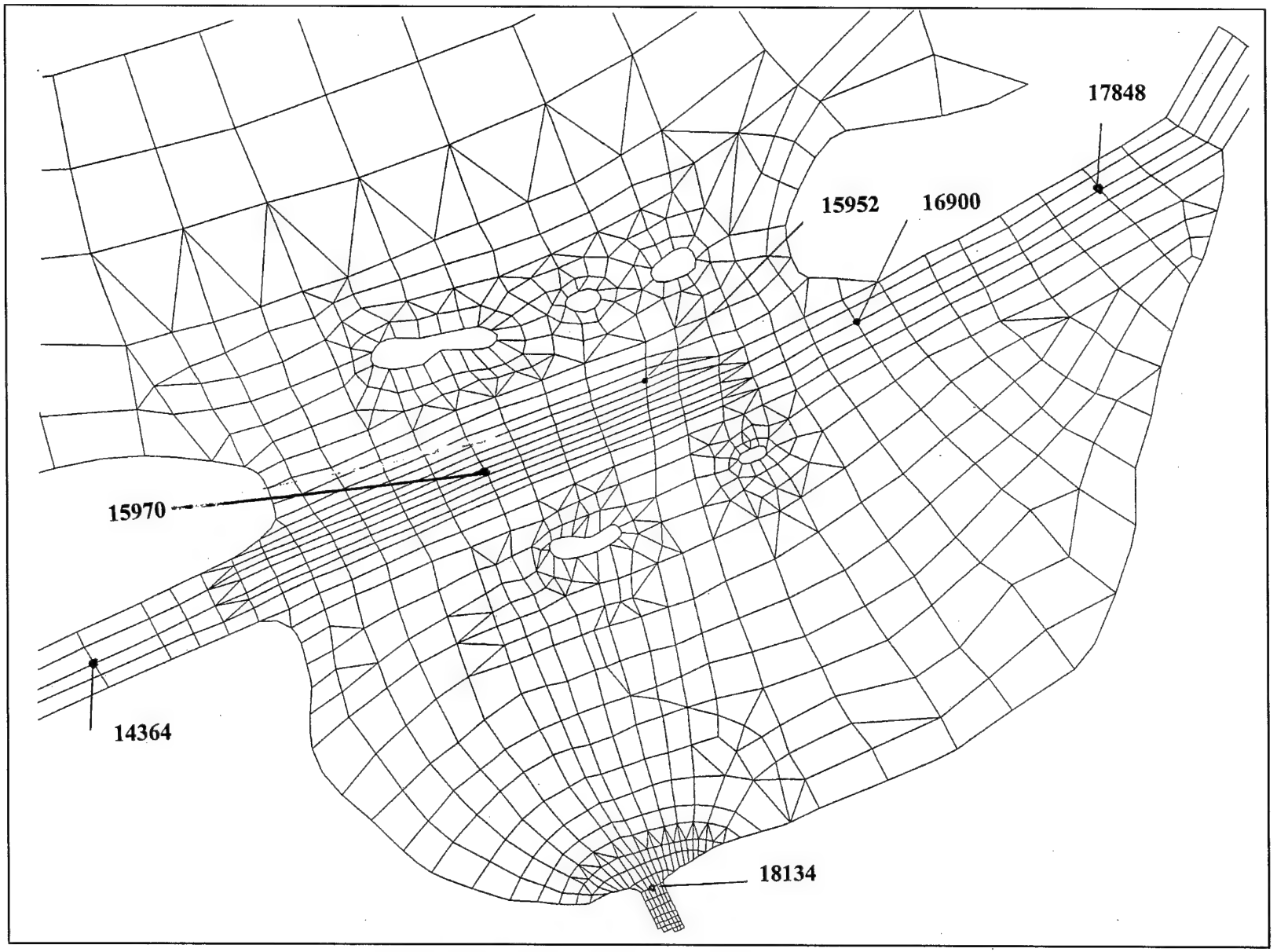

Figure 37. Locations of model nodes 14364, 15970, 15952, 16900, and 17848

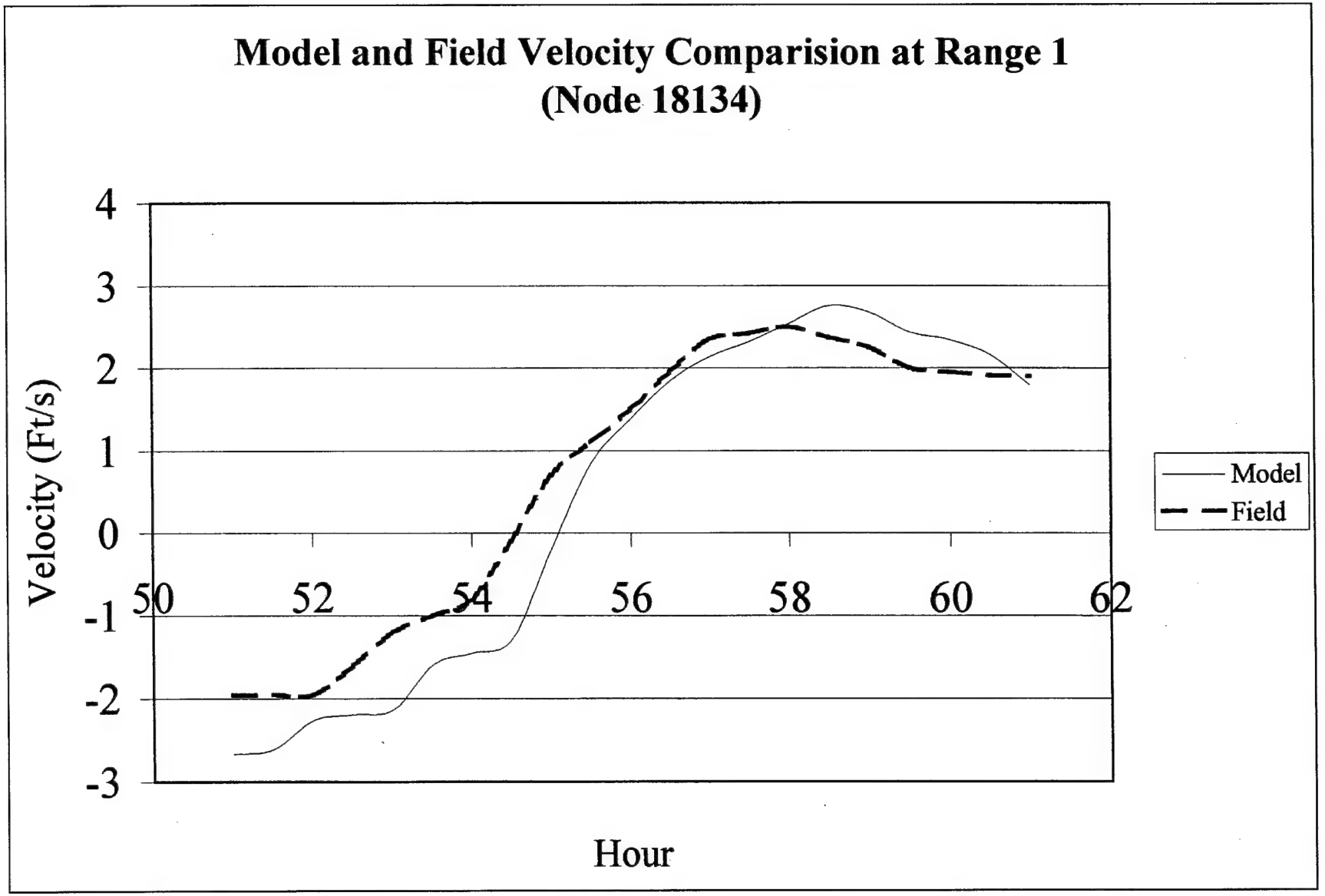

Figure 38. Comparison of model and field tides at Range 1 (Node 18134) (Velocity Is in feet per second. To convert to meters per second, multiply by 0.3048)

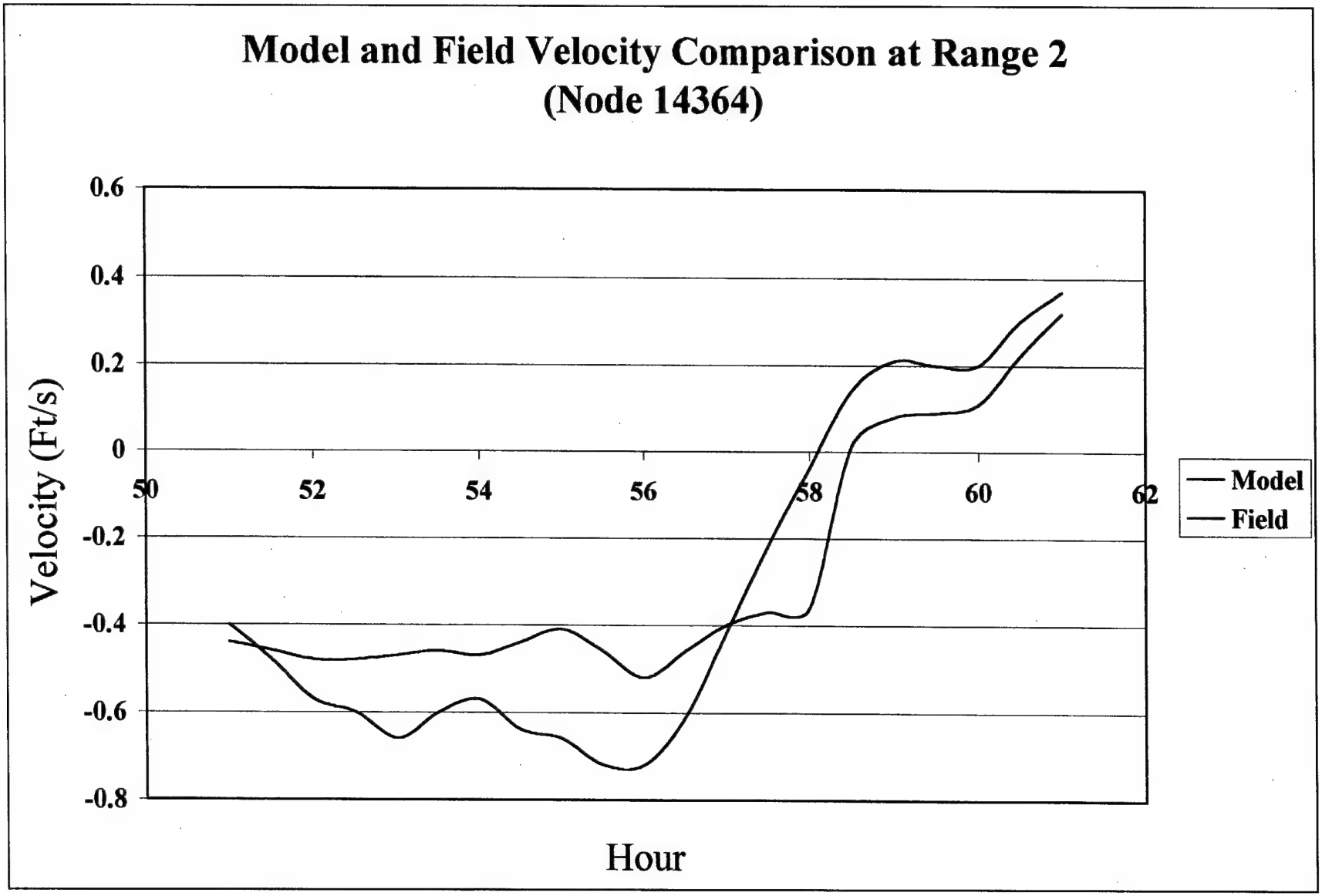

Figure 39. Comparison of model and field tides at Range 2 (Node 14364) (Velocity is in feet per second. To convert to meters per second, multiply by 0.3048)

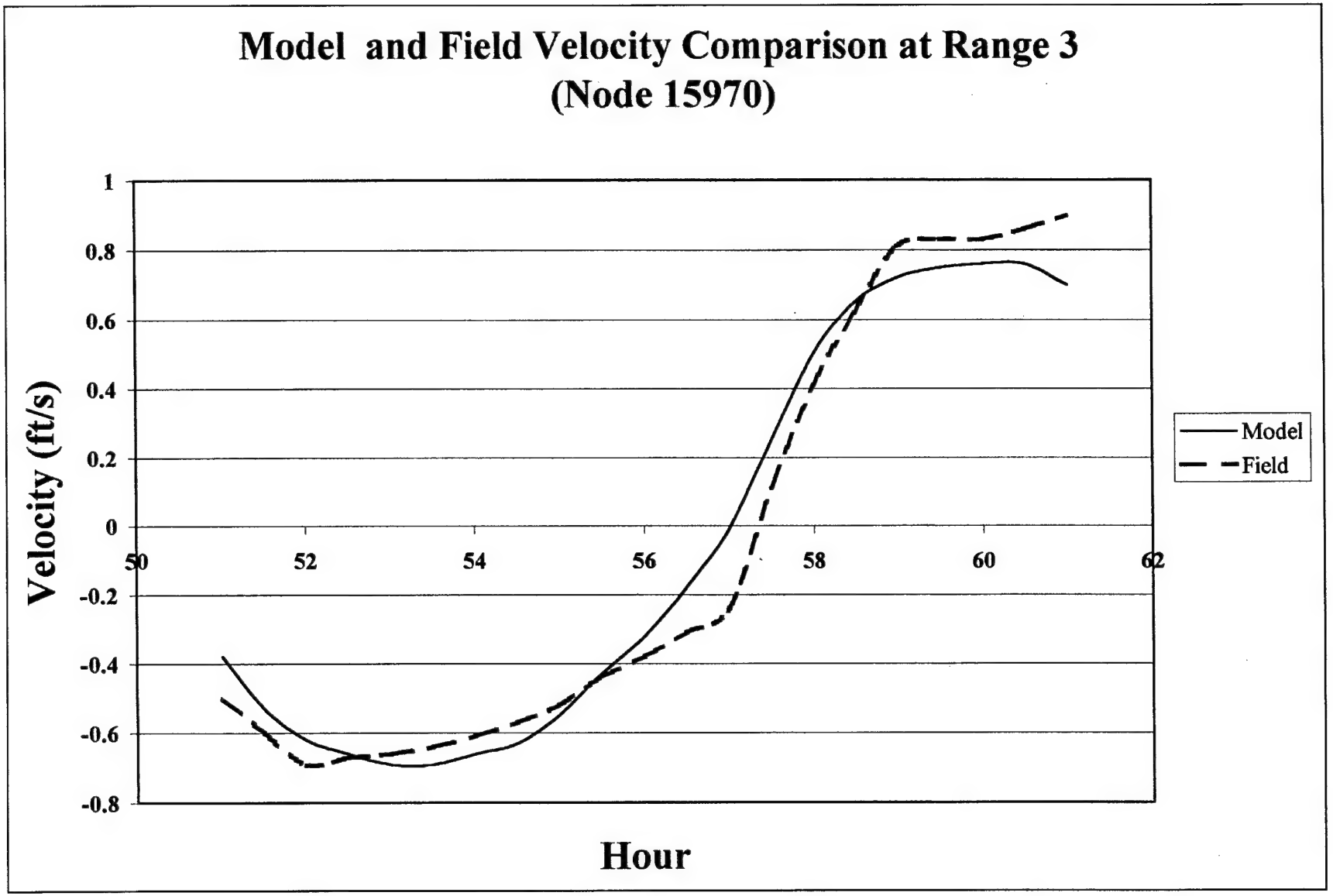

Figure 40. Comparison of model and field tides at Range 3 (Node 15970) (Velocity is in feet per second. To convert to meters per second, multiply by 0.3048)

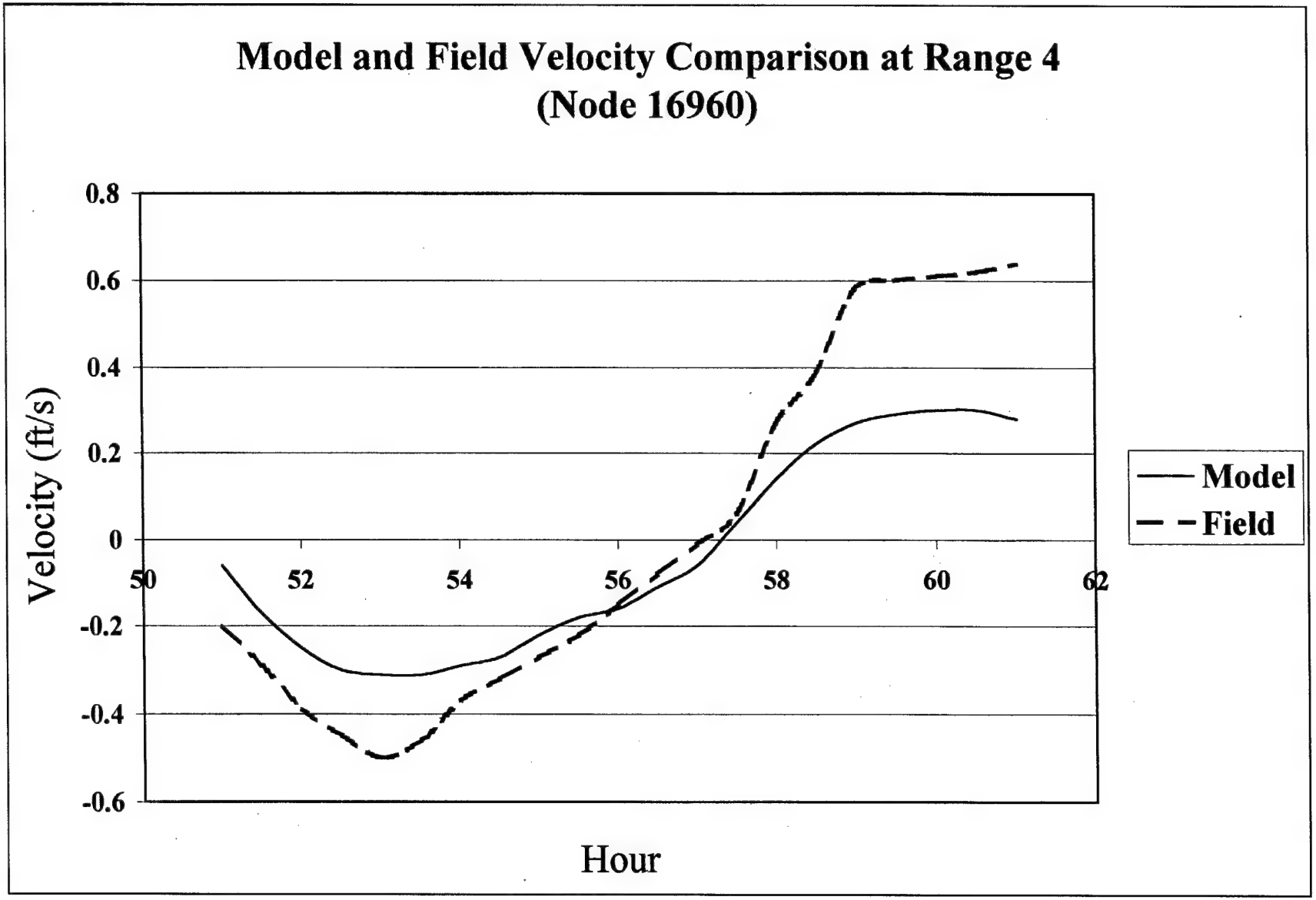

Figure 41. Comparison of model and field tides at Range 4 (Node 16960) (Velocity is in feet per second. To convert to meters per second, multiply by 0.3048)

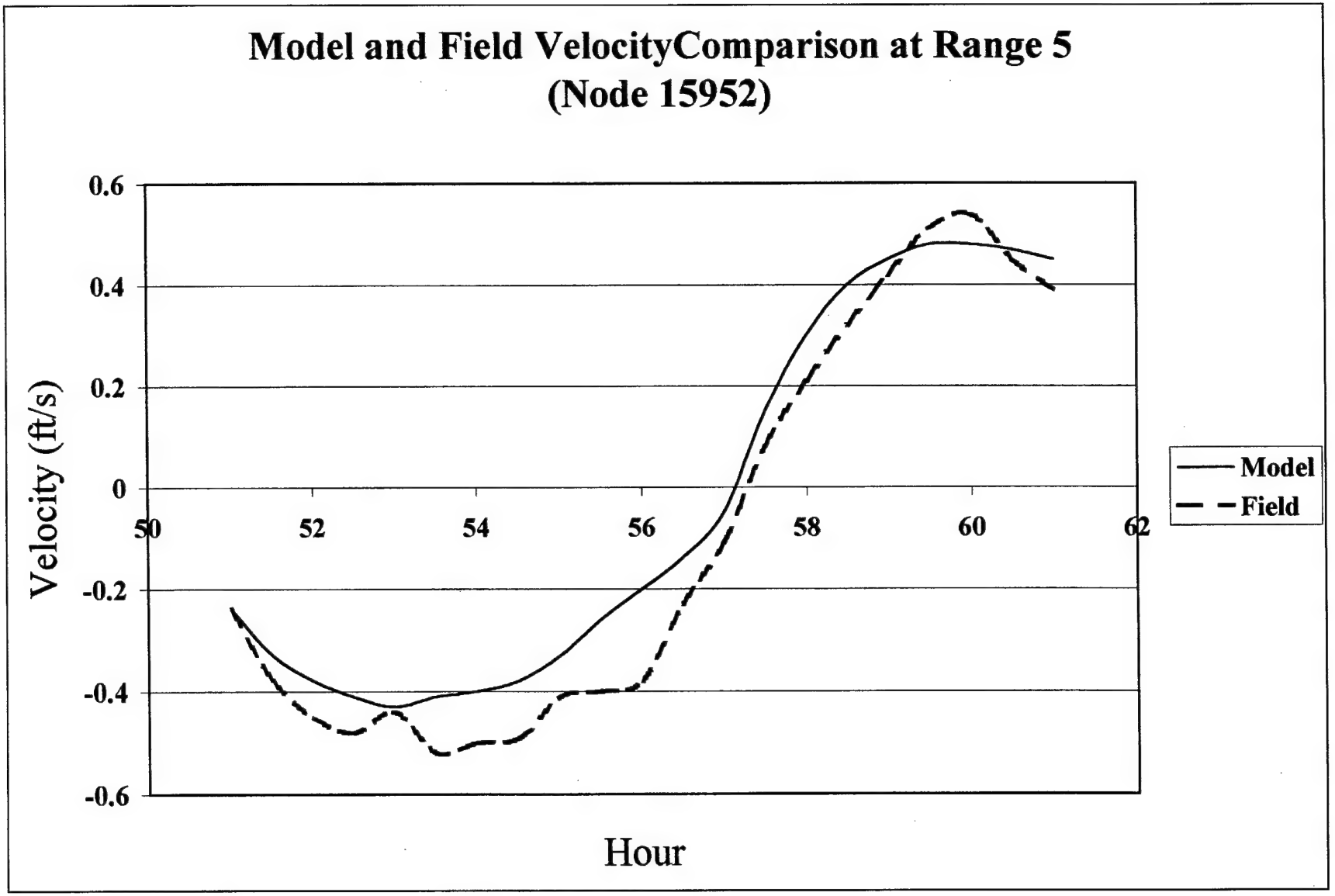

Figure 42. Comparison of model and field tides at Range 5 (Node 15952) (Velocity is in feet per second. To convert to meters per second, multiply by 0.3048)

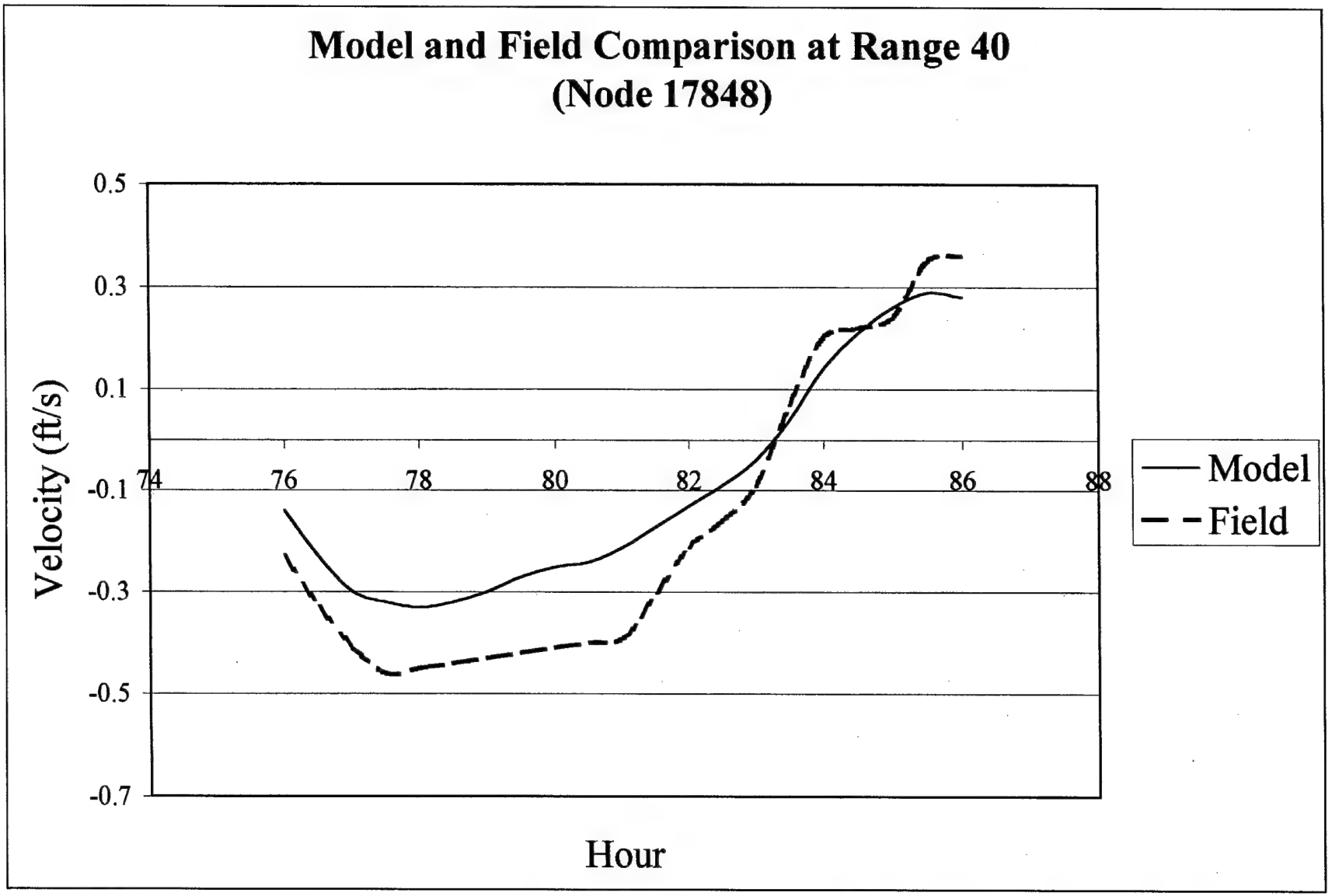

Figure 43. Comparison of model and field tides at Range 40 (Node 17848) (Velocity is in feet per second. To convert to meters per second, multiply by 0.3048)

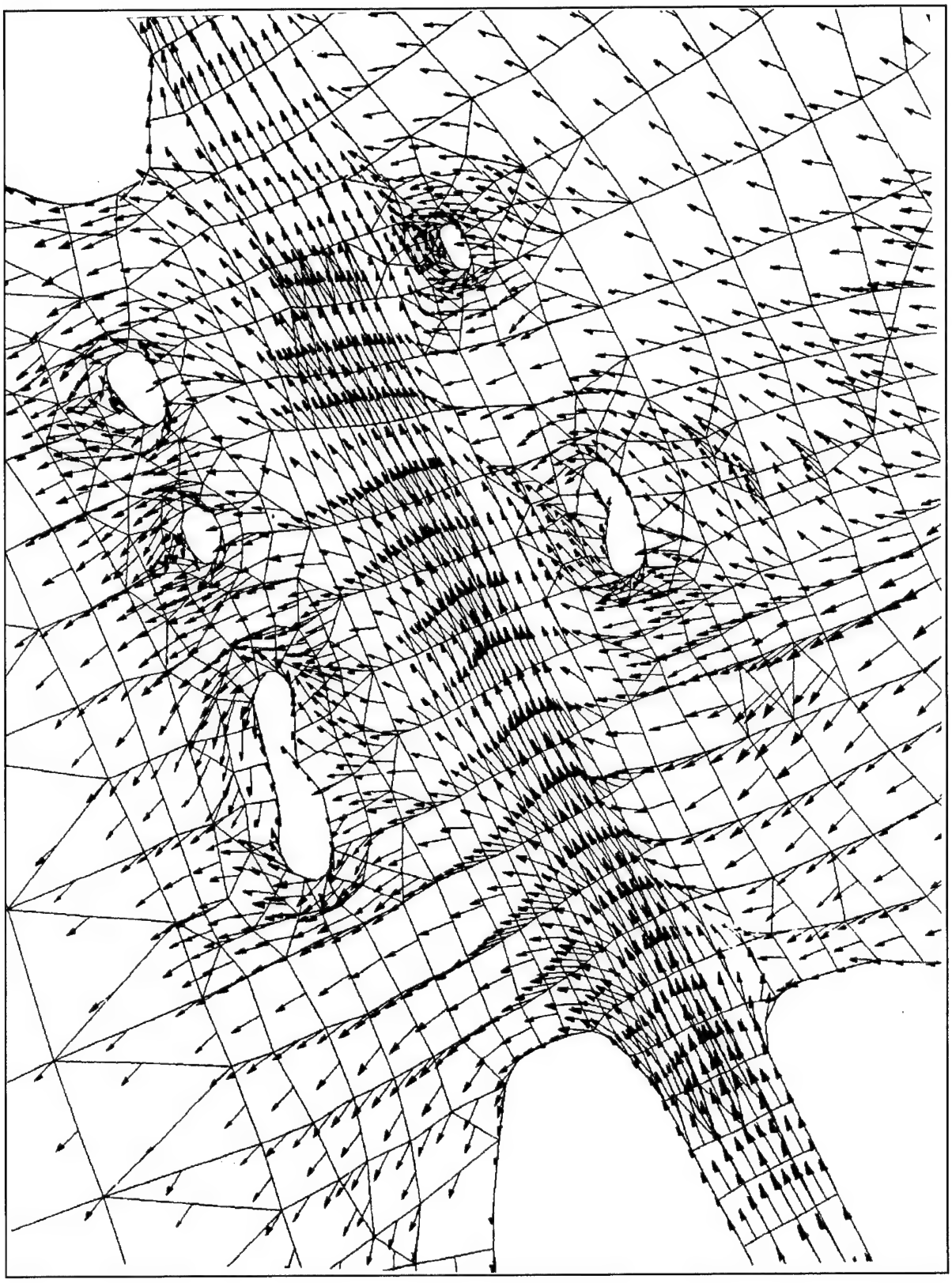

Figure 44. Illustration of flow pattern in model for flood

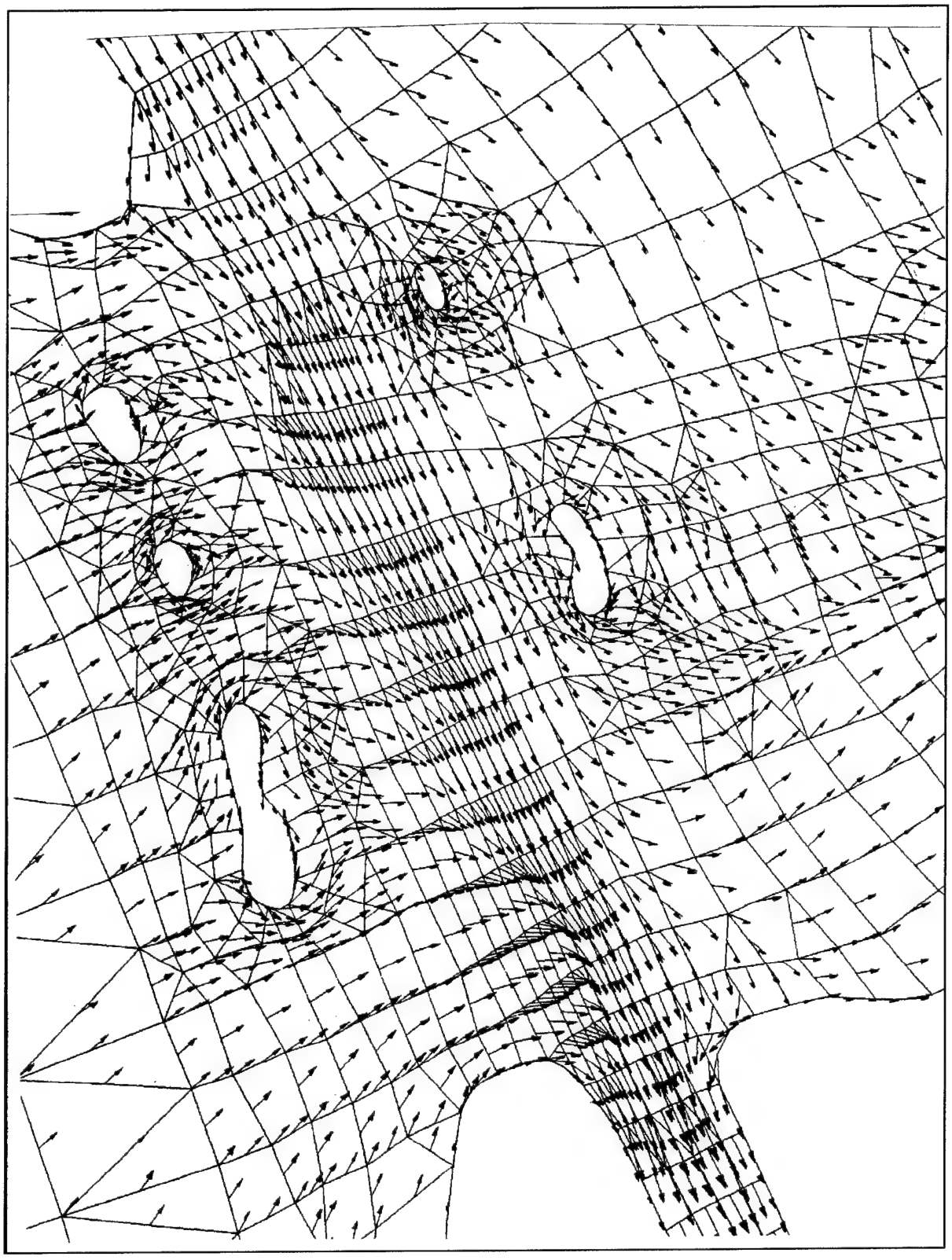

Figure 45. Illustration of flow pattern in model for ebb

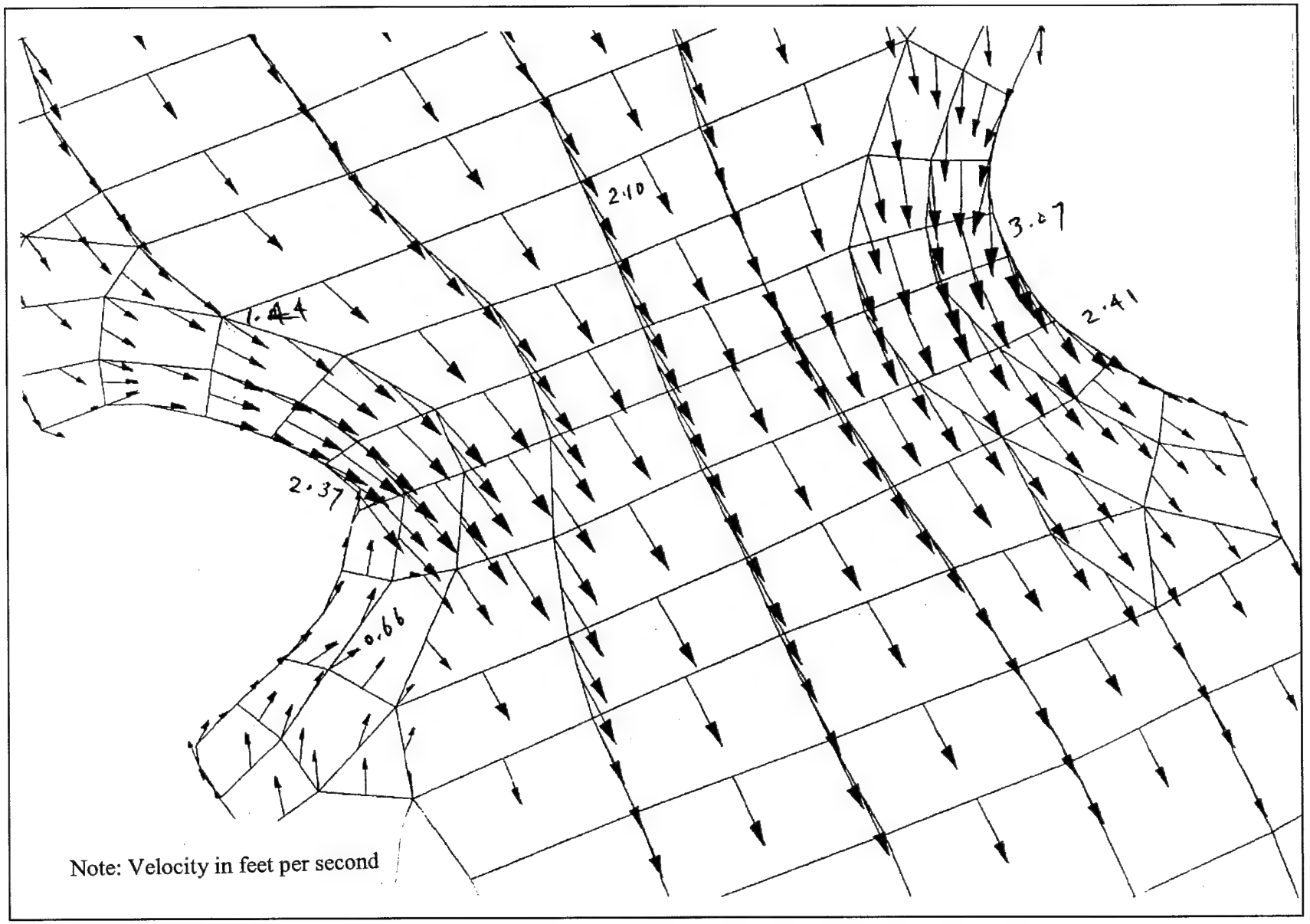

Figure 46. Illustration of flow pattern in the entrance channel (To convert to meters per second, multiply by 0.3048)

Bed Shear Stress

Among various parameters, transport rate of noncohesive sediment has been shown to be a function of a certain power of velocity or a function of bed shear stress. The velocity vectors obtained from the model have been replotted with the cube of velocity magnitude but maintaining the same directions. Such plots for the flood and ebb condition are shown in Figures 47 and 48, respectively. A comparison of these two figures indicates that the flood current has a higher potential for sediment transport than the ebb current. As would be expected from the geometry and depths in the area, sediment transport would be predominant along a natural channel between the GIWW and the entrance to Rollover Bay. Bed shear stress values were calculated using the velocity magnitudes obtained from the numerical model. Representative plots for the flood and ebb condition are shown in Figures 49 and 50, respectively. The magnitudes of bed shear stresses in the area of interest are low. Hence, both the figures do not indicate any substantial variation in the bed shear stress values indicated by the ranges selected with the color code. As would be expected, the bed shear stresses are relatively higher within the area of Rollover Pass channel because of higher tidal velocities.

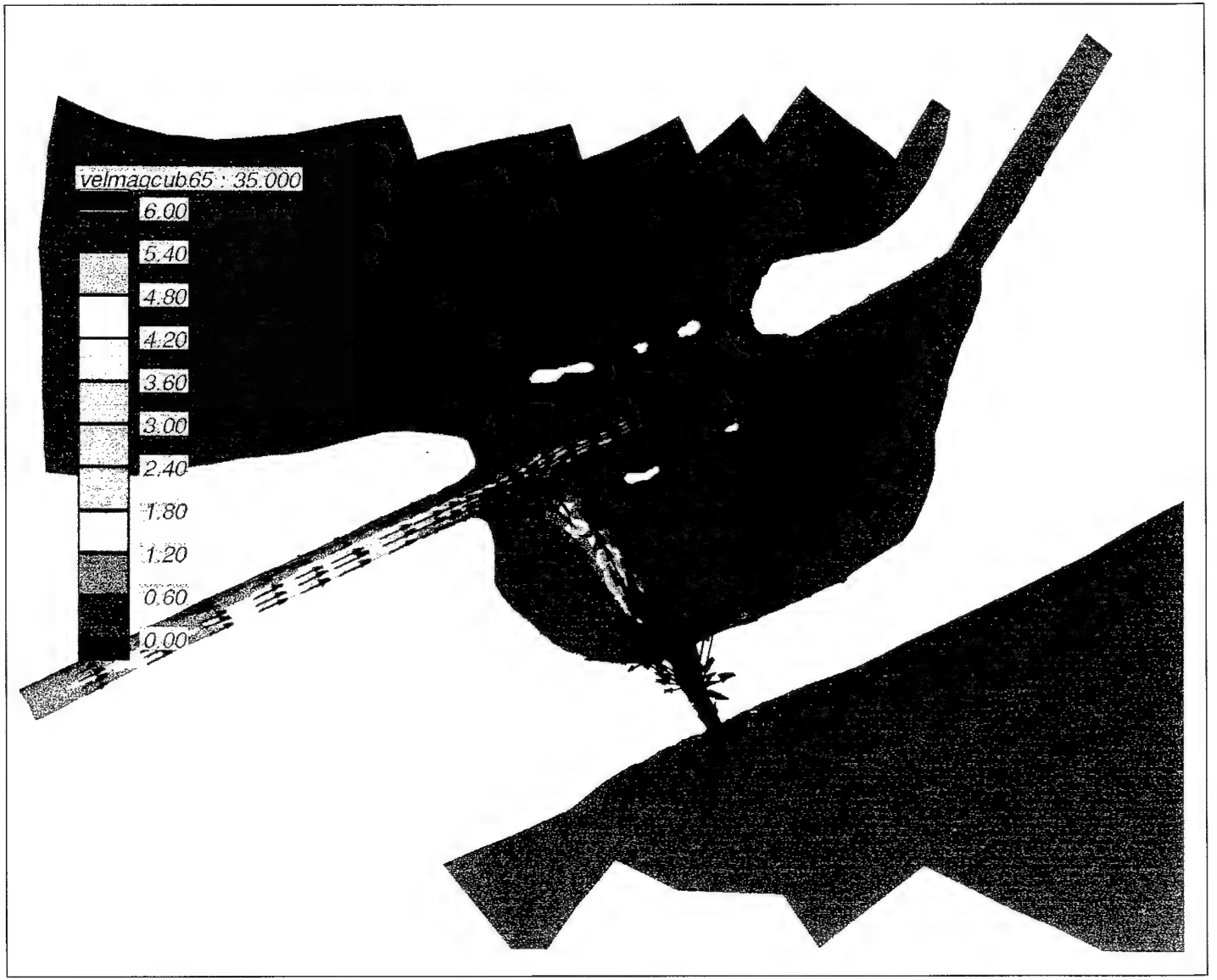

Figure 47. Illustration of velocity cubed values in model during flood

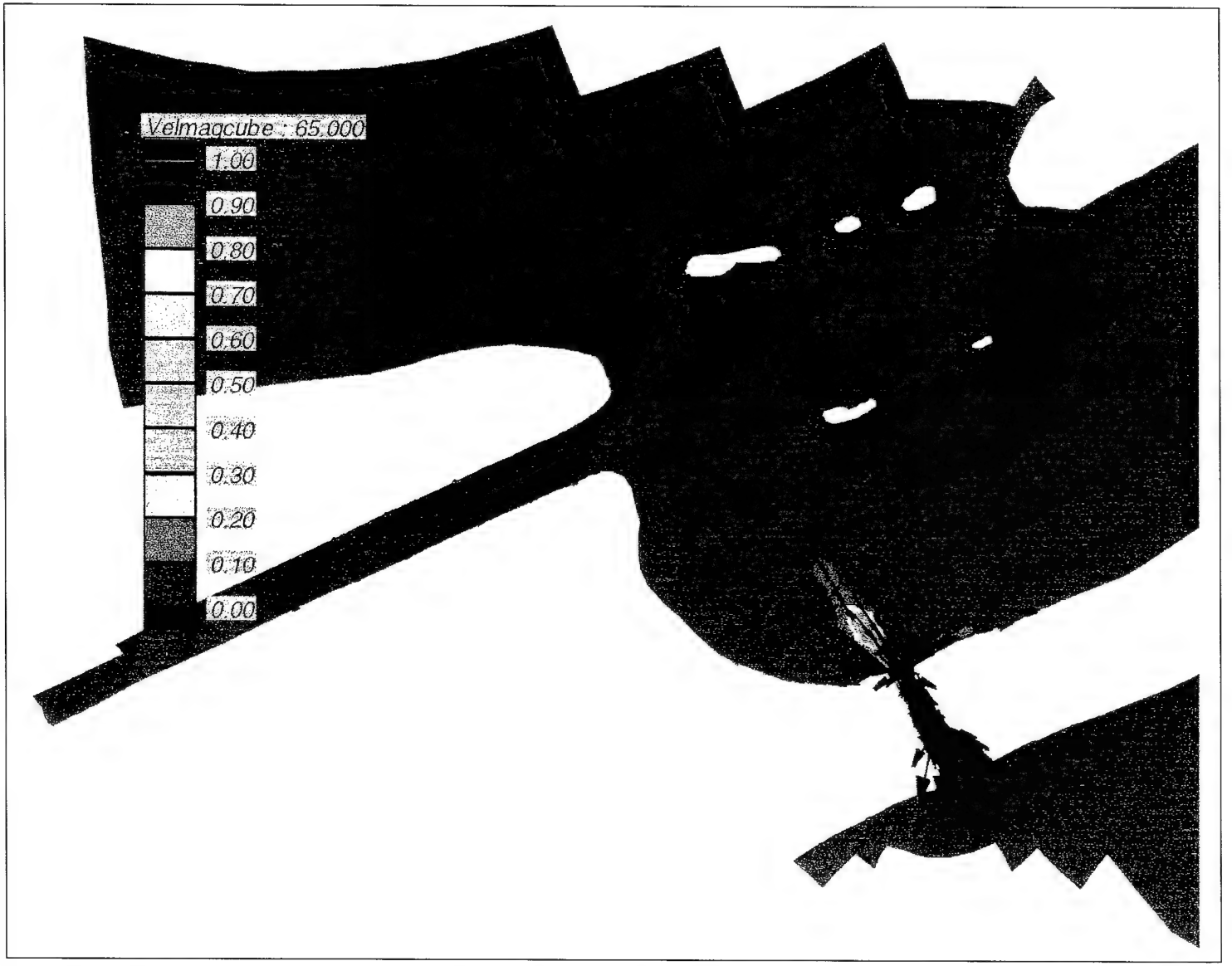

Figure 48. Illustration of velocity cubed values in model during ebb (Velocity is in feet per second. To convert to meters per second, multiply by 0.3048)

Figure 49. Illustration of bed shear stress distribution in model during flood

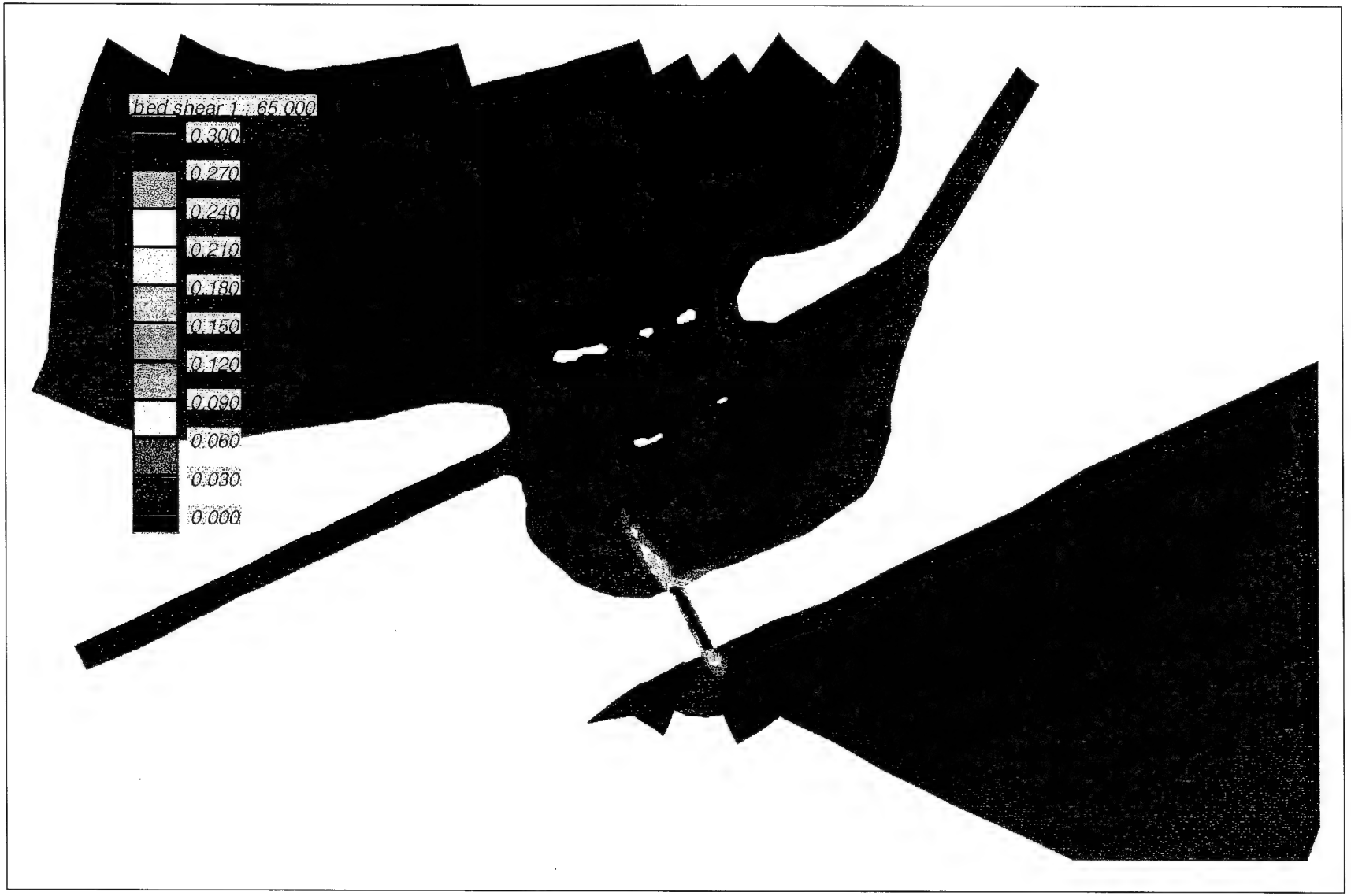

Figure 50. Illustration of bed shear stress distribution in model during ebb

4 Sediment Trap Configuration

Design Factors

The following factors are taken into account while designing the sediment trap:

a. The trap needs to be located at a place of maximum sediment transport, and it needs to be close to the GIWW.

b. It should have appropriate navigational access for a dredge to get in and get out without difficulty.

c. The depth and size of the trap should permit safe operation of a dredge.

d. The storage volume of the trap should permit adequate temporary storage of the sediment.

e. Preferably, the trap should catch both fine and coarse sediment.

f. The prevailing flow pattern should be approximately normal to the longer side of trap.

Trap Layout/Plan Configuration

Three main types of layouts were considered:

a. Trap isolated from GIWW with access from the existing deep channel.

b. Trap with its entire length connected to the GIWW.

c. Trap isolated from GIWW with a navigation connection to the GIWW.

Flow patterns obtained from the numerical model for the flood tide and ebb tide are shown in Figures 51 and 52, respectively. The traps are located in the path of the flood and ebb currents so the currents are close to normal direction

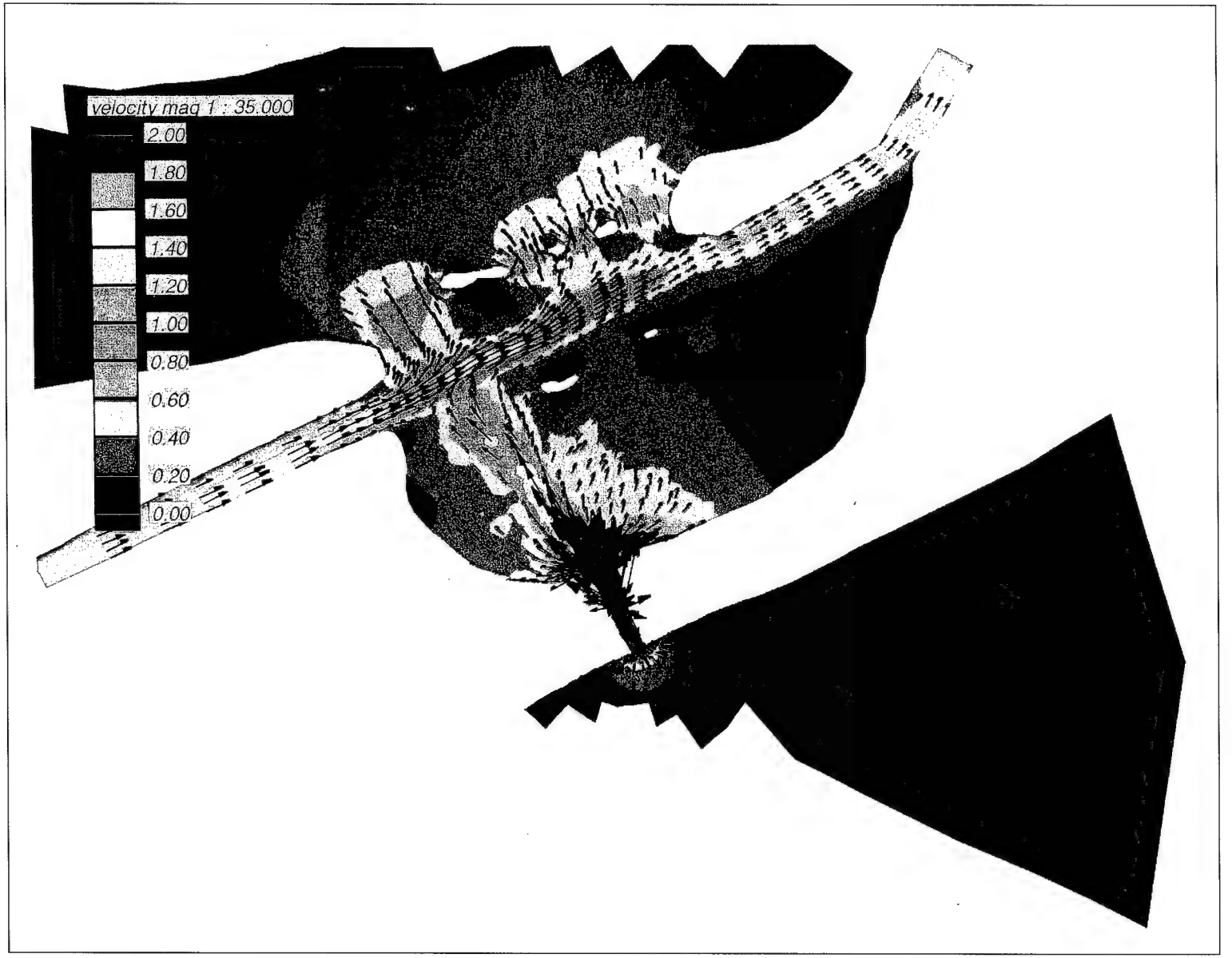

Figure 51. Illustration of flow pattern in model for flood (Velocity is in feet per second. To convert to meters per second, multiply by 0.3048)

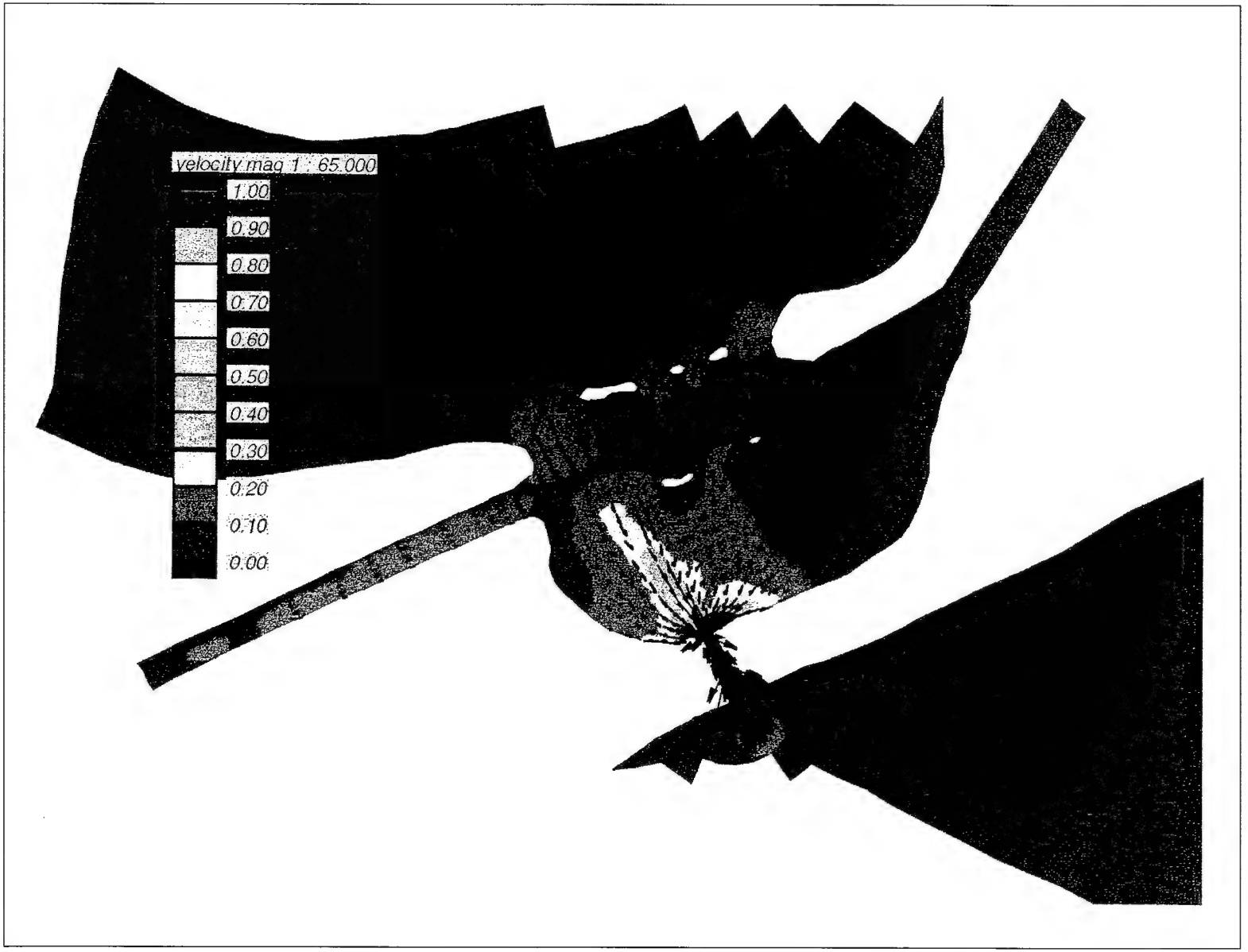

Figure 52. Illustration of flow pattern in model for ebb (Velocity is in feet per second. To convert to meters per second, multiply by 0.3048)

with respect to the longer dimension of the trap. Eleven different geometrical shapes were considered (Figures 53 through 63). All the drawings show bottom dimensions of a sediment trap. Side slopes are not shown, which will depend upon the natural angle of repose at the site.

Layout 1

Layout 1 (Figure 53) consists of a long, narrow rectangular trap covering the entire length of GIWW within the Rollover Bay from Section 2085 to 2170. In essence, the trap would represent a widening of the present navigation channel on both sides from the present base width of 38 to 68 m (125 to 225 ft). The Galveston District wanted this simple layout evaluated for its merits and demerits for comparison with other layouts.

Merits of the layout are:

a. Simple to dredge and operate.

b. No separate navigational access to the sediment trap is needed.

Demerits are:

a. It will trap more sediment within the GIWW requiring removal of larger volume of sediment with an increased frequency of dredging.

b. Since sediment moving across the GIWW is not uniform, the entire length of the trap will not be effective in trapping sediment. Hence, unwanted initial dredging is involved.

Layout 2

Layout 2 (Figure 54) consists of a square-shaped trap isolated from the channel. Flow pattern in the Rollover Bay during the flood and ebb is fan-shaped. Flood water entering the bay spreads over a wider area inside the bay. The length of such a trap normal to the flow would not be adequate to trap the sediment, which may bypass the trap.

Layout 3

Layout 3 (Figure 55) consists of a trapezoidal trap isolated from the channel. This would trap sediment coming through the deep channel connected to the pass. However, the length is inadequate and it will not be efficient for the same reasons applicable for Layout 2.

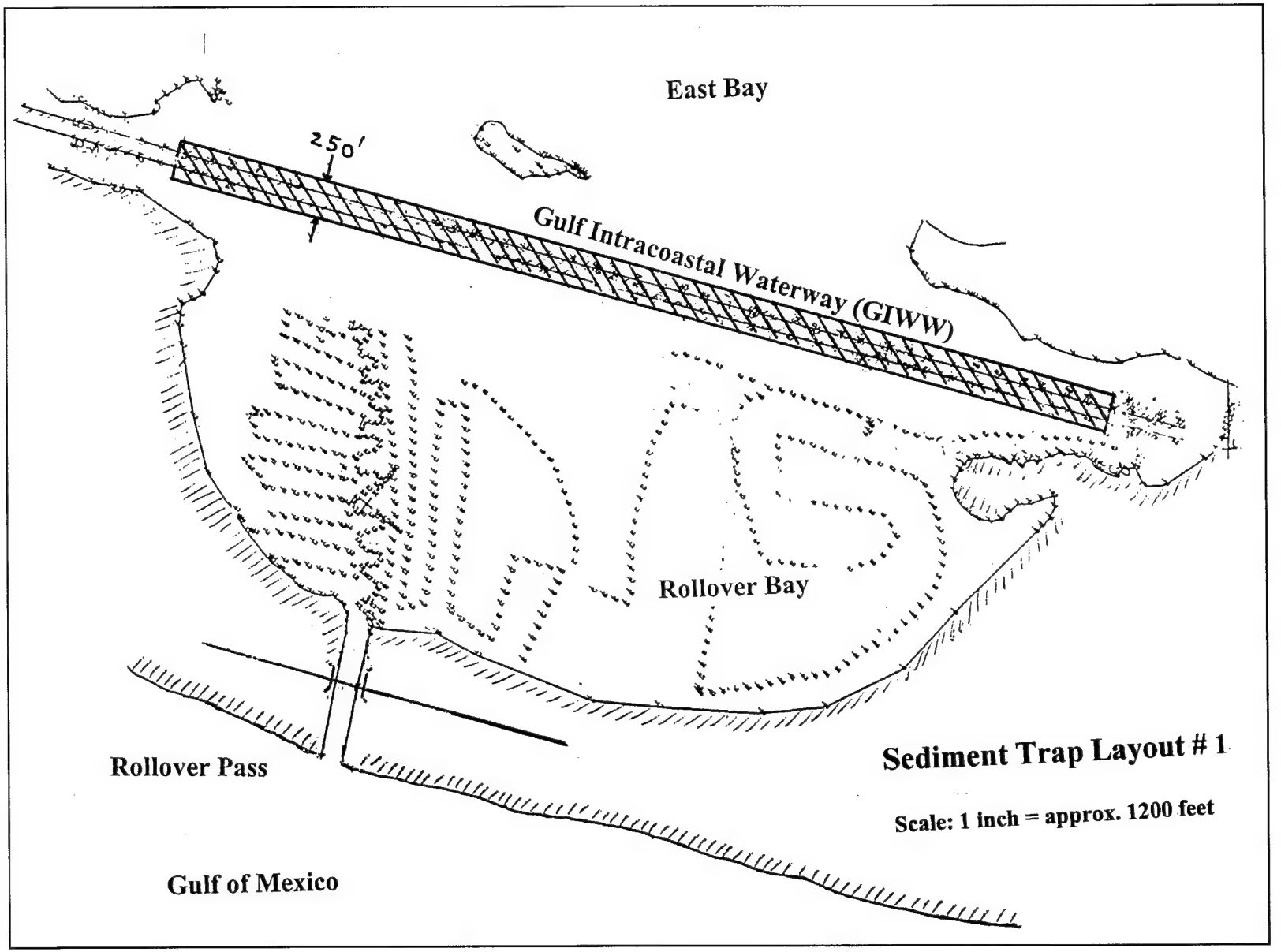

Figure 53. Sediment trap Layout 1 (Distance is in feet. To convert feet to meters, multiply by 0.3048)

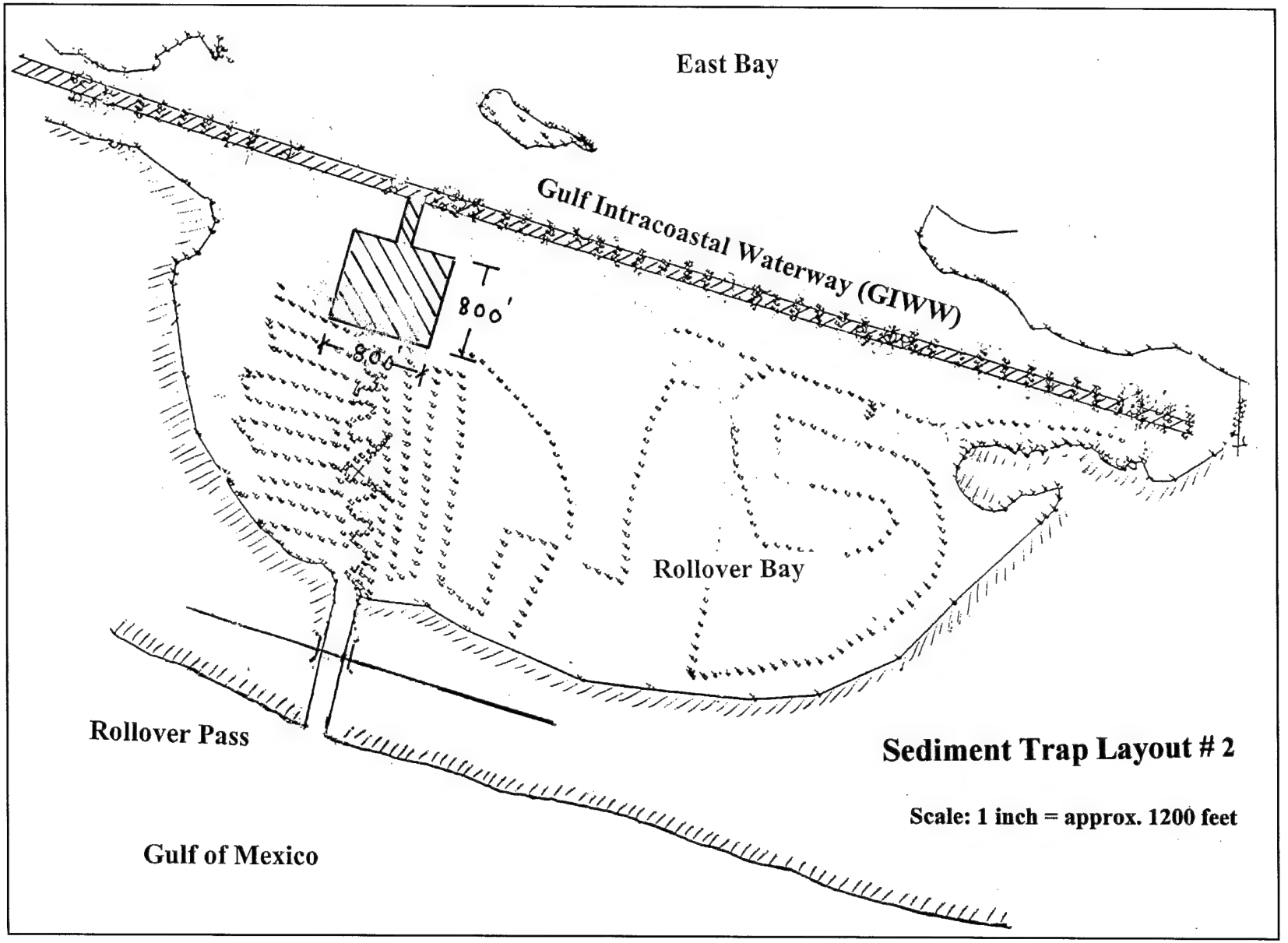

Figure 54. Sediment trap Layout 2 (Distance is in feet. To convert feet to meters, multiply by 0.3048)

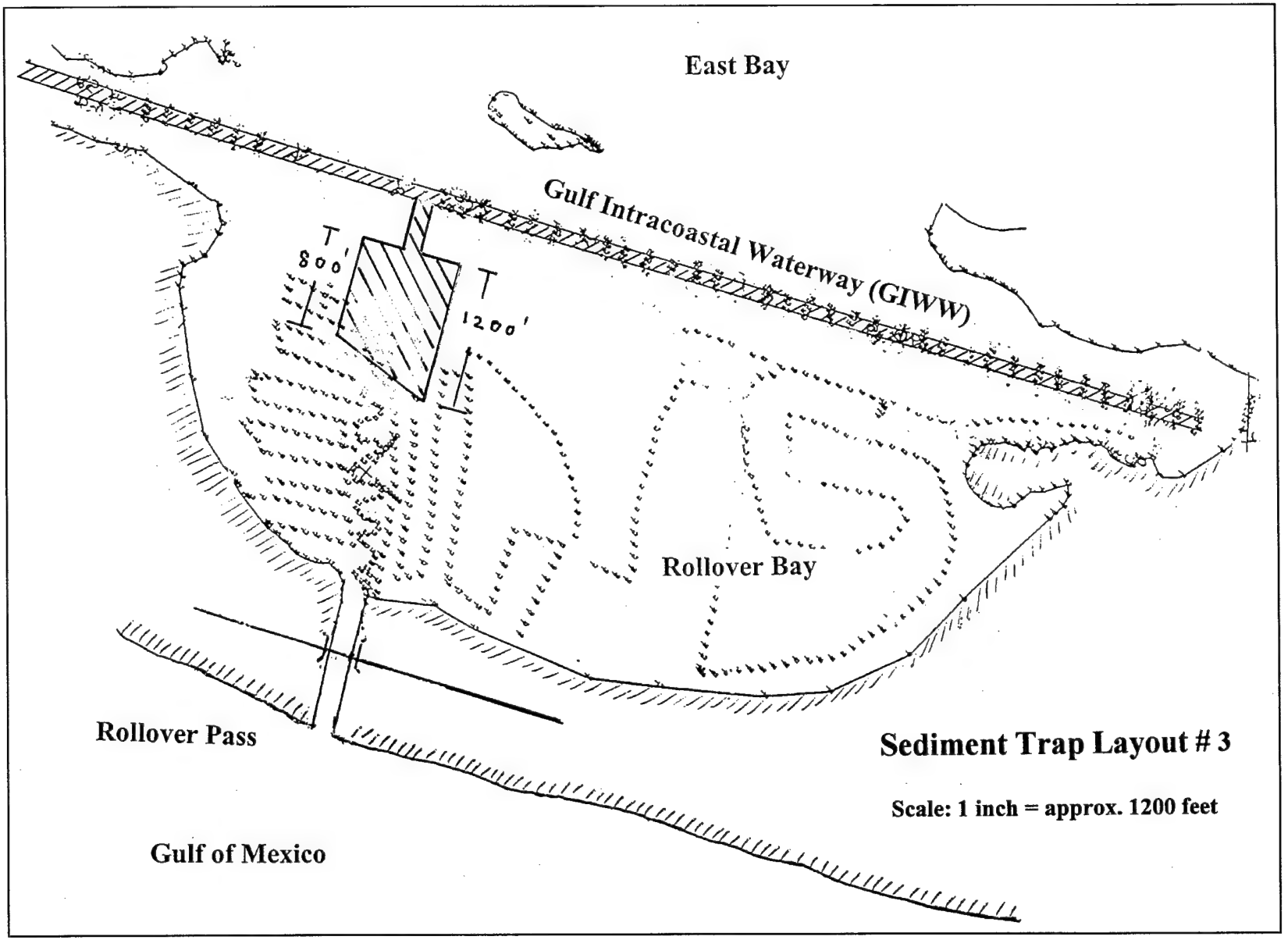

Figure 55. Sediment trap Layout 3 (Distance is in feet. To convert feet to meters, multiply by 0.3048)

Layout 4

Layout 4 (Figure 56) consists of a trapezoidal trap oriented parallel to the channel, but detached from the GIWW. This type planform for a sediment trap would be expected to function well.

Layout 5

Layout 5 (Figure 57) consists of a trap aligned symmetrically on both sides of the GIWW. This is a modified version of Layout 1 in that the length is substantially smaller and the width is larger. This layout is expected to be better than Layout 1 because it involves a smaller volume of initial dredging, and it covers the critical portion of the channel that has higher siltation. Hence, formation of local shallowing in the channel might be reduced because sediment would be spread out over a wider area.

Layout 6

Layout 6 (Figure 58) consists of a bowl-shaped planform trap connected longitudinally to the channel. The length of the trap is 762 m (2,500 ft) and the maximum width is 244 m (800 ft). This would be expected to trap sediment, but it would not be contained within the newly dredged area. Some of the sediment would spread over the present channel.

Layout 7

Layout 7 (Figure 59) consists of a trap with the same width as that of Layout 6, but the length of trap covers the entire length of higher siltation zone, referred to in Chapter 2 of this report as D-D, from Transect 2136 to 2166. The length of the trap is 914 m (3,000 ft) and the maximum width is 244 m (800 ft). Since this trap has a larger volume and covers the appropriate zone of siltation, it would trap a larger volume of sediment; however the direct connection between the trap and GIWW would permit transfer of sediment from the trap to the GIWW, which is not a desirable feature.

Layout 8

Layout 8 (Figure 60) consists of a trapezoidal-shaped trap connected to the channel over a length of 914 m (3,000 ft) with a maximum width of 122 m (400 ft). This trap has a smaller volume and has the same disadvantages as Layout 7 because of its direct connection with the GIWW.

Layout 9

Layout 9 (Figure 61) consists of a triangular-shaped trap isolated from the channel with two navigational connections to the GIWW. This would permit

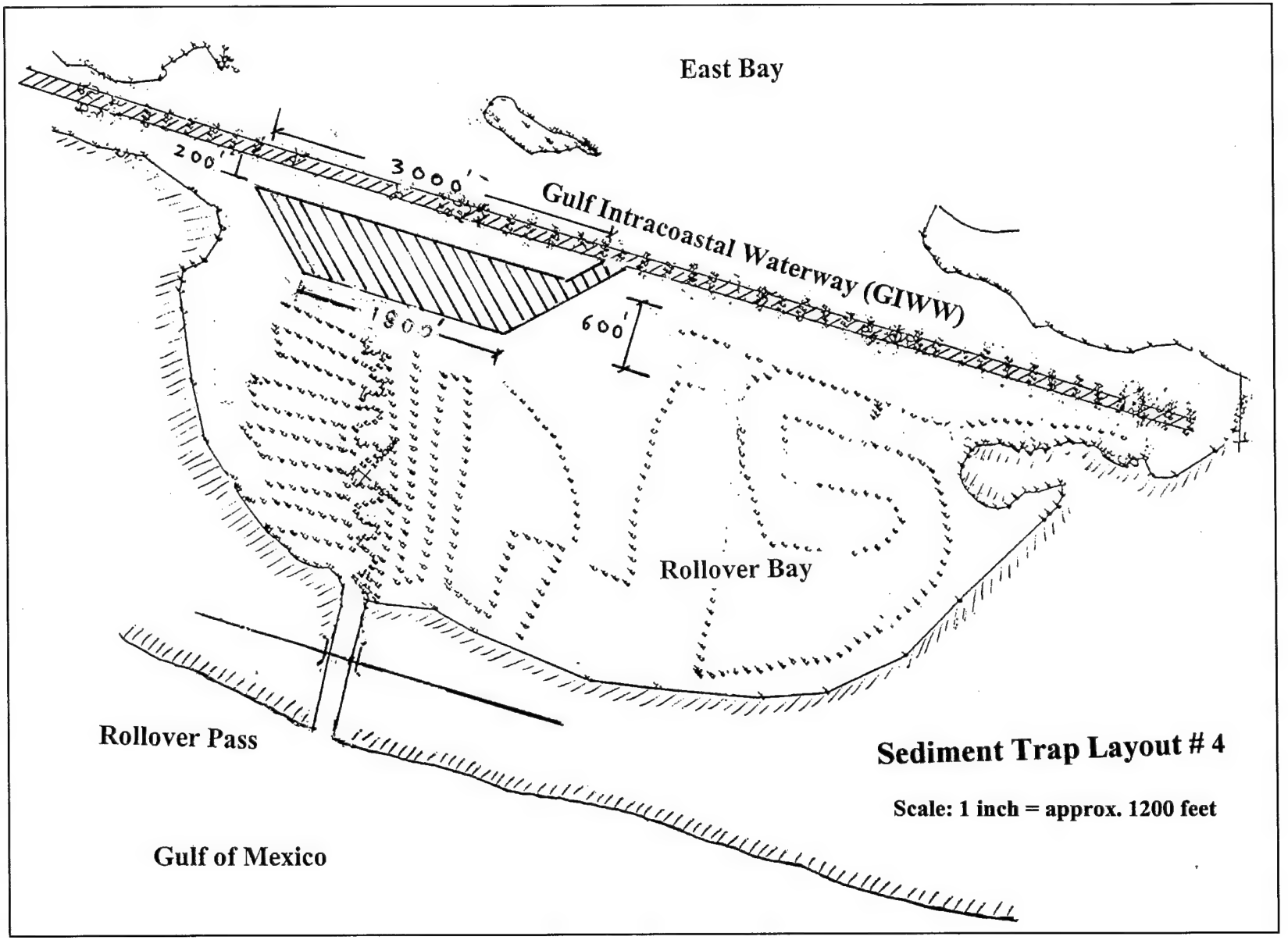

Figure 56. Sediment trap Layout 4 (Distance is in feet. To convert feet to meters, multiply by 0.3048)

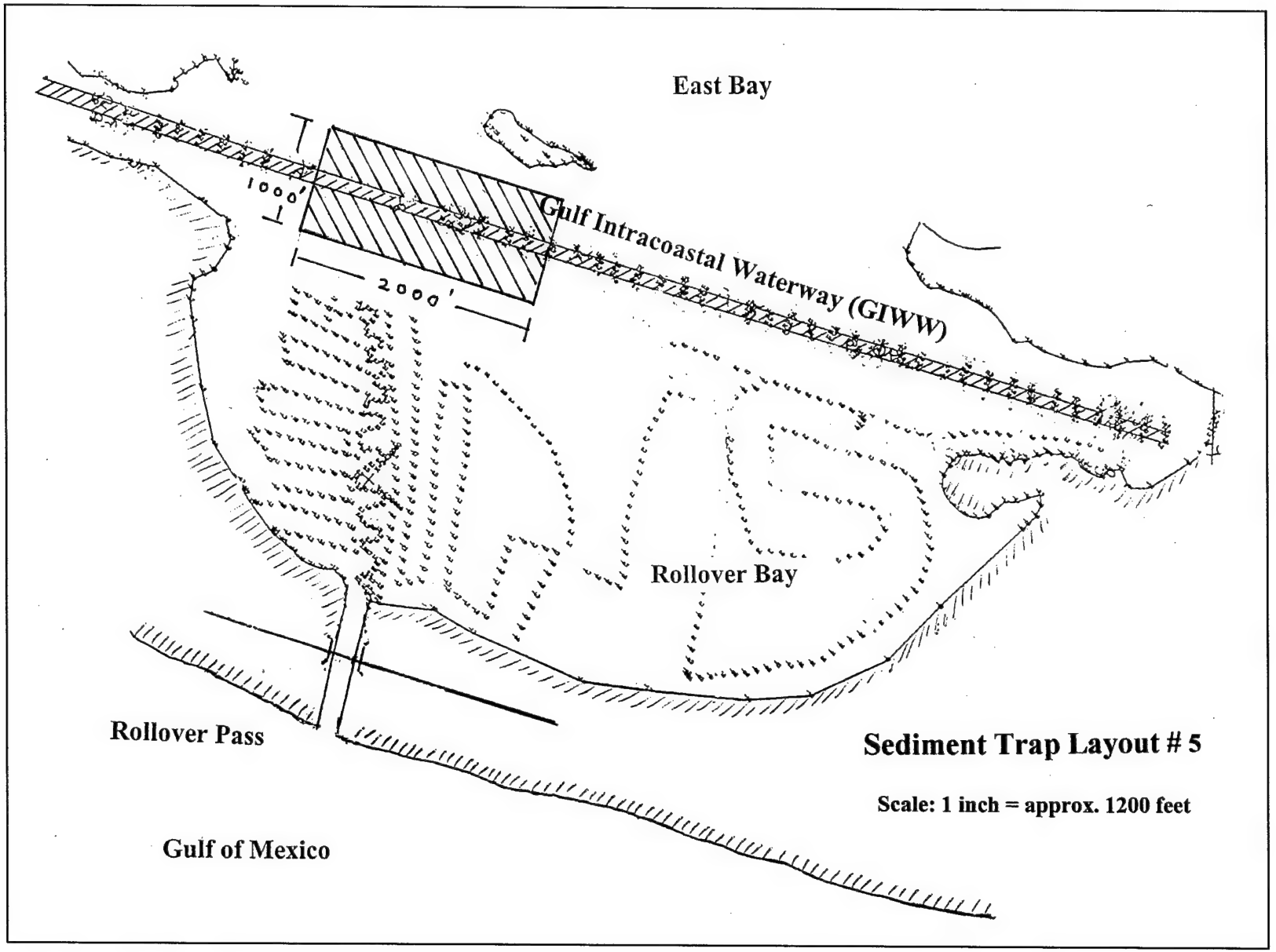

Figure 57. Sediment trap Layout 5 (Distance is in feet. To convert feet to meters, multiply by 0.3048)

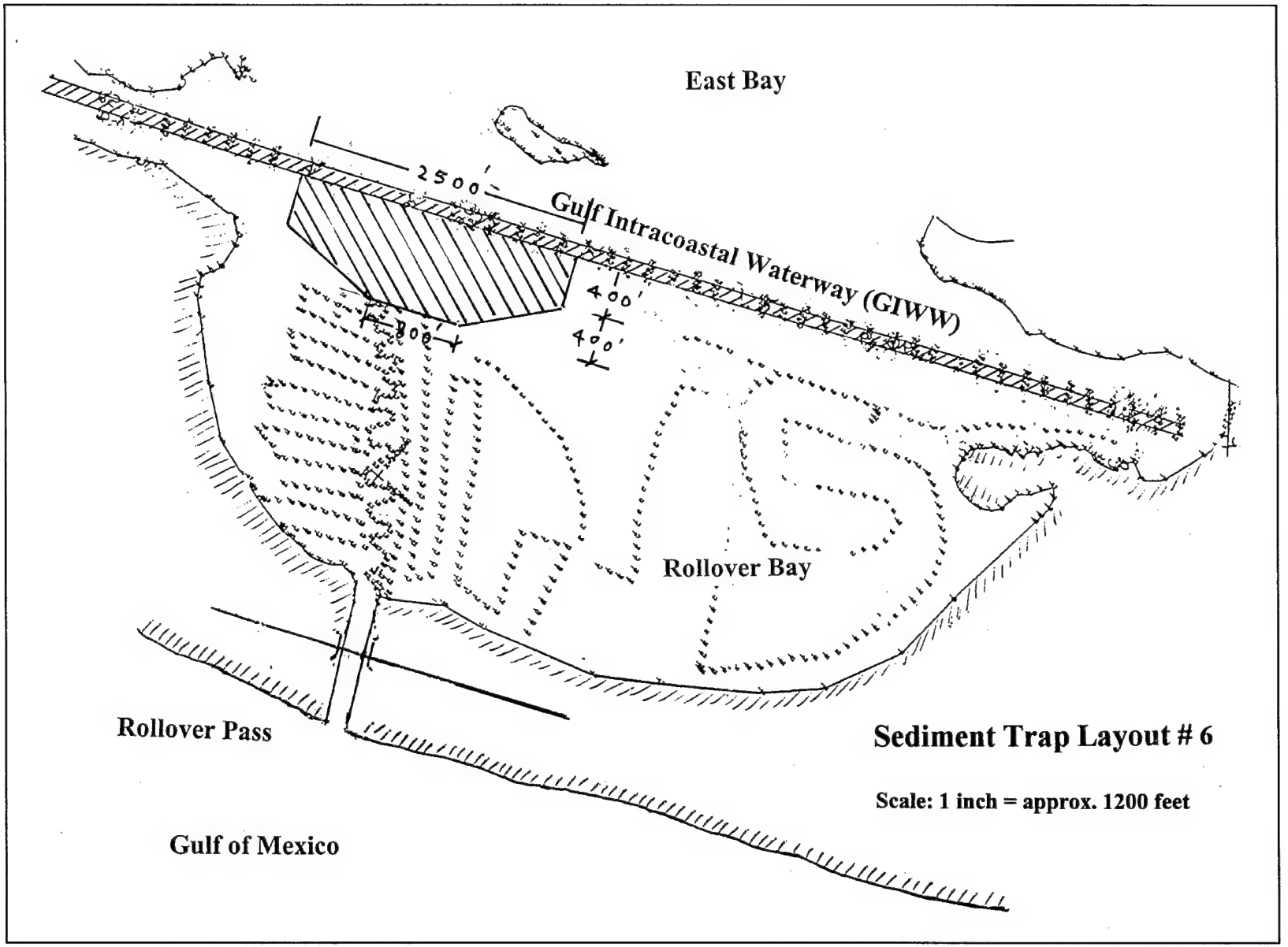

Figure 58. Sediment trap Layout 6 (Distance is in feet. To convert feet to meters, multiply by 0.3048)

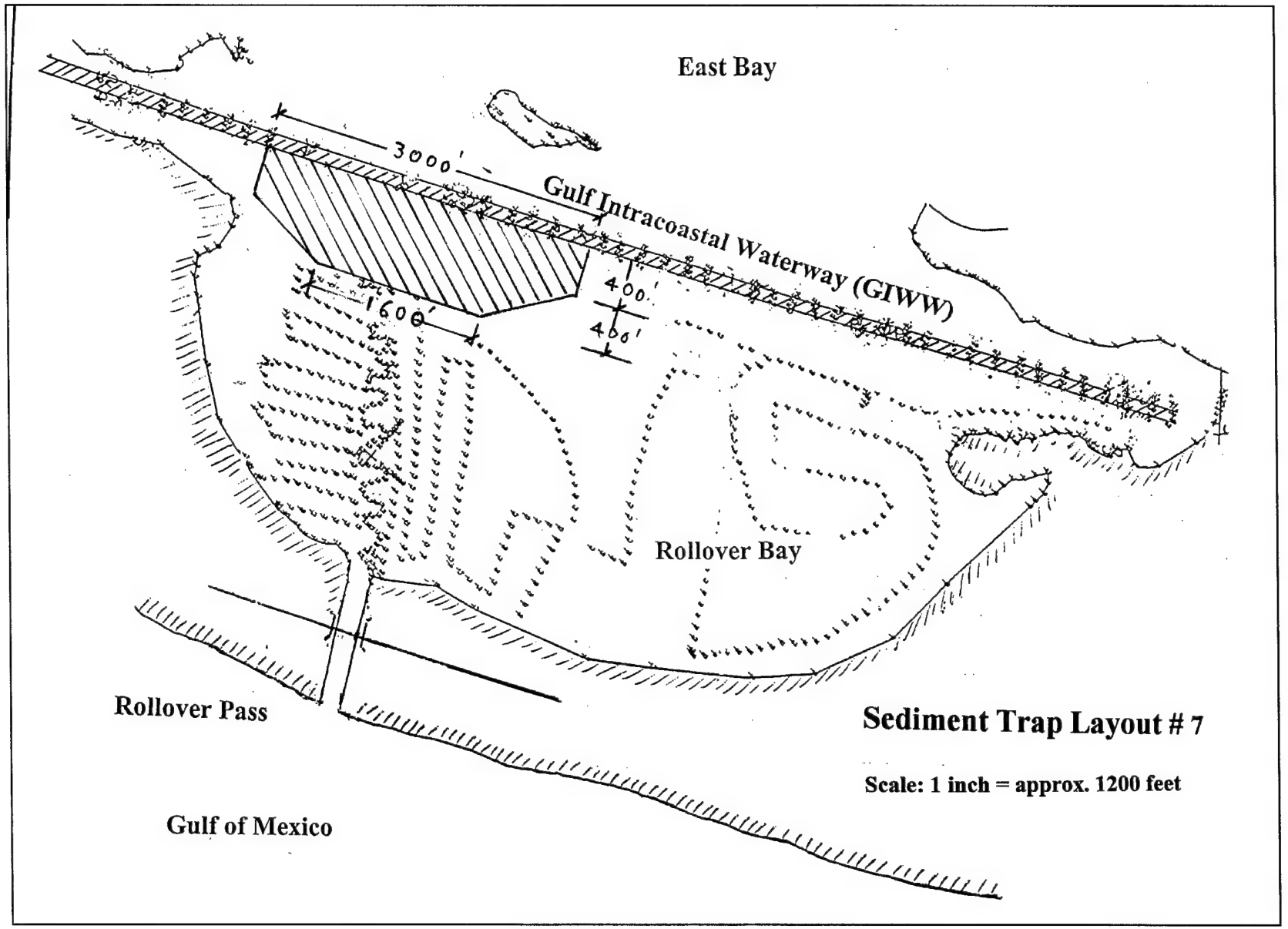

Figure 59. Sediment trap Layout 7 (Distance is in feet. To convert feet to meters, multiply by 0.3048)

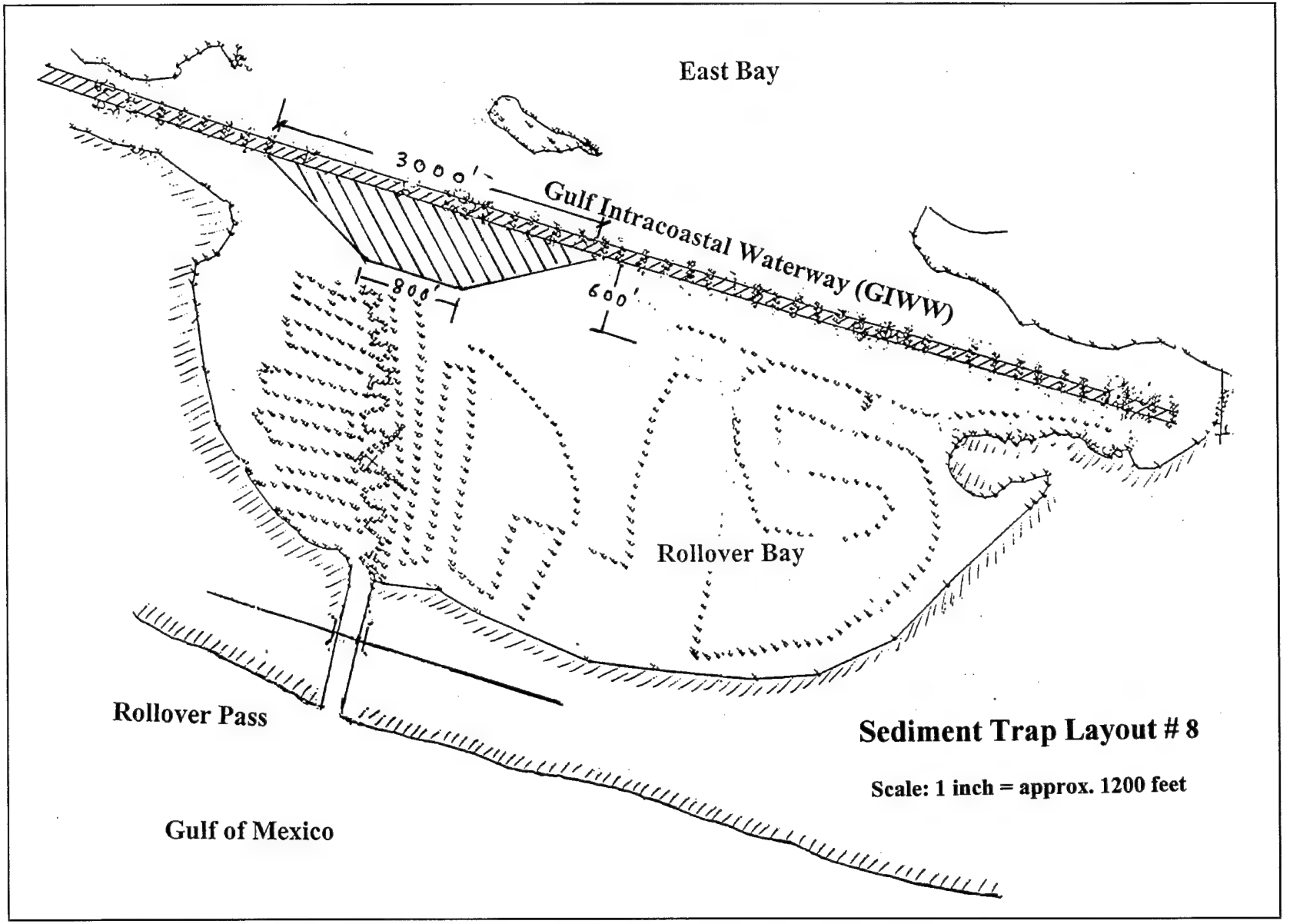

Figure 60. Sediment trap Layout 8 (Distance is in feet. To convert feet to meters, multiply by 0.3048)

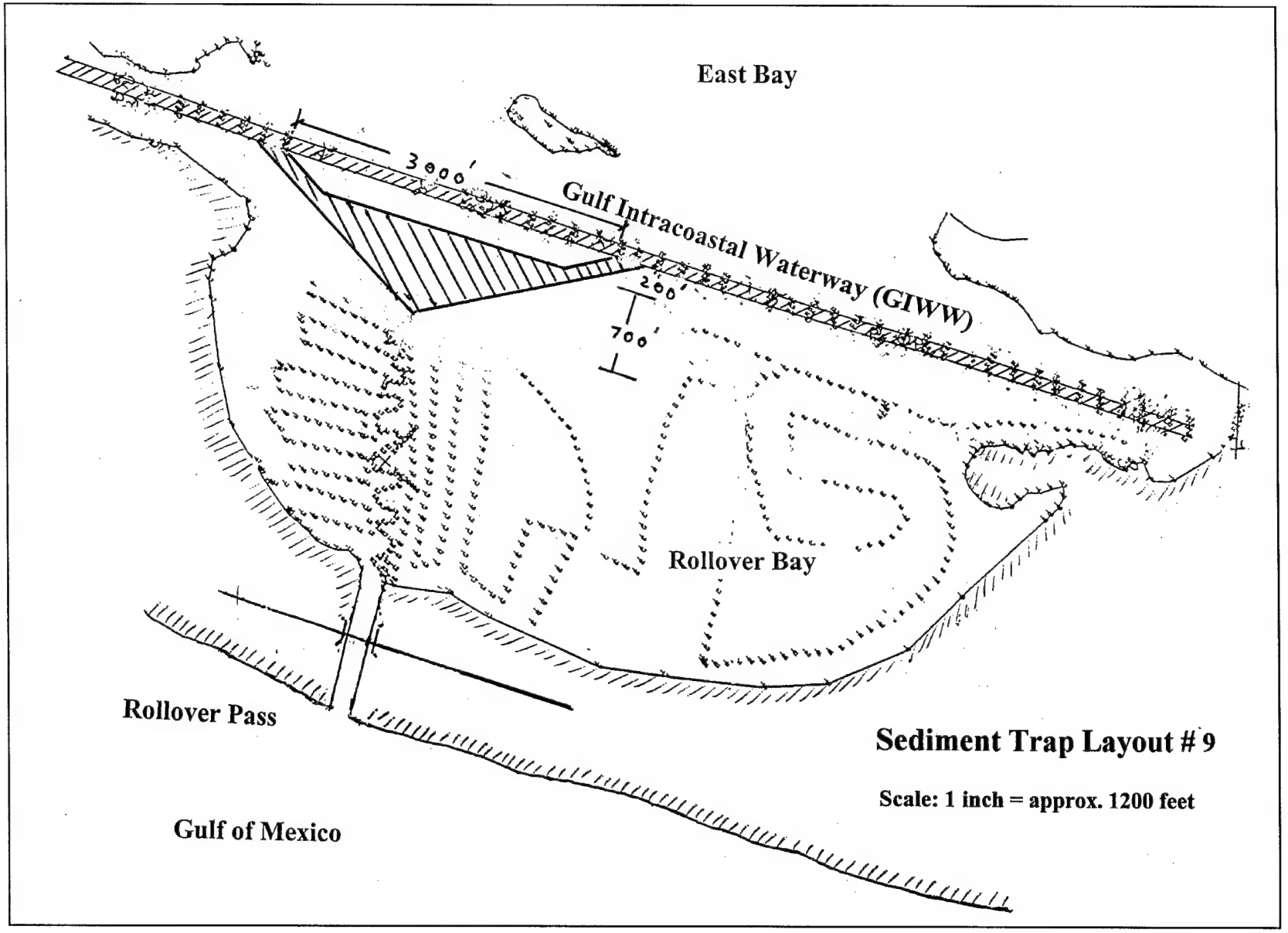

Figure 61. Sediment trap Layout 9 (Distance is in feet. To convert feet to meters, multiply by 0.3048)

some flow through the trap, washing away some of the accumulated sediment to the GIWW.

Layout 10

Layout 10 (Figure 62) consists of a rectangular trap isolated from the channel with two navigational connections with the channel. Because of the right-angled connection with the main channel, the currents inside the trap would not be high. Therefore, the trapping efficiency would be better than that of Layout 9.

Layout 11

Layout 11 (Figure 63) consists of a rectangular trap isolated from the channel by 61 m (200 ft) and has only one navigational connection with the channel. Because of a single connection with the main channel, there would be no through currents inside the trap. Therefore, the trapping efficiency would be high. The proposed sediment trap may be provided in three phases, if needed, as shown in Figure 64. The advantage of phasing the work would be lower initial costs and it would provide an opportunity of field testing of the proposal for its efficacy.

Discussion on Sediment Trap Design

a. Among the various layouts described, the layouts detached from GIWW and having their longer dimension parallel to the GIWW are preferred.

b. If a strip or higher elevation is left between the channel and the trap, it would act advantageously as a barrier for the bed load crossing the trap and entering the channel.

c. Only one navigational connection is suggested between the trap and the channel. The advantage of a single connection with the main channel would be to avoid longitudinal through-currents inside the trap, and hence, achieve a higher trapping efficiency. It is suggested that the width of connection to be 38 m (125 ft), which is the width of the GIWW at its base.

d. A connection located at the center of the trap would be directly in the path of high sediment transport, which may carry sediment into the GIWW. Hence, a connection at the eastern end of the trap is recommended rather than at the center of the trap.

e. Sediment is generally transported consistent with the flow pattern. Sediment particle size analysis suggests that ocean sediment enters the bay during flood tide, which then deposits in the GIWW. Taking into account the flow pattern obtained from the hydrodynamic model, there does not appear to be much scope for changing the principal location of the trap relative to the GIWW (Figure 65).

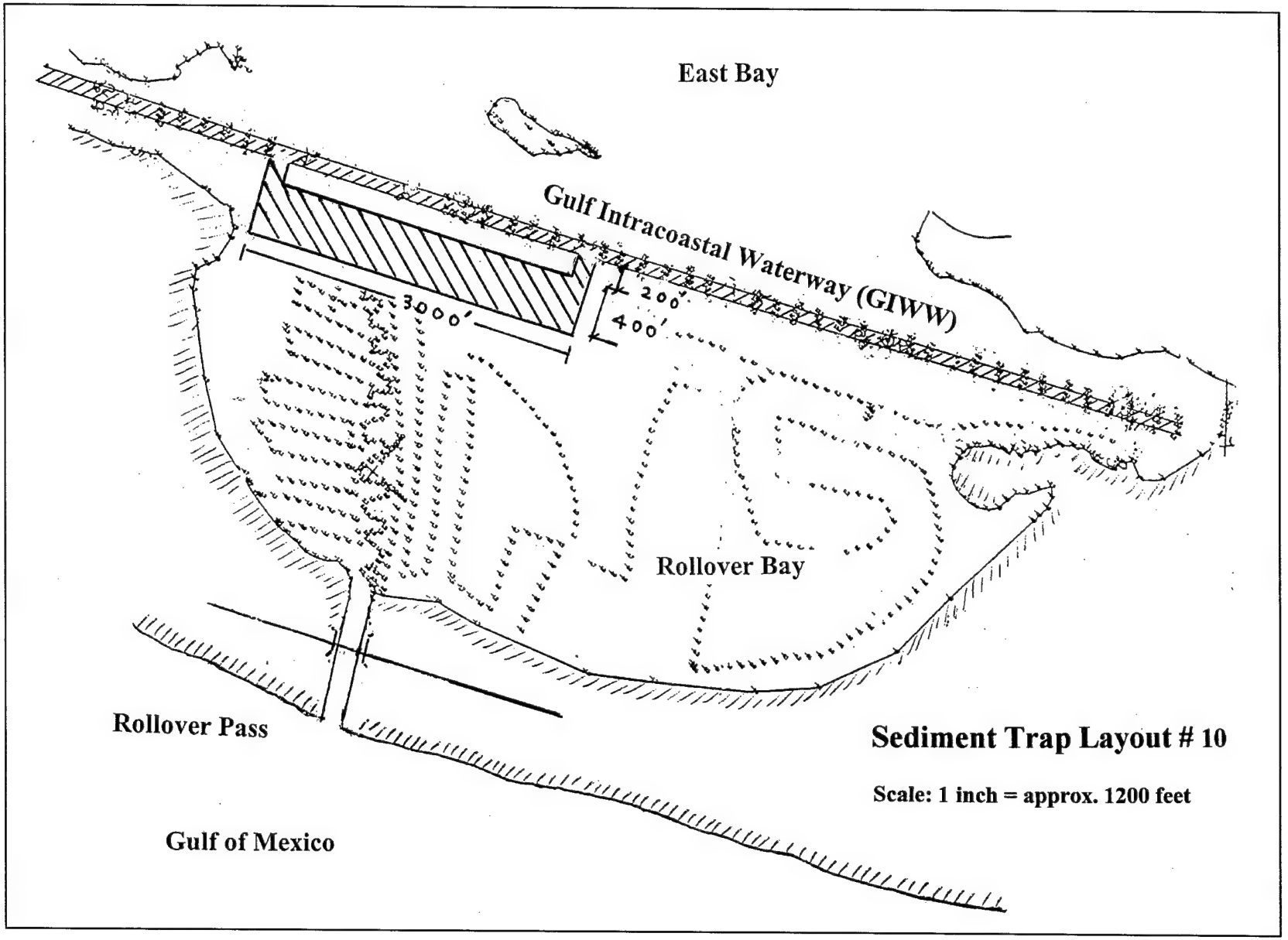

Figure 62. Sediment trap Layout 10 (Distance is in feet. To convert feet to meters, multiply by 0.3048)

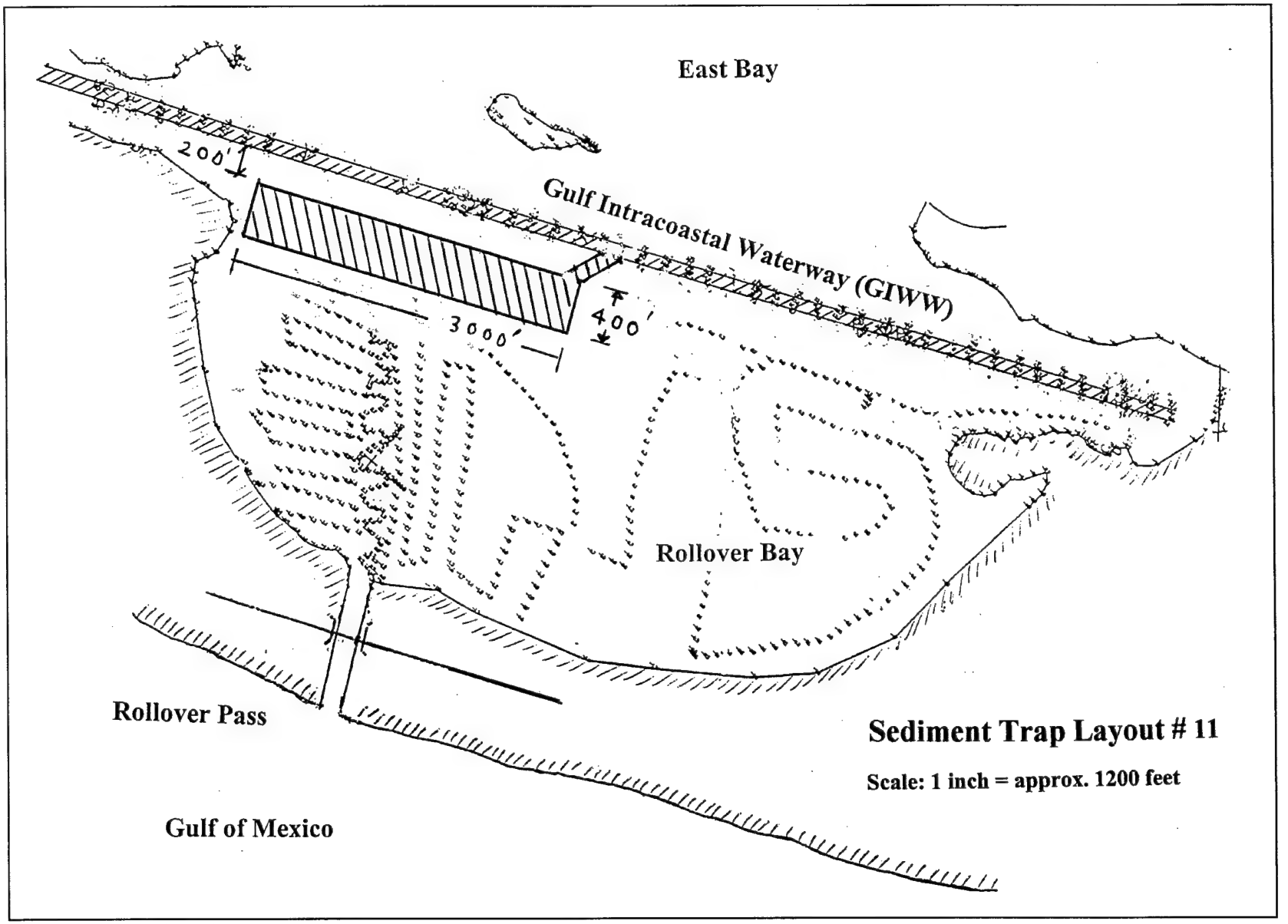

Figure 63. Sediment trap Layout 11 (Distance is in feet. To convert feet to meters, multiply by 0.3048)

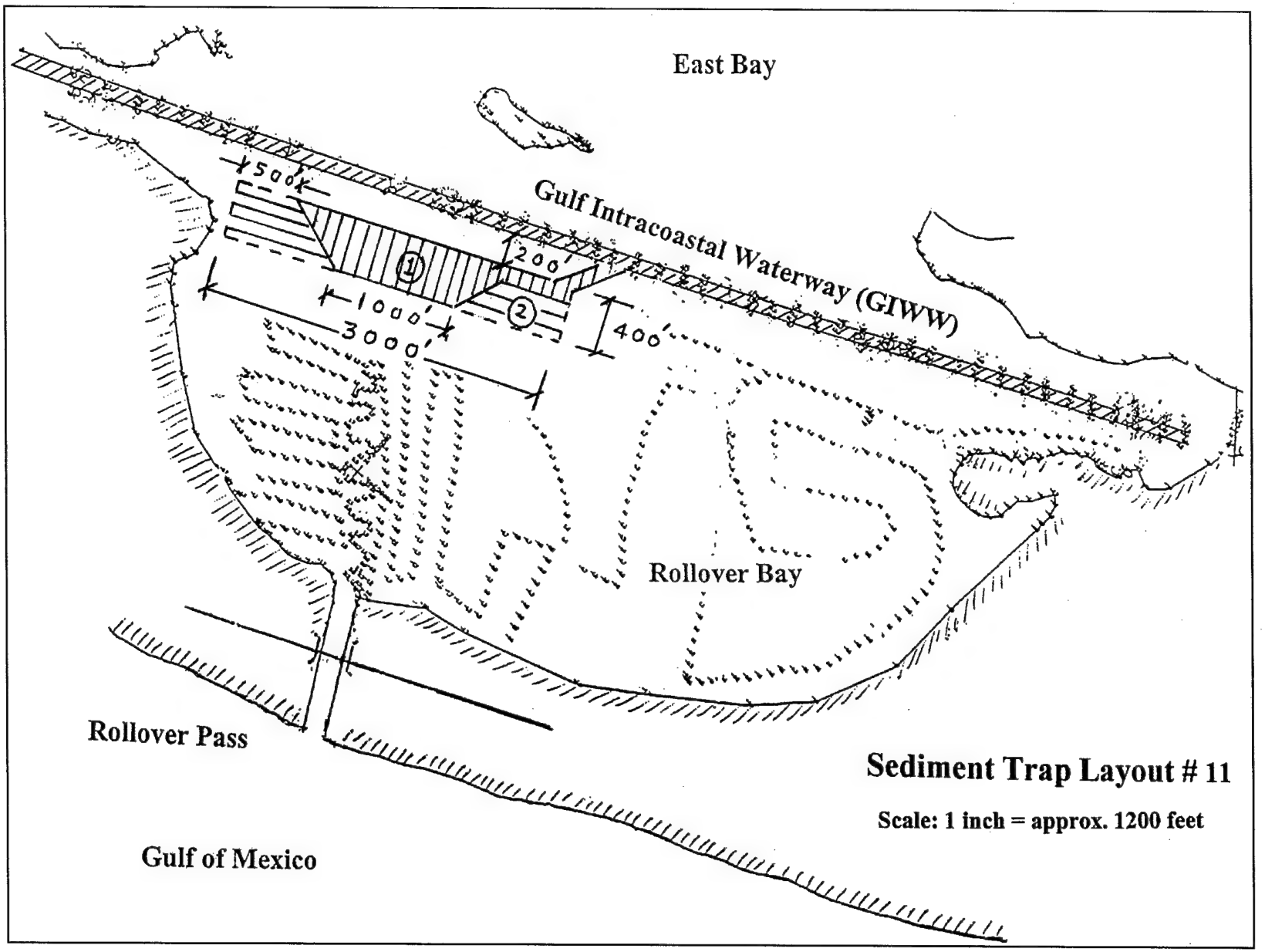

Figure 64. Construction phasing of sediment trap Layout 11 (Distance is in feet. To convert feet to meters, multiply by 0.3048)

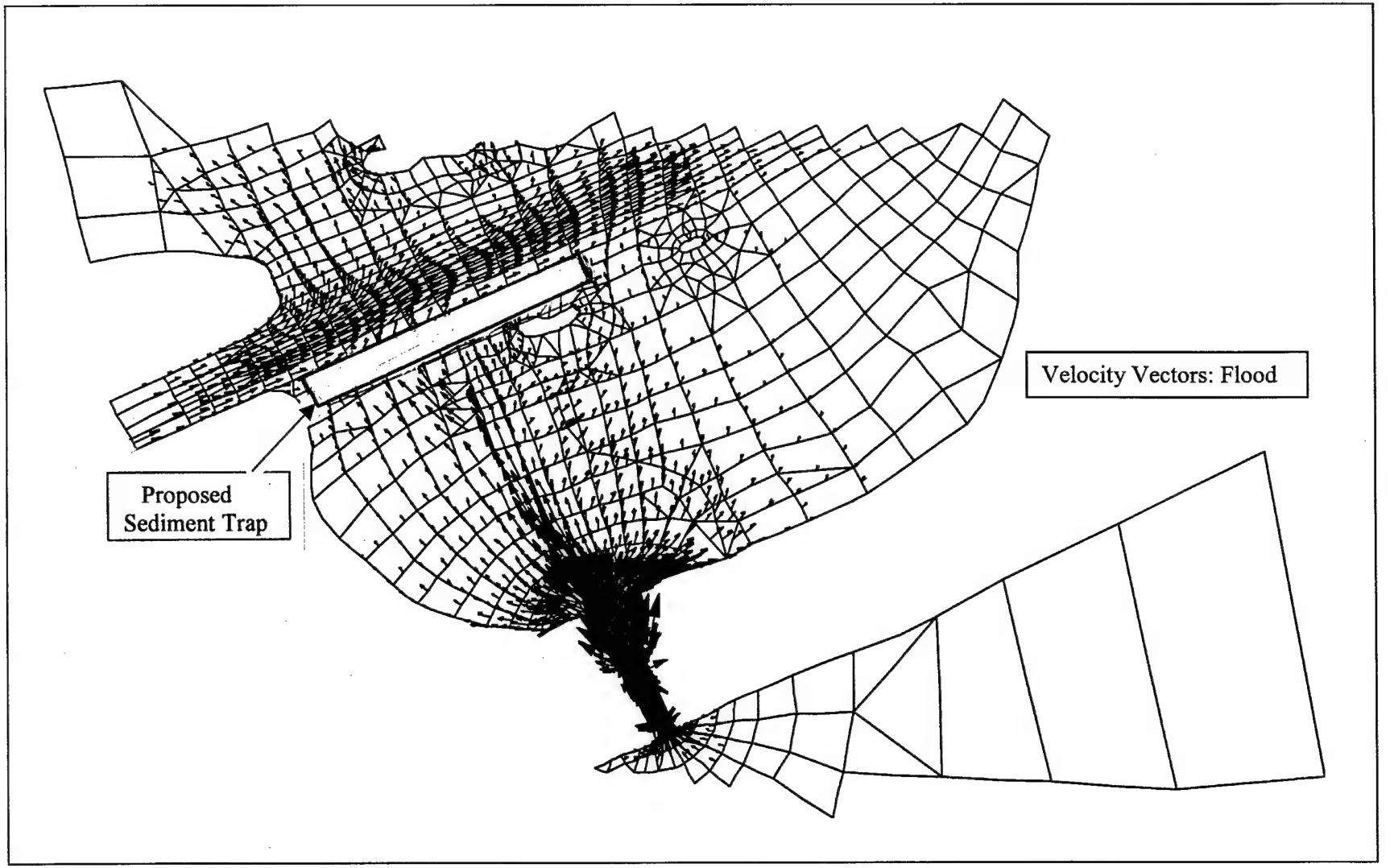

Figure 65. Proposed sediment trap superposed on flow pattern during flood

f. Three sources of sediment may be considered which include ocean, East Bay, and previous dredge material disposal areas. It is difficult to determine the relative contribution of each. The presence of coarse sediment within the GIWW indicates a possibility of the ocean acting as a source; however, the strong currents within the GIWW may be washing away finer sediments leaving behind coarse sediments.

g. Analysis of dredging data showed that siltation was considerably higher in Zone D-D between Sections 2166 and 2136. This reach consists of 15 elements of 61 m (200 ft) each. The length of sediment trap is suggested at 914 m (3,000 ft), which is equal to the length of the high siltation zone.

h. A width of 122 m (400 ft) is recommended for the trap, assuming that this will provide adequate room for a dredge to maneuver inside the trap. The second reason for keeping this width was to permit settling of a fraction of suspended sediment entering the bay from the seaside and crossing the GIWW. If a wider trap was considered necessary for providing more room for a dredge, it would be advantageous.

i. Table 3 shows that an estimated volume of sediment deposition in the zone of high siltation (between Sections 2166 and 2136) is on the order of 0.09 million cu m (3.2 million cu ft) over a two-year period. Since the general bed level in the area of the trap is about 0.9 m (3 ft), dredging to 2.7 m (9 ft) would provide a 1.8-m- (6-ft-) depth for the trap. This would provide a maximum storage volume of 0.20 million cu m (7.2 million cu ft), which is more than double the volume of estimated siltation. Hence, a 2.7-m- (9-ft-) depth is recommended.

j. While a depth of 2.7 m (9 ft) appears adequate for the sediment trap for storage and safe dredging operation, greater depth may be provided if found necessary or advantageous from other considerations. The GIWW is overdredged to a depth of 4.87 m (16 ft) for a design navigable depth of 3.66 m (12 ft). The depth of trap need not be greater than 4.88 m (16 ft).

k. After the trap is dredged for the first time, collapsing of side slopes inside the trap and washing of adjacent sediment into the trap because of tidal currents should be expected. No attempt is made in this report to estimate the average or the maximum rate of filling of the sediment trap. The site conditions would be expected to stabilize with time after an initial faster filling of the trap. Table 5 gives excess siltation in Zone D-D relative to the siltation in other reach of GIWW. The quantity is on the order of 226,400 cu m (800,000 cu ft). If a sand trap could collect at least this volume before it reached the GIWW, then excessive local shoaling in Zone D-D could be reduced, which would result in reduced frequency of dredging and hence, a reduced maintenance cost.

l. It may be reasonable to assume that the base siltation in the entire length of the GIWW within Rollover Bay and beyond would not have any

major impact caused by the new trap. If the trap functions effectively, the present dredging frequency of about two years would hopefully become two and a half to three years depending upon the annual rates of siltation. The most convenient practice would be to dredge the sediment trap at the same time when the GIWW would be dredged for maintenance dredging irrespective of the amount of sediment accumulation. However, if the trap continues to fill up at a much faster rate than the GIWW, it may have to be emptied earlier to enable its functioning as a trap.

Impact of Other Dredging in Rollover Bay

The Galveston District received a Permit Application No. 21755 issued on 27 August 1999 for dredging about 526,000 sq m (130 acres) of borrow area inside Rollover Bay. Figure 66 shows the area, which is proposed to be dredged for removing sediment and supplying it to the eroding beach. It covers a reach south of the GIWW extending to the inner entrance of the manmade cut joining Rollover Bay to the sea. The drawing also shows a small area to the northwest of the earlier dredge deposits. The area is proposed to be dredged to 1.22 m (4 ft) below mean low tide (mlt). Since the existing ground elevation of the area is about 0.46 m (1.5 ft) below mlt level; the depth of cut will be about 0.76 m (2.5 ft) below the present bed. This amounts to essentially surficial scraping rather than digging.

The following comments on the above proposal are restricted only to the removal of sediment and not to its placement on the beach. Also, the environmental impact is not addressed.

a. Dredging the area as proposed on the south side of the GIWW to a depth of 1.22 m (4 ft) below mtl is not likely to cause any significant adverse effect on the existing sedimentation pattern in the area. The dredging may even have a marginal beneficial effect. A part of the sediment entering the bay from the sea side would be expected to be deposited in the newly dredged area and to that extent reduce the amount of sediment deposition for some time over a small reach of the GIWW, which is adjacent to the proposed dredging.

b. It would be desirable to restrict the area of dredging to the south of the earlier dredged deposits. Leaving a strip of higher elevation between the GIWW and the dredged area would arrest northbound bed-load transport into the GIWW to some extent. This would also prevent sloughing of dredged banks into the GIWW.

Dredged Sediment Disposal

Currently, sediment dredged from the GIWW is deposited on the eroding beach outside the Rollover Pass entrance on a needed basis. ERDC, CHL

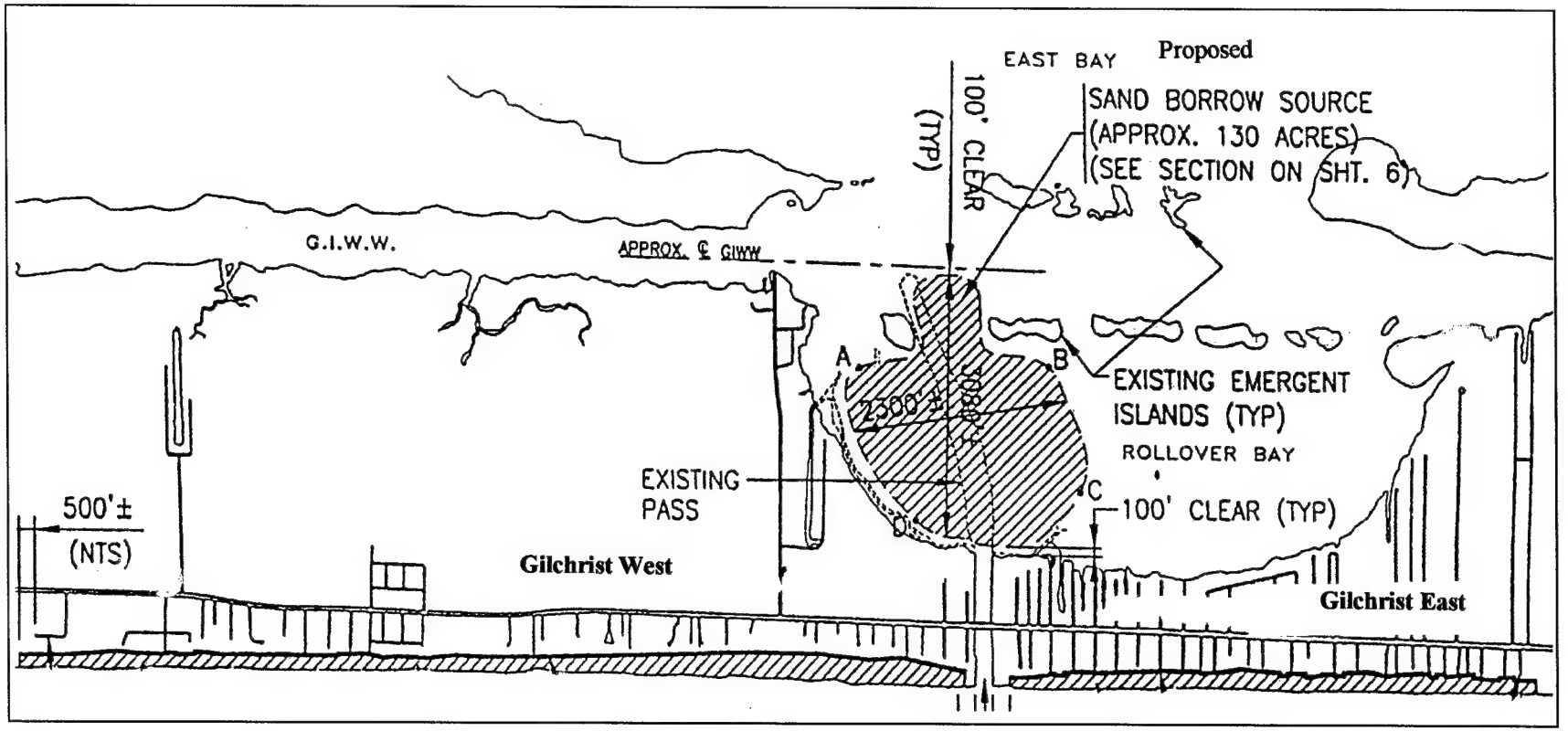

Figure 66. Dredging proposed in East Bay

collected surface sediment samples from different locations in Rollover Bay and East Bay including the GIWW area. A particle size analysis of sediment collected from the GIWW adjacent to the area where the new trap is proposed showed that the material consists of predominantly coarse sediment. It would be expected that the sediment trap would collect material very similar to this since the trap is located on the south side of the GIWW, which is the supply side from the sea. Such material is highly suitable for beach nourishment. Hence, it is recommended that the material removed from the trap be deposited on the eroding beach.

Recommended Design

The sediment trap Layout 11 shown in Figure 63 is recommended for adoption. The trap has a length of 914 m (3,000 ft) and a width of 122 m (400 ft). The recommended width is expected to be required for obtaining better trapping efficiency and also to provide adequate room for maneuvering a dredge inside the trap. The trap is isolated from the GIWW by at least 61 m (200 ft). Recommended design depth in the trap is 2.7 m (9 ft), which is expected to be adequate for safe dredging operation; however, it could be deeper if found necessary or advantageous. Similarly, the width of the trap could be more than recommended, provided the extension is towards the inlet entrance.

Layout 11 has the following merits:

a. It is not connected to the GIWW over the entire trap length. Hence, it is not influenced by the longitudinal flow pattern in the GIWW.

b. It does not include construction of any structures.

c. It provides only one navigational connection with the GIWW for a dredge to enter and leave.

d. The trap does not permit a "flow-through" hydraulic condition.

e. Phasing of dredging work for future expansion is easy and feasible.

f. Sediment from the trap can be removed without hindering traffic in the GIWW.

The new sediment trap should be initially dredged over a smaller area as shown in Figure 64 under Phase 1. Its effectiveness needs to be monitored over the next two years or so after construction. Expansion of the trap over larger areas in the next two phases should be done later if experience shows that the first phase is having the desired effect.

Among the various layouts suggested in this report, only the layouts detached from GIWW and having their longer dimension parallel to the GIWW are preferred. The order of preference of layouts are: Layout 11 (Figure 63); Layout 10 (Figure 62); Layout 9 (Figure 61); and Layout 4 (Figure 56).

Further Studies

An important product of the present study is the formulation of a working numerical hydrodynamic model of the Rollover Pass area. This model can be used for the following further studies:

a. Examine the effect of dredging other areas of the bay.

b. Examine the effect of closure of Rollover Pass.

c. Conduct numerical sedimentation studies.

5 Conclusions and Recommendations

a. Sediment dredged from the GIWW has the following average composition:
Sand 30 percent, Silt 50 percent, Clay 20 percent

b. Coarse sediment appears to be traveling from the sea all the way to the GIWW.

c. East Bay is a source of finer sediment.

d. Present GIWW is a sediment trap.

e. A short length of GIWW between sections 2136 and 2166 is the most suitable zone for locating sediment trap.

f. Configuration # 11 (Figure 63) of the report is recommended for the trap. It has the following features:

1. It is not connected to the GIWW over its entire length.
2. It does not include construction of any structures.
3. It provides one connection with GIWW for a dredge to enter.
4. The trap does not permit a "flow-through" hydraulic condition.
5. Phasing of dredging work for future expansion is easy and feasible.

g. The recommended sediment trap layout # 11 has a length of 915 m (3,000 feet) and a width of 122 m (400 feet). The recommended width would be needed for obtaining better trapping efficiency and also for providing adequate room for maneuvering a dredge inside the trap. The trap is isolated from GIWW by at least 61 m (200 feet). Recommended design depth in the trap is 2.75 m (9 feet), which is expected to be adequate for safe dredging operation, however, it could be deeper if found necessary or advantageous. The proposed trap will be effective in collecting a substantial proportion of coarse sediment traveling mainly as bed load from the seaside.

h. Providing a sediment trap on the north side of GIWW will not be effective because it will not trap suspended sediment unless the depth is greater than the depth of GIWW and also the width will have to be substantial, which will also make it expensive.

i. Although some of the suspended sediment crossing the GIWW will be trapped, the amount is expected to be small.

j. Suspended sediment coming from the East Bay will continue to accumulate within the GIWW.

k. The proposed trap is expected to catch the excessive sediment between sections 2136 and 2166 and prevent formation of a local hump, which at present necessitates more frequent dredging. Hence with the presence of the sediment trap, frequency between consecutive dredging operations and hence the average annual cost of dredging are expected to be reduced.

l. The new sediment trap should be dredged over a smaller area under Phase 1. Its effectiveness should be monitored over the next two years or so after construction. Expansion of trap over larger areas in the next two phases should be done later if experience shows that the first phase is having desired effect.

m. The sediment removed for making the trap should be deposited on the eroding beach, provided it is suitable for beach nourishment.

n. Environmental impacts of sediment trap have not been addressed in this report.

References

Ackers, P., and White, W. R. (1973). "Sediment Transport: New Approach and Analysis," *Journal of the Hydraulics Division,* American Society of Civil Engineers, 99 (HY-11), 2041-2060.

Ariathurai, R., MacArthur, R. D., and Krone, R. C. (1977). "Mathematical model of estuarial sediment transport," Technical Report D-77-12, U.S. Army Engineer Waterways Experiment Station, Vicksburg, MS.

Brigham Young University. (1995). "Surface water modeling system," Reference Manual, Computer Graphics Laboratory, Provo, UT.

Fagerburg T. L, Fisackerly, G. M., Parman, J. W, and Coleman, C. J. (1994). "Houston-Galveston navigation channels, Texas project, Report 1 Galveston Bay field investigation," Technical Report HL-92-7, U. S. Army Engineer Waterways Experiment Station, Vicksburg, MS.

Fischer W. L., McGowan, J. H., Brown, L. F., Jr., and Groat, C. G. (1972). "Environmental geologic atlas of the Texas coastal zone - Galveston-Houston area," Bureau of Economic Geology, University of Texas, Austin, TX.

King, Ian P., and Rachiele, R. (1989). "Program documentation: RMA4 – a two-dimensional water quality model; version 3.0," Resource Management Associates, Lafayette, CA.

Krone, R. B. (1962). "Flume studies of transport of sediment in estuarial shoaling processes," Final Report, Hydraulics Engineering Research Laboratory, University of California, Berkeley, CA.

Lin H. C. (1992). "Houston-Galveston navigation channels, Texas Project: Report 2, two-dimensional numerical modeling of hydrodynamics," Technical Report HL-92-7, U.S. Army Engineer Waterways Experiment Station, Vicksburg, MS.

Norton, W. R., and King, I. P. (1977). "Operating instructions for the computer program RMA-2V," Resource Management Associates, Lafayette, CA.

Partheniades, E. (1962). "A study of erosion and deposition of cohesive soils in salt water," Ph.D. diss., University of California, Berkeley, CA.

Swart, D. H. (1976). "Coastal sediment transport, computation of longshore transport," R968, Part 1, Delft Hydraulics Laboratory, The Netherlands.

Thomas, W. A., and McAnally, W. H. (1985). "User's manual for the generalized computer program system; open-channel flow and sedimentation, TABS-2, main text and Appendices A through O," Instruction Report HL-85-1, U.S. Army Engineer Waterways Experiment Station, Vicksburg, MS.

White, W. R., Milli, H., and Crabbe, A. D. (1975). "Sediment transport theories: an appraisal of available methods," Report Int. 119, Vols 1 and 2, Hydraulics Research Station, Wallingford, England.

Appendix A
The TABS-MD System

TABS-MD is a collection of generalized computer programs and utility codes integrated into a numerical modeling system. TABS-MD is capable of one-, two-, and/or three-dimensional computations; however, only the one- and two-dimensional vertically averaged capability will be discussed in this summary. The system is used for studying hydrodynamics, sedimentation, and transport problems in rivers, reservoirs, bays, and estuaries. A schematic representation of the system is shown in Figure A1. It can be used either as a stand-alone solution technique or as a step in the hybrid modeling approach. The basic concept is to calculate water surface elevations, current patterns, sediment erosion, transport and deposition, the resulting bed surface elevations, and the feedback to hydraulics. Existing and proposed geometry can be analyzed to determine the impact on sedimentation of project designs and to determine the impact of project designs on salinity and on the stream system. The system is described in detail by Thomas and McAnally (1985).[1]

The three basic 2D depth-averaged components of the system are as follows:

a. "A Two-Dimensional Model for Free Surface Flows," RMA2.

b. "Sediment Transport in Unsteady Two-Dimensional Flows, Horizontal Plane," SED2D.

c. "Two-Dimensional Finite Element Program for Water Quality," RMA4.

RMA2 is a finite element solution of the Reynolds form of the Navier-Stokes equations for turbulent flows. Friction is calculated with Manning's equation and eddy viscosity coefficients are used to define the turbulent exchanges. A velocity form of the basic equation is used with side boundaries treated as either slip or static. The model has a marsh porosity option as well as the ability to automatically perform wetting and drying. Boundary conditions may be water surface elevations, velocities, discharges, or tidal radiation.

[1] References cited in this appendix are listed in the References at the end of the main text.

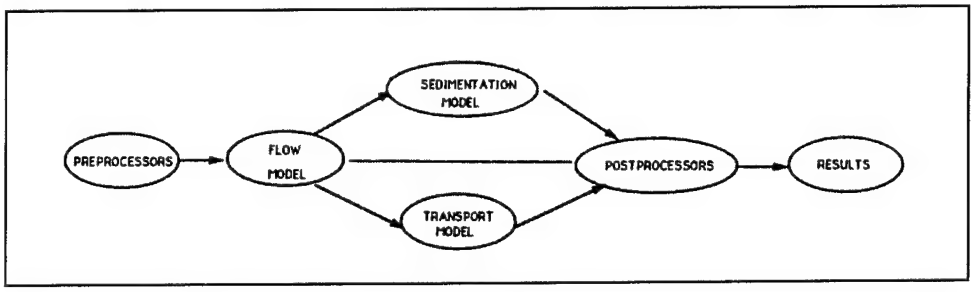

Figure A1. TABS-MD schematic

The sedimentation model, SED2D, solves the convection-diffusion equation with bed source-sink terms. These terms are structured for either sand or cohesive sediments. The Ackers-White (1973) procedure is used to calculate a sediment transport potential for the sands from which the actual transport is calculated based on availability. Clay erosion is based on work by Partheniades (1962) and Ariathurai and the deposition of clay utilized Krone's equations (Ariathurai, MacArthur, and Krone 1977). Deposited material forms layers and bookkeeping allows up to 10 layers at each node for maintaining separate material types, deposit thickness, and age. The code uses the same mesh as RMA2.

Salinity calculations, RMA4, are made with a form of the convective-diffusion equation which has general source-sink terms. Up to six conservative substances or substances requiring a decay term can be routed. The code uses the same mesh as RMA2. The model accommodates a mixing zone outside of the model boundaries for estimation of retrainment.

Each of these generalized computer codes can be used as a stand-alone program, but to facilitate the preparation of input data and to aid in analyzing results, a family of utility programs was developed for the following purposes:

a. Digitizing

b. Mesh generation

c. Spatial data management

d. Graphical output

e. Output analysis

f. File management

g. Interfaces

h. Job control language

Finite Element Modeling

The TABS-MD numerical models used in this effort employ the finite element method to solve the governing equations. To help those who are unfamiliar with the method to better understand the system, a brief description of the method is given here.

The finite element method approximates a solution to governing equations by dividing the area of interest into smaller subareas, which are called elements. The dependent variables (e.g., water surface elevations and sediment concentrations) are approximated over each element by continuous functions which interpolate based on unknown point (node) values of the variables. An error, defined as the deviation of the governing equations using the approximate solution from the equation using the correct solution, is minimized. Then, when boundary conditions are imposed, a set of solvable simultaneous equations is created. The solution is continuous over the area of interest.

In one-dimensional problems, elements are line segments. In two-dimensional problems, the elements are polygons, usually either triangles or quadrilaterals. Nodes are located on the edges of elements and occasionally inside the elements. The interpolating functions may be linear or higher order polynomials. Figure A2 illustrates a quadrilateral element with eight nodes and a linear solution surface where F is the interpolating function.

Most water resource applications of the finite element method use the Galerkin method of weighted residuals to minimize error. In this method the residual, the local error in the equations use of the approximate and solution, is weighted by a function that is identical to the interpolating function and then minimized. Minimization results in a set of simultaneous equations in terms of nodal values of the dependent variable (e.g. water surface elevations or sediment concentration). The time portion of time-dependent problems can be solved by the finite element method, but it is generally more efficient to express derivatives with respect to time in finite difference form.

The Hydrodynamic Model, RMA2

Applications

This program is designed for far-field problems in which vertical accelerations are negligible and the velocity vectors at a node generally point in the same directions over the entire depth of the water column at any instant of time. It expects a vertically homogeneous fluid with a free surface. The model will define the response to a specified horizontally inhomogeneous fluid. Both steady and unsteady state problems can be analyzed. A surface wind stress can be imposed and the effects of the earth's rotation can be included.

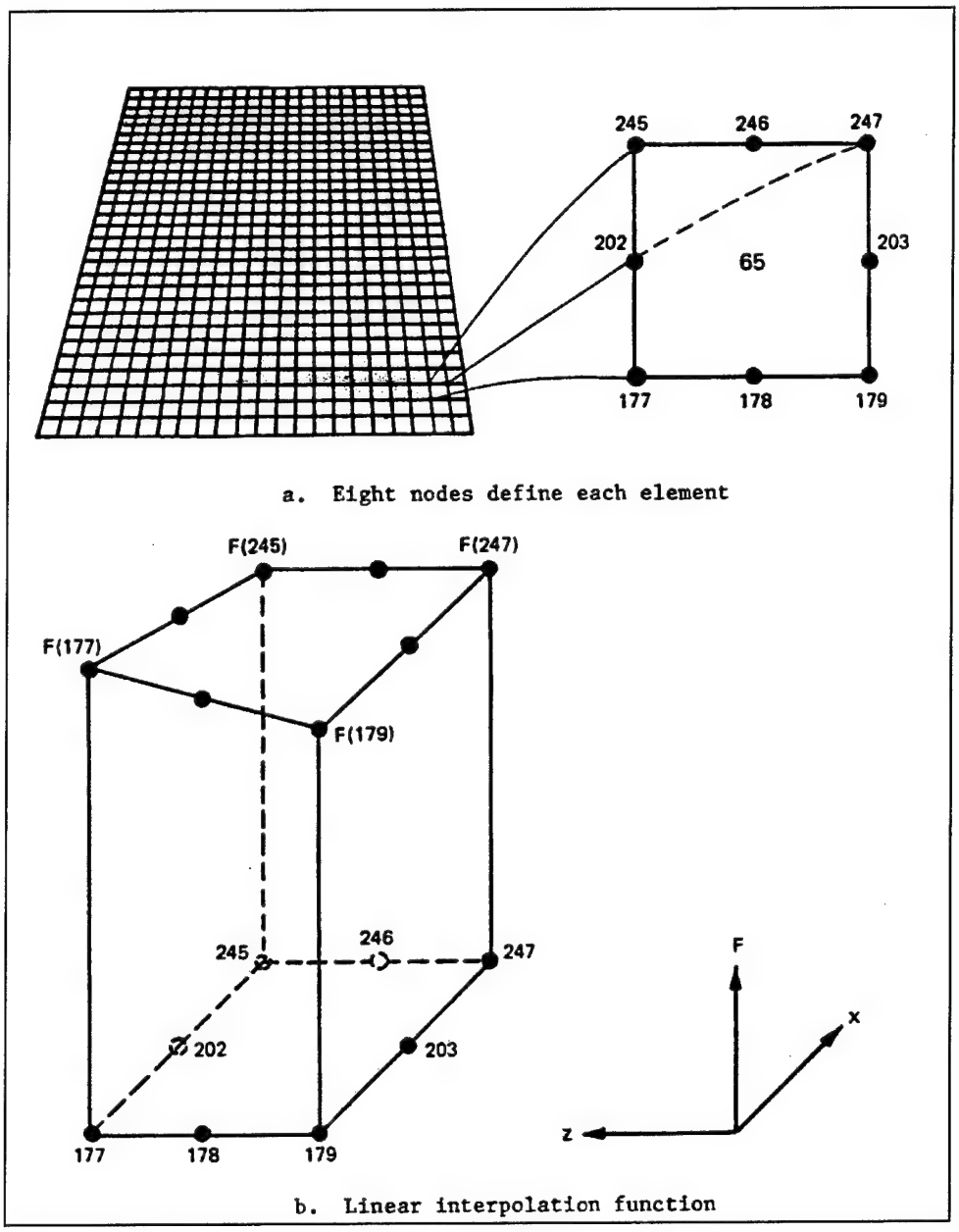

Figure A2. Two-dimensional finite element mesh

The program has been applied to calculate water levels and flow distribution around islands; flow at bridges having one or more relief openings, in contracting and expanding reaches, into and out of off-channel hydropower plants, at river junctions, and into and out of pumping plant channels; circulation and transport in waterbodies with wetlands; and general water levels and flow patterns in rivers, reservoirs, and estuaries.

Limitations

This program is not designed for near-field problems where flow structure interactions (such as vortices, vibrations, or vertical accelerations) are of interest. Areas of vertically stratified flow are beyond this program's capability unless it is used in a hybrid modeling approach. It is two-dimensional in the horizontal plane, and zones where the bottom current is in a different direction from the surface current must be analyzed with considerable subjective judgment. It is a free-surface calculation for subcritical flow problems.

Governing equations

The generalized computer program RMA2 solves the depth-integrated equations of fluid mass and momentum conservation in two horizontal directions. The form of the solved equations is:

$$h\frac{\partial u}{\partial t} + hu\frac{\partial u}{\partial x} + hu\frac{\partial u}{\partial y} - \frac{h}{r}\left(e_{xx}\frac{\partial^2 u}{\partial x^2} + exy\frac{\partial^2 u}{\partial y^2}\right) + gh\left(\frac{\partial a}{\partial x}\frac{\partial h}{\partial x}\right) + \frac{gun}{\left(1.48h^{1/6}\right)^2}\left(u^2 + v^2\right)^{1/2} - zV_a^2 \cos j - 2hwv \sin f = 0 \quad \text{(A1)}$$

$$h\frac{\partial v}{\partial t} + hv\frac{\partial v}{\partial x} + hv\frac{\partial v}{\partial y} - \frac{h}{\rho}\left(\varepsilon_{yx}\frac{\partial^2 v}{\partial y^2} + \varepsilon_{yy}\frac{\partial^2 v}{\partial y^2}\right) + gh\left(\frac{\partial a}{\partial y} + \frac{\partial h}{\partial y}\right) + \frac{gun}{\left(1.48h^{1/6}\right)^2}\left(u^2 + v^2\right)^{1/2} - \zeta V_a^2 \sin\varphi + 2\omega hu \sin\phi = 0 \quad \text{(A2)}$$

$$\frac{\partial h}{\partial t} + h\left(\frac{\partial u}{\partial x} + \frac{\partial v}{\partial y}\right) + u\frac{\partial h}{\partial x} + v\frac{\partial h}{\partial y} = 0 \quad \text{(A3)}$$

where

h = depth
u,v = velocities
x,y,t = Cartesian coordinates and time
ρ = density of fluid
ϵ = eddy viscosity coefficient, for xx = normal direction on x-axis surface; yy= normal direction on y-axis surface; xy and yx = shear direction on each surface
g = acceleration due to gravity
a = elevation of bottom
n = Manning's n value
1.486 = conversion from SI (metric) to non-SI units
ζ = empirical wind shear coefficient

V_a = wind speed
ψ = wind direction
ω = rate of earth's angular rotation
ϕ = local latitude

Equations A1, A2, and A 3 are solved by the finite element method using Galerkin weighted residuals. The elements may be one-dimensional lines or two-dimensional quadrilaterals or triangles and may have curved (parabolic) sides. The shape functions are quadratic for velocity and linear for depth. Integration in space is performed by Gaussian integration. Derivatives in time are replaced by a nonlinear finite difference approximation. Variables are assumed to vary over each time interval in the form:

$$f(t) = f(0) + at + bt^c \quad t_o \leq t < t \tag{A4}$$

which is differentiated with respect to time, and cast in finite difference form. Letters *a, b,* and *c* are constants. It has been found by experiment that the best value for *c* is 1.5 (Norton and King 1977).

The solution is fully implicit and the set of simulataneous equations is solved by Newton-Raphson nonlinear iteration. The computer code executes the solution by means of a front-type solver that assembles a portion of the matrix and solves it before assembling the next portion of the matrix. The front solvers' efficiency is largely independent of bandwidth and thus does not require as much care in formation of the computational mesh as do earlier traditional solvers.

The code RMA2 is based on the earlier versions (Norton and King 1977) but differs in several ways. It is formulated in terms of velocity (v) instead of unit discharge (vh), which improves some aspects of the code's behavior; it permits drying and wetting of areas within the grid; it permits specification of turbulent coefficients in directions other than along the x- and z-axes; it accommodates the specifications of hydraulic control structures in the network; it permits wetlands to be simulated as either totally wet/dry or as gradually changing wetting; and it permits input in either English system or international units. For a more complete description, see Appendix F of Thomas and McAnally (1985).

The Sediment Transport Model, SED2D

Applications

SED2D can be applied to clay and/or sand bed sediments where flow velocities can be considered two-dimensional (i.e., the speed and direction can be satisfactorily represented as a depth-averaged velocity). It is useful for both deposition and erosion studies and, to a limited extent, for stream width studies. The program treats two categories of sediment: noncohesive, which is referred to as sand here, and cohesive, which is referred to as clay.

Limitations

Both clay and sand may be analyzed, but the model considers a single, effective grain size for each and treats each separately. Fall velocity must be prescribed along with the water surface elevations, x-velocity, y-velocity, diffusion coefficients, bed density, critical shear stresses for erosion, erosion rate constants, and critical shear stress for deposition.

The program does not compute water surface elevations or velocities; therefore these data must be provided. For complicated geometries, the numerical model for hydrodynamic computations, RMA2, is used. However, SED2D can only accept a two-dimensional network.

Governing equations

The generalized computer program SED2D solves the depth-integrated convection-dispersion equation in two horizontal dimensions for a single sediment constituent. For a more complete description, see Appendix G of Thomas and McAnally (1985). The form of the solved equation is:

$$\frac{\partial C}{\partial t}+u\frac{\partial C}{\partial x}+v\frac{\partial C}{\partial y}=\frac{\partial}{\partial x}\left(Dx\frac{\partial C}{\partial x}\right)+\frac{\partial}{\partial y}\left(Dy\frac{\partial C}{\partial y}\right)+\alpha 1C+\alpha 2=0 \qquad \text{(A5)}$$

where

C = concentration of sediment
u = depth-integrated velocity in x-direction
D_x = dispersion coefficient in x-direction
D_y = dispersion coefficient in y-direction
α_1 = coefficient of concentration-dependent source/sink term
α_2 = coefficient of source/sink term

The source/sink terms in Equation A5 are computed in routines that treat the interaction of the flow and the bed. Separate sections of the code handle computations for clay bed and sand bed problems.

Sand transport

The source/sink terms are evaluated by first computing a potential sand transport capacity for the specified flow conditions, comparing that capacity with the amount of sand actually being transported, and then eroding from or depositing to the bed at a rate that would approach the equilibrium value after sufficient elapsed time.

The potential sand transport capacity in the model is computed by the method of Ackers and White (1973), which uses a transport power (work rate) approach. It has been shown to provide superior results for transport under

steady-flow conditions (White, Milli, and Crabbe 1975) and for combined waves and currents (Swart 1976). Flume tests at the U.S. Army Engineer Research and Development Center, Waterways Experiment Station have shown that the concept is valid for transport by estuarine currents.

The total load transport function of Ackers and White is based upon a dimensionless grain size:

$$D_{gr} = D\left[\frac{g(s-1)}{v^2}\right]^{1/3} \tag{A6}$$

where

D = sediment particle diameter

s = specific gravity of the sediment

v = kinematic viscosity of the fluid

and a sediment mobility parameter

$$F_{gr} = \left[\frac{\tau^{n'}\tau^{(1-n)}}{\rho g D(s-1)}\right]^{1/2} \tag{A7}$$

where

τ = total boundary shear stress = ρgRS

where

R = hydraulic radius

S = slope of water surface

n = a coefficient expressing the relative importance of bed-load and suspended-load transport, given in Equation A9

NOTE:

n = 1 for fine sediments

n = 0 for coarse sediments

τ = boundary surface shear stress

The surface shear stress is that part of the total shear stress which is due to the rough surface of the bed only, i.e., not including that part due to bed forms and geometry. It therefore corresponds to that shear stress that the flow would exert on a plane bed.

The total sediment transport is (in kg/m^3) expressed as an effective concentration:

$$G_P = C\left(\frac{F_{gr}}{A} - 1\right)^m \frac{sD}{h}\left(\frac{\rho}{\tau} U\right)^{n'} \tag{A8}$$

where U is the average flow speed, and for $1<D_{gr}\leq 60$

$$n' = 1.00 - 0.56\ log\ D_{gr} \tag{A9}$$

$$A = \frac{0.23}{\sqrt{D_{gr}}} + 0.14 \tag{A10}$$

$$log\ C = 2.86\ log\ D_{gr} - (log\ D_{gr})^2 - 3.53 \tag{A11}$$

$$m = \frac{9.66}{D_{gr}} + 1.34 \tag{A12}$$

For $D_{gr}<60$

$$n' = 0.00 \tag{A13}$$

$$A = 0.17 \tag{A14}$$

$$C = 0.025 \tag{A15}$$

$$m = 1.5 \tag{A16}$$

Note the C_a has units consistent with G_p (kg/m^3 for SED2D).

Equations A6 - A16 result in a potential sediment concentration G_p. This value is the depth-averaged concentration of sediment that will occur if an equilibrium transport rate is reached with a nonlimited supply of sediment. The rate of sediment deposition (or erosion) is then computed as:

$$R = \frac{G_p - C}{t_c} \tag{A17}$$

where

C = present sediment concentration

t_c = time constant

For deposition, the time constant is:

$$t_c = larger\ of \begin{cases} \Delta t \\ or \\ \dfrac{C_d H}{V_s} \end{cases} \tag{A18}$$

and for erosion it is:

$$t_c = larger\ of \begin{cases} \Delta t \\ or \\ \dfrac{C_e h}{U} \end{cases} \tag{A19}$$

where

Δt = computational time-step

C_d = response time coefficient for deposition

V_s = sediment settling velocity

C_e = response time coefficient for erosion

The sand bed has a specified initial thickness which limits the amount of erosion to that thickness.

Cohesive sediments transport

Cohesive sediments (usually clays and some silts) are considered to be depositional if the bed shear stress exerted by the flow is less than a critical value τ_d. When that value occurs, the deposition rate is given by Krone's (1962) equation

$$S = \begin{cases} -\dfrac{2V_s}{h} C \left(1 - \dfrac{\tau}{\tau_d}\right) for\ C<C_c & \text{(A20)} \\ -\dfrac{2V_s}{hC_c^{4/3}} C^{5/3} \left(1 - \dfrac{\tau}{\tau_d}\right) for\ C>C_c & \text{(A21)} \end{cases}$$

where

S = source term

V_s = fall velocity of a sediment particle

h = flow depth

C = sediment concentration in water column

τ = bed shear stress

τd = critical shear stress for deposition

Cc = critical concentration = 300 mg/ℓ

If the bed shear stress is greater than the critical value for particle erosion τ_e, material is removed from the bed. The source term is then computed by Ariathurai's (Ariathurai, MacArthur, and Krone 1977) adaptation of Partheniades' (1962) findings:

$$S = \frac{P}{h}\left(\frac{\tau}{\tau_e} - 1\right) \tag{A22}$$

where P is the erosion rate constant, unless the shear stress is also greater than the critical value for mass erosion. When this value is exceeded, mass failure of a sediment layer occurs and

$$S = \frac{T_L P_L}{h \Delta t} \tag{A23}$$

where

T_L = thickness of the failed layer

ρ_L = density of the failed layer

Δ_t = time interval over which failure occurs

τ_s = bulk shear strength of the layer

The cohesive sediment bed consists of 1 to 10 layers, each with a distinct density and erosion resistance. The layers consolidate with overburden and time.

Bed shear stress

Bed shear stresses are calculated from the flow speed according to one of four optional equations: the smooth-wall log velocity profile or Manning's equation for flows alone; and a smooth bed or rippled bed equation for combined currents and wind waves. Shear stresses are calculated using the shear velocity concept where:

$$\tau_b = \rho u_*^2 \tag{A24}$$

where

τ_b = bed shear stress

u_* = shear velocity

and the shear velocity is calculated by one of four methods:

a. Smooth-wall log velocity profiles

$$\frac{\bar{u}}{u_*} = 5.75 \log\left(3.23\frac{u_* h}{\nu}\right) \tag{A25}$$

where $\bar{U}$ is the mean flow velocity (resultant of u and v components)
Equation A25 is applicable to the lower 15 percent of the boundary layer when

$$\frac{u_* h}{\nu} > 30$$

b. The Manning's shear stress equation

$$u_* = \frac{\sqrt{g\,\bar{u}\,n}}{CME\,h^{1/6}} \tag{A26}$$

where *CME* is a coefficient of 1 for SI (metric) units and 1.486 for English units of measurement.

c. A Jonsson-type equation for surface shear stress (plane beds) caused by waves and currents

$$u_* = \frac{1}{2}\left(\frac{f_w u_{om} + f_c \bar{u}}{u_{om} + \bar{u}}\right)\left(\bar{u} + \frac{u_{om}}{2}\right) \tag{A27}$$

where

f_w = shear stress coefficient for waves

u_{om} = maximum orbital velocity of waves

f_c = shear stress coefficient for currents

d. A Bijker-type equation for total shear stress caused by waves and current

$$u* = \sqrt{\frac{1}{2} f_c \bar{u}^2 + \frac{1}{4} f_w u_{om}^2} \tag{A28}$$

Solution method

Equation A5 is solved by the finite element method using Galerkin weighted residuals. Like RMA2, which uses the same general solution technique, elements are quadrilateral and may have parabolic sides. Shape functions are quadratic. Integration in space is Gaussian. Time-stepping is performed by a Crank-Nicholson approach with a weighting factor (φ) of 0.66. A front-type solver similar to that in RMA2 is used to solve the simultaneous equations.

The Water Quality Transport Model, RMA4

Applications

The water quality model, RMA4, is designed to simulate the depth-average advection-diffusion process in most water bodies with a free surface. The model is used for investigating the physical processes of migration and mixing of a soluble substance in reservoirs, rivers, bays, estuarines and coastal zones. The model is useful for evaluation of the basic processes or for defining the effectiveness of remedial measures. For complex geometries the model utilizes the depth-averaged hydrodynamics form RMA2.

The water quality model has been applied to define the horizontal salinity distribution; to trace temperature effects from power plants; to calculate residence times of harbors or basins; to optimize the placement of outfalls; to identify potential critical areas for oil spills or other pollutants spread; to evaluate turbidity plume extent; and to monitor other water quality criterion within game and fish habitats.

Limitations

The formulation of RMA4 is limited to one-dimensional (cross-sectionally averaged) and two-dimensional (depth-averaged) situations in which the concentration is fairly well-mixed in the vertical. It will not provide accurate concentrations for stratified situations in which the constituent concentration influences the density of the fluid. In addition, the accuracy of the transport model is dependent on the accuracy of the hydrodynamics (e.g., as supplied from RMA2).

Governing equations

The USACE - ERDC version of RMA4 is a revised version of RMA4 as developed by King (1989). The generalized computer program solves the depth-integrated equations of the transport and mixing process. The form of the equations solved is:

$$h\left(\frac{\partial c}{\partial t} + u\frac{\partial c}{\partial x} + v\frac{\partial c}{\partial y} - \frac{\partial}{\partial x}D_x\frac{\partial c}{\partial x} - \frac{\partial}{\partial y}D_y\frac{\partial c}{\partial y} - \sigma + kc\right) = 0 \quad \text{(A29)}$$

where

h = water depth
c = constituent concentration
t = Time
$u,v,$ = velocity components
D_x, D_y = turbulent mixing coefficients
k = first order decay
σ = source/sink of constituent

Note that the basic governing equation for RMA4 is the same as for the sediment transport model, SED2D. The differences between the two models lies in the source/sink terms.

Equation A29 is solved by the finite element method using Galerkin weighted residuals. As with the hydrodynamic model, RMA2, the transport model RMA4 handles one-dimensional segments or two-dimensional quadrilaterals or triangles with the option for curved sides. Spatial integration of the equation is performed by Gaussian techniques and the temporal variations are handled by nonlinear finite differences, consistent with the method described in paragraph 15 above. The frontal solution method is also used in RMA4, as with the other programs in the TABS-MD system, to provide an efficient solution algorithm.

The boundary conditions for RMA4 are specified in several optional ways. The boundary concentration may be specified absolutely at a certain level regardless of the flow direction; the concentration can be specified to be applied

only when the water is leaving the model; or a mixing zone may be specified just beyond the model boundary to provide the possibility of reentertainment of constituent into the model that may have crossed the boundary earlier. For a more detailed description of the constituent transport model, RMA4, see King and Rachiele, 1989.

Within the one-dimensional formulation of the model, there is a provision for defining the constituent concentration mixing and transport at control structures as they may have been specified in RMA2. These allow for either a flow-through condition, as for example for a wier-type flow, or for a mixing chamber type of flux, which would be appropriate for a navigation lock.

REPORT DOCUMENTATION PAGE

Form Approved
OMB No. 0704-0188

1. REPORT DATE *(DD-MM-YYYY)*	2. REPORT TYPE	3. DATES COVERED *(From - To)*
September 2000	Final Report	

4. TITLE AND SUBTITLE

Design of Sediment Trap at Rollover Pass, Texas

5a. CONTRACT NUMBER

5b. GRANT NUMBER

5c. PROGRAM ELEMENT NUMBER

6. AUTHOR(S)

Trimbak M. Parchure, Ben Brown, Robert T. McAdory

5d. PROJECT NUMBER

5e. TASK NUMBER

5f. WORK UNIT NUMBER

7. PERFORMING ORGANIZATION NAME(S) AND ADDRESS(ES) AND ADDRESS(ES)

U.S. Army Engineer Research and Development Center
Coastal and Hydraulics Laboratory
3909 Halls Ferry Road
Vicksburg, MS 39180-6199

8. PERFORMING ORGANIZATION REPORT NUMBER

ERDC/CHL TR-00-23

9. SPONSORING / MONITORING AGENCY NAME(S) AND ADDRESS(ES)

Headquarters, U.S. Army Corps of Engineers
Washington, DC 20314-1000

10. SPONSOR/MONITOR'S ACRONYM(S)

11. SPONSOR/MONITOR'S REPORT NUMBER(S)

12. DISTRIBUTION / AVAILABILITY STATEMENT

Approved for public release; distribution is unlimited.

13. SUPPLEMENTARY NOTES

14. ABSTRACT

Rollover Pass is a narrow manmade channel, which connects the Gulf of Mexico and Rollover Bay. The Gulf Intracoastal Water Way (GIWW) crosses the Rollover Bay on the north side of Rollover Pass. The U.S. Army Engineer District, Galveston, maintains a navigation channel, 38 m (125 feet) wide and 3.6 m (12 feet) deep within the GIWW for commercial barge traffic. Over the past several years considerable siltation has been taking place within the GIWW in the vicinity of the Rollover Pass area and periodic dredging is required for maintaining navigable depths. The objective of the study was to construct a working numerical model of the Rollover Pass area, and to use the model for design of a sediment trap, which will be feasible and effective in reducing the frequency of dredging in the GIWW.

The hydrodynamic model code RMA2, available at ERDC-CHL, was used to calculate the hydrodynamics of the system with a two-dimensional numerical model. The model was verified using field data. Velocity patterns under selected tidal conditions were generated. Computation and analysis of bed shear stress patterns were used along with the velocity data to estimate where and by how much sediment deposition is expected to occur. Several alternatives of sediment trap in terms of location, shape, size and depth were considered for evaluation. The factors taken into account in the design of the trap are described in the report. Three configurations out of these were

(Continued)

15. SUBJECT TERMS

Dredging Sand trap
Rollover Pass Sediment

16. SECURITY CLASSIFICATION OF:			17. LIMITATION OF ABSTRACT	18. NUMBER OF PAGES	19a. NAME OF RESPONSIBLE PERSON
a. REPORT	b. ABSTRACT	c. THIS PAGE			19b. TELEPHONE NUMBER *(include area code)*
UNCLASSIFIED	UNCLASSIFIED	UNCLASSIFIED		113	

14. (Concluded).

examined with the model: (1) a sand trap proposed by the Galveston District, (2) a tentative layout of sand trap based on field data and (3) modified final layout based on the results of the tentative layout.

The final layout has a length of 915 m (3,000 feet) and a width of 122 m (400 feet). The trap is separate a from the GIWW by at least 61 m (200 feet). Recommended design depth in the trap is 2.75 m (9 feet). The merits of this layout are described in the report. The width and depth of the trap may be varied in the future, if found necessary or advantageous.

It was noted that suspended sediment coming from the East Bay would continue to accumulate within the GIWW but the trap is expected to capture substantial bed load from the sea side. It is recommended that the new sediment trap should be initially dredged over a smaller area under Phase 1. Its effectiveness should be monitored over the next two years or so after construction. Expansion of the trap over larger areas in the next two phases should be done later if experience shows that the first phase is having desired effect. The proposed trap is expected to catch the excessive sediment between sections 2136 and 2166 and prevent formation of a local hump, which at present necessitates more frequent dredging. With the presence of the sediment trap, frequency between consecutive dredging operations, and hence, the average annual cost of dredging are expected to be reduced.